



저작자표시-비영리-변경금지 2.0 대한민국

이용자는 아래의 조건을 따르는 경우에 한하여 자유롭게

- 이 저작물을 복제, 배포, 전송, 전시, 공연 및 방송할 수 있습니다.

다음과 같은 조건을 따라야 합니다:



저작자표시. 귀하는 원저작자를 표시하여야 합니다.



비영리. 귀하는 이 저작물을 영리 목적으로 이용할 수 없습니다.



변경금지. 귀하는 이 저작물을 개작, 변형 또는 가공할 수 없습니다.

- 귀하는, 이 저작물의 재이용이나 배포의 경우, 이 저작물에 적용된 이용허락조건을 명확하게 나타내어야 합니다.
- 저작권자로부터 별도의 허가를 받으면 이러한 조건들은 적용되지 않습니다.

저작권법에 따른 이용자의 권리는 위의 내용에 의하여 영향을 받지 않습니다.

이것은 [이용허락규약\(Legal Code\)](#)을 이해하기 쉽게 요약한 것입니다.

[Disclaimer](#)

Doctoral Thesis

Development of Functional Protein-based
Target-specific Labeling Nanoplatfoms
for Biological Applications

Yoonji Bae

Department of Biological Sciences

Ulsan National Institute of Science and Technology

2021

Development of Functional Protein-based
Target-specific Labeling Nanoplatfoms
for Biological Applications

Yoonji Bae

Department of Biological Sciences

Ulsan National Institute of Science and Technology

Development of Functional Protein-based Target-specific Labeling Nanoplatfoms for Biological Applications

A thesis/dissertation submitted to
Ulsan National Institute of Science and Technology
in partial fulfillment of the
requirements for the degree of
Doctor of Philosophy

Yoonji Bae

11/25/2020 of submission

Approved by


Advisor

Sebyung Kang

Development of Functional Protein-based
Target-specific Labeling Nanoplatfoms
for Biological Applications

Yoonji Bae

This certifies that the thesis/dissertation of Yoonji Bae is approved.

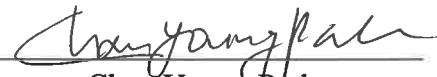
11/25/2020 of submission



Advisor: Sebyung Kang



Tae Joo Park



Chan Young Park



Young Chan Chae



Jongnam Park

Abstract

Qualitative and quantitative analyses of target biomolecules in the cell are essential for the early detection of diseases and the prognosis of treatment in various biomedical research and clinical applications. To selectively detect and quantify biomolecules of interest in complicated biological samples, various methods have been developed in the biotechnology fields. Target biomolecules in the cells can be specifically visualized with labeling probes by fluorescent cell imaging and quantified with immunoassay based on antigen-antibody interactions.

The aim of the thesis is to develop the functional protein-based target-specific labeling nanoplatfoms for application in fluorescent cell imaging and immunoassays. Target biomolecules within the cell can be detected with target-specific fluorescent cell imaging probes. Protein cage nanoparticles as attractive polyvalent nanoplatfoms have been applied to bioimaging probes and biosensor components because they have a well-defined symmetric hollow shell structure with uniform nanoscale particle sizes. Their polyvalent nature allows uniform multiple targeting ligands or fluorescent probes to genetically and/or chemically adhere to their surface. A new class of protein cage nanoparticles, encapsulin, was developed as a tunable dual-functional nanoplatfom, which has its target-specific capability with multiple combinations of targeting ligands and colors, using bacterial glue, the SpyTag/SpyCatcher (ST/SC) protein ligation system.

Next, target-specific signal amplifiers were developed as secondary antibody mimics to be applied in immunoassays. Immunoassays are utilized to selectively detect and quantify low-abundance biomolecules in biological samples through antigen-antibody interaction. HRP-conjugated IgG-binding nanobodies were established using ST/SC protein ligation system. They have selective and strong binding to specific IgG and show signal amplifying capability in various types of immunoassays, such as western blot, ELISA, and the multiplex TSA cell and tissue imaging.

A variety of target-specific labeling probes demonstrated that they could be utilized in fluorescent cell imaging and immunoassays by combining fluorescent molecules or signal generating enzyme with targeting ligands, including affibody molecules or nanobodies.

Contents

| | |
|--|----|
| Abstract | 1 |
| Contents | 3 |
| List of figures | 5 |
| Abbreviations | 7 |
| | |
| Chapter 1. Introduction | |
| 1.1 Qualitative and Quantitative Analyses of Target Biomolecules in Cells | 9 |
| 1.1.1 Visualization of Target Biomolecules | 9 |
| 1.1.2 Quantitation of Target Biomolecules | 12 |
| 1.2 Functional Proteins-based Nanoplatfoms | 13 |
| 1.2.1 Protein cage nanoparticles | 13 |
| 1.2.2 Monomeric proteins | 14 |
| 1.2.3 Genetic Encoded Protein Tags | 16 |
| 1.3 Research Outline | 17 |
| 1.3.1 Objective for the Thesis | 17 |
| 1.3.2 Outline of the Thesis | 17 |
| | |
| Chapter 2. Target-specific Fluorescent Probes for Fluorescence Cell Imaging based on Protein Cage Nanoparticles | |
| 2.1 Summary | 18 |
| 2.2 Introduction | 18 |
| 2.3 Materials and Methods | 20 |
| 2.4 Results and Discussion | 22 |
| 2.5 Conclusion | 36 |
| | |
| Chapter 3. Target-specific Signal Amplifiers for Immunoassays | |
| 3.1 Summary | 37 |
| 3.2 Introduction | 37 |
| 3.3 Materials and Methods | 40 |
| 3.4 Results and Discussion | 44 |

| | |
|--|----|
| 3.5 Conclusion | 61 |
| Chapter 4. Concluding Remarks | |
| 4.1 Summary and Conclusions | 62 |
| References | 63 |
| Acknowledgements | 71 |
| Appendix | |
| A. Microperoxidase study | 72 |
| B. Target-specific Labeling Tools to Detect Intracellular Proteins | 76 |
| C. References | 81 |

List of figures

Chapter 1. Introduction

| | |
|---|----|
| Figure 1.1 Overview of fluorescent probes | 10 |
| Figure 1.2 Examples of self-labeling tag systems and applications in microscopy | 11 |
| Figure 1.3 Immunofluorescence using antibody-antigen interaction | 12 |
| Figure 1.4 A example of immunoassay, enzyme-linked immunosorbent assay (ELISA) | 12 |
| Figure 1.5 Surface diagram representations of various types of protein cage nanoparticles | 13 |
| Figure 1.6 Schematic representation of various types of monomeric proteins | 15 |
| Figure 1.7 Cartoon of SpyTag/SpyCatcher protein ligation system | 16 |

Chapter 2. Target-specific Fluorescent Probes for Fluorescent Cell Imaging based on Protein Cage Nanoparticles

| | |
|---|----|
| Figure 2.1 Schematic illustration of target-specific fluorescent probes | 20 |
| Figure 2.2 Molecular mass measurements of two different SC-Afbs | 24 |
| Figure 2.3 Characterization of fEncap-L-ST | 24 |
| Figure 2.4 SDS-PAGE analyses of reaction results of SC-Afb and fEncap-L-ST | 25 |
| Figure 2.5 Fluorescent microscopic images with affibody molecule-ligated fEncap-L-ST | 25 |
| Figure 2.6 Characterizations of SC-proteins ligated Encap | 27 |
| Figure 2.7 Optimization of input ratio of SC-proteins to subunit of Encap using SDS-PAGE | 29 |
| Figure 2.8 SDS-PAGE analyses of reaction results of SC-proteins and Encap | 30 |
| Figure 2.9 Fluorescent microscopic images of with dual functional Encap | 31 |
| Figure 2.10 Characterization of aEncap-L-ST | 33 |
| Figure 2.11 Characterization of reaction products for fluorescent microscopic images using SDS-PAGE | 33 |
| Figure 2.12 Fluorescent microscopic images with dual targeting Encap | 34 |
| Figure 2.13 Fluorescent microscopic images of HEK293T cells treated with dual targeting Encap --- | 35 |

Chapter 3. Target-specific Signal Amplifiers for Immunoassays

| | |
|---|----|
| Figure 3.1 Schematic illustration of target-specific signal amplifiers | 39 |
| Figure 3.2 Characterization of purified proteins and reaction proteins using SDS-PAGE | 44 |
| Figure 3.3 SDS-PAGE analysis of reaction results of HRP-SC and Nb-STs | 46 |
| Figure 3.4 Characterization of purified proteins and reaction proteins using analytical methods | 46 |
| Figure 3.5 SPR sensorgrams of Nb-STs and HRP:Nbs | 47 |
| Figure 3.6 Western blots | 49 |
| Figure 3.7 Quantitative analyses of signal enhancement of western blots | 50 |

Figure 3.8 Indirect ELISA ----- 52
 Figure 3.9 SDS-PAGE analysis of reaction results of dye conjugated SCs and Nb-STs ----- 55
 Figure 3.10 Fluorescent cell imaging and tyramide signal amplification (TSA) assays ----- 56
 Figure 3.11 Tyramide signal amplification (TSA) assays with negative cells ----- 57
 Figure 3.12 Tyramide signal amplification (TSA) assays in FLAG-HaloTag gene-transfected HEK293T cells - 58
 Figure 3.13 Tyramide signal amplification (TSA) assays in *Xenopus* whole embryos ----- 60

Appendix A. Microperoxidase study

Figure A1 Schematic representation of the heme attachment process mediated by the Ccm system -- 73
 Figure A2 Expression test of microperoxidase fusion proteins ----- 74
 Figure A3 Characterization of microperoxidase-SpyCatcher ----- 74
 Figure A4 Comparison of catalytic activity of peroxidases ----- 75

Appendix B. Target-specific labeling tools to detect intracellular proteins

Figure B1 Schematic representation of target-specific labeling tools ----- 79
 Figure B2 Fluorescent microscopic images with target-specific labeling tools ----- 79
 Figure B3 Confirmation of SpyTag/SpyCatcher ligation using western blots ----- 80

Abbreviations

DAPI: 4', 6-diamidino-2-phenylindole

ABD: antibody binding domain

APEX2: ascorbate peroxidase-2

BFP: blue fluorescent protein

CFP: cyan fluorescent protein

DLS: dynamic light scattering

DMEM: Dulbecco's modified Eagle's medium

ECL: enhanced chemiluminescence

EGFR: epidermal growth factor receptor

ELISA: enzyme-linked immunosorbent assay

Encap: encapsulin protein cage nanoparticles

EpCAM: epithelial cell adhesion molecule

ESI-TOF MS: electrospray ionization time-of-flight mass spectrometer

F5M: fluorescein-5-maleimide

FAM: 5(6)-carboxyfluorescein

FBS: fetal bovine serum

GFP: green fluorescent protein

GSH: glutathione

GST: glutathione S-transferase

HCC: hepatocellular carcinoma

hCG: human chorionic gonadotropin

HER2: Human epidermal growth factor receptor

HRP: horseradish peroxidase

ICG: indotricarbocyanine

IgG: immunoglobulin G

IPTG: isopropyl β -D-1-thiogalactopyranoside

mSA: monostreptavidin (mSA)

Nanoluc: nanoluciferase

PBS: phosphate buffered saline

PCR: polymerase chain reaction

PVDF: polyvinylidene difluoride

RU: response unit

SDS-PAGE: sodium dodecyl sulfate-polyacrylamide gel electrophoresis

SEC: size exclusion chromatography

SPR: surface plasmon resonance

ST/SC: SpyTag/SpyCatcher

TEM: transmission electron microscopy

TMB: 3,3',5,5'-tetramethylbenzidine

TSA: tyramide signal amplification

YFP: yellow fluorescent proteins

Chapter 1. Introduction

1.1. Qualitative and Quantitative Analyses of Target Biomolecules in Cells

Cells have various expression level of proteins, which play important roles in cell structure, regulation of metabolism and cell to cell communication in cellular life. Therefore, qualitative and quantitative analyses of target proteins in cell are essential to understand molecular and cellular processes within living system. Various techniques have been developed in biomedical research and clinical applications to selectively visualize and quantify target proteins of interest in complex biological samples.

1.1.1 Visualization of Target Biomolecules

Fluorescence cell imaging is useful method to selectively detect and visualize cell components and morphology as well as to investigate cellular behaviors and responses derived from internal and/or external stimuli within biological complex. Fluorescence is produced by target proteins or fluorophore conjugated to target proteins and is excited and emitted at certain wavelength. Therefore, this method requires detectable fluorescent probes, which usually are labeled around the target proteins. Three kinds of labeling probes will be described here.

Target-Specific Fluorescent probes

Fluorescent probes are useful tools for fluorescent cell imaging due to their sensitivity and versatility while minimizing perturbation of target cells (Figure 1.1).¹⁻³ Typically, fluorescent probes consist of fluorophores, which have no specificity for the target protein. For clinical applications, most fluorescent probes are combined with targeting moiety for targeting efficiency. First, many cancer-specific fluorescent probes have been established by targeting cancer cell markers such as growth signaling receptors, angiogenesis growth factors, and tumor cell markers. Current strategies for cancer targeting probes are established by incorporating imaging agents with cancer-specific ligands by chemical conjugation or genetic insertion. Cancer targeting probes recognize cancer sites and bind to specific molecular targets. Becker, et al. reported serum protein-dye conjugates consisting of transferrin or human serum albumin and an indotricarbocyanine (ICG) derivatives for the optical imaging of breast cancer.⁴ Ogawa, et al. demonstrated the breast cancer targeting probes by combining ICG with monoclonal antibodies directed at cell surface markers overexpressed on breast cancers.⁵ There are target-specific fluorescent probes by combining fluorescent dye and biomolecules-targeting peptide as well as cancer. Wei, et al. suggested fluorescent peptide probes by combining collagen targeting peptide with the repetitive Gly-Pro-Pro and Gly-Hyp-Hyp sequences, and fluorescent dye, 5(6)-carboxyfluorescein (FAM).⁶ Even though these strategies have many advantages such as high

fluorescence intensity and specificity to targets, they still need chemical modification to conjugate fluorophore, which may induce heterogeneity with high manufacturing costs and a long preparation time. Recently, target-specific fluorescent probes are generated by combining biocompatible nanomaterials with targeting ligands, including antibody, affibody molecules, or nanobody. They can recognize specific biomolecules in target cells with enhanced stability, reduced toxicity, and improved targeting efficiency.

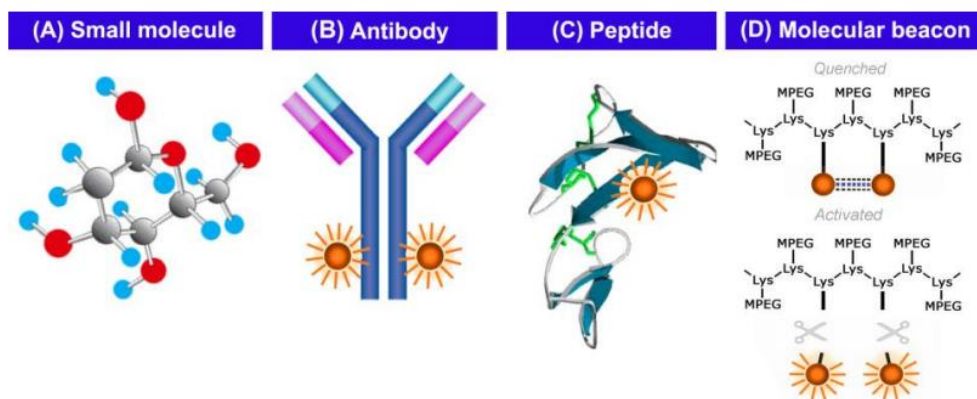


Figure 1.1 Overview of fluorescent probes. (A) Non-specific small fluorescent molecules, (B) fluorescent agents conjugated to antibodies, (C) targeted peptides, or (D) molecular beacon.⁷

Self-labeling Tag Systems

In self-labeling tag system, genetically encoded tags with targeting specificity can be fused to target proteins, which are recognized by cognate ligand and catalyzed for covalent attachment.⁸ HaloTag, SNAP-Tag, and CLIP-Tag are representative self-labeling tags, which are used for protein purification, cellular imaging, and protein-protein interaction analysis.⁹⁻¹² These tags possess several advantages; rapid labeling kinetics, high labeling intensity, and thermal stability. Each tag is expressed with the target proteins in the cell, and covalently conjugated with specific ligands conjugated to a fluorescent dye (Figure 1.2). Many of these ligands have produced with cell-permeable property across cellular membranes allowing for live cell labeling and imaging analysis. Los, et al. demonstrated the utility of HaloTag system for cellular imaging and protein immobilization by analyzing multiple molecular processes associated with NF- κ B-mediated cellular physiology, including imaging of subcellular protein translocation and capture of protein-protein and protein-DNA complexes.¹³ In Charubin's group, they used HaloTag and SNAP-tag to label the anaerobic organisms with fluorescent ligands commercially available.¹⁴ HaloTag can be utilized to study cellular signaling on the proteins regulating biological processes. However, they do not share fluorescent ligands and the appropriate ligand must be changed each time a specific tag is used. Also, the size of the protein tag is not small, which can affect the resolution of fluorescence imaging or cause other problems.

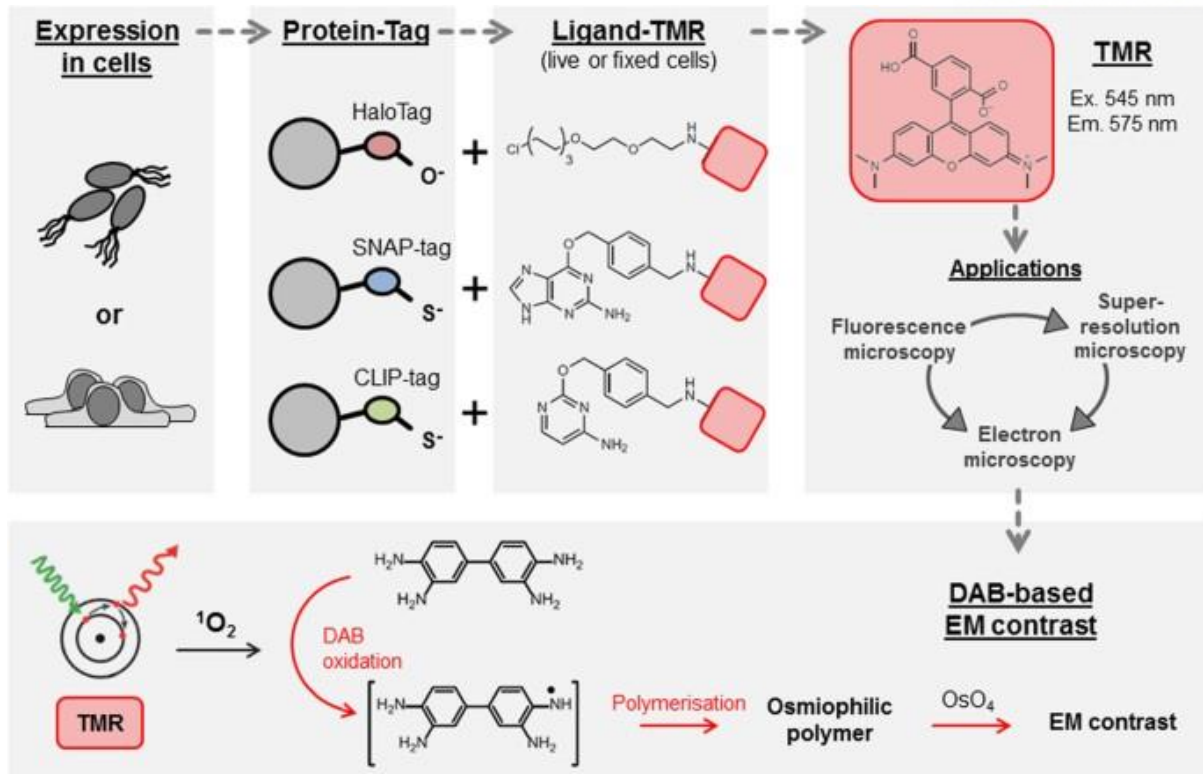


Figure 1.2 Examples of self-labeling tag systems and applications in microscopy.⁸

Visualization using Antibody-Antigen Interaction

Immunofluorescence is commonly used for visualization of target proteins based on antibody-antigen interaction. This method is preferred due to its high sensitivity and specificity toward its target. Generally, this method is based on two different antibodies – primary antibody and secondary antibody. The primary antibody binds to the target proteins itself or its epitope, followed by binding with fluorescent dye or enzyme conjugated secondary antibodies, which emit light at certain wavelength or reacts with the substrate to produce colored product, respectively (Figure 1.3A). Tyramide signal amplification (TSA) assay is one of the representative signal amplification methods for detecting low-abundant target molecules in various type of biological samples.^{15, 16} In this assay, biotin- or fluorophore-conjugated tyramide is activated by peroxidase, which is conjugated to secondary antibody. Phenolic group of the tyramide is catalyzed with hydrogen peroxide, and generated reactive tyramide radicals, which covalently binds to nearby tyrosine residues (Figure 1.3B).

1.1.2 Quantitation of Target Biomolecules

It is important to determine how much proteins exist in biological complex. That is measured as the concentration or the relative amount in quantity of proteins.

Immunoassays

Immunoassay is one of biochemical methods which use antibodies to detect the presence and concentration of target molecules in biological samples. The immunoassay is based on antigen-antibody interaction and utilize two different types of antibodies-primary antibody and secondary antibody. The purpose of primary antibody detects the target molecules with high binding affinity. The purpose of secondary antibody is to amplify the primary signal. Therefore, secondary antibodies are typically conjugated with signal amplifying enzymes such as horseradish peroxidases (HRP), which repeatedly convert inactive substrates to signal-generating active products.^{17, 18} HRP has various kinds of substrates such as 2,2' -azino-di-[3-ethylbenzthiazoline-6-sulfonic acid (ABTS), 3,3',5,5'-tetramethylbenzidine (TMB), which have been utilized in immunoassay, immunochemistry, and electro-analytical chemistry. As a result, they can generate considerable amplification of low primary signals in a concentration-dependent manner. Amplified signals can be quantitatively detected via colorimetric, fluorescent, and chemiluminescent measurements (Figure 1.4). Therefore, low-abundance biomolecules in biological samples are selectively detected and quantified by immunoassays.

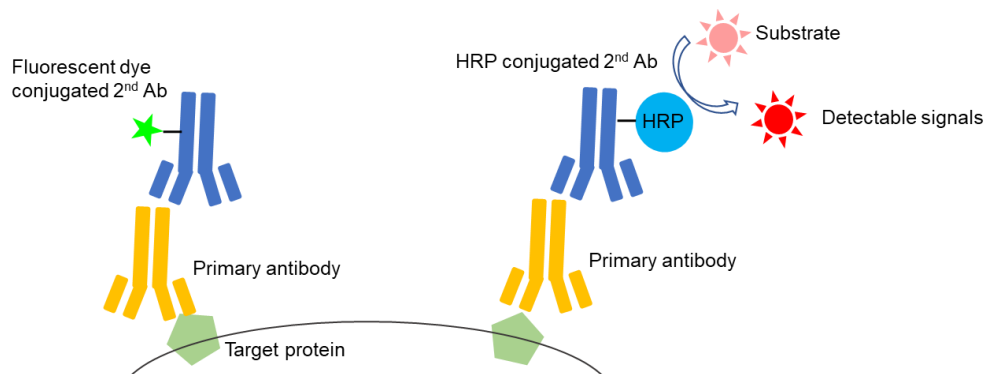


Figure 1.3 Immunofluorescence using antibody-antigen interaction

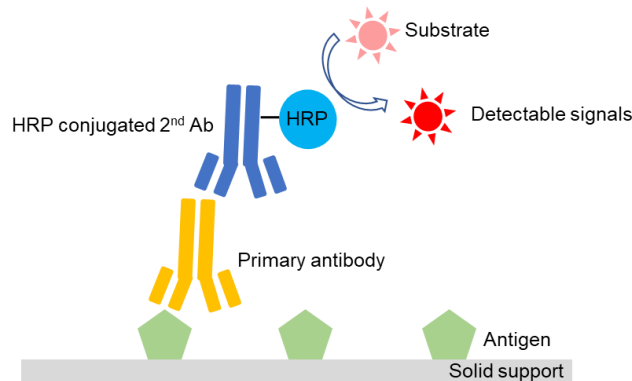


Figure 1.4 A example of immunoassay, enzyme-linked immunosorbent assay (ELISA)

1.2 Functional Proteins-based Nanoplatfoms

1.2.1 Protein cage nanoparticles

A wide range of nanoparticles have been developed as nanoscale delivery templates including liposomes,^{19, 20} micelles,^{21, 22} inorganic and polymeric nanoparticles,²³⁻²⁷ and protein cage nanoparticles,²⁸ for effective therapeutic and/or diagnostic reagents to the target sites *in vitro/in vivo*. Especially, protein cage nanoparticles, including virus-like particles,^{29, 30} P22 viral capsid,^{31, 32} and lumazine synthase,³³ are derived from nature, and have well-controlled structure, biocompatibility and solubility (Figure 1.5). They have a symmetric protein structure and are made up of identical subunits with a highly uniform size distribution, and their atomic resolution crystal structures have been investigated. They are stable to chemical and genetic modifications of their surface. Therefore, the exterior surfaces of protein cage nanoparticles could be modified for presenting various types of molecules including affinity tags, antibodies, fluorophore, and targeting peptides. They have been utilized as polyvalent nanoplatfoms for developing bioimaging probes and biosensor.

Encapsulin protein cage nanoparticles (Encap) is isolated from thermophile *Thermotoga maritima*.^{34, 35} They are self-assembled from 60 copies of identical subunit in a precisely controlled manner. Encap is developed as effective nanocarriers of antigenic peptides and therapeutic and/or diagnostic reagents using protein engineering. The exterior surfaces of Encap is displayed with hepatocellular carcinoma (HCC) cell binding peptide (SP94-peptides, SFSIIHTPILPL) through genetic insertion. SP94-peptide displaying Encap effectively and selectively targeted HepG2 cells, and was detected by fluorescent microscopy imaging.³⁴

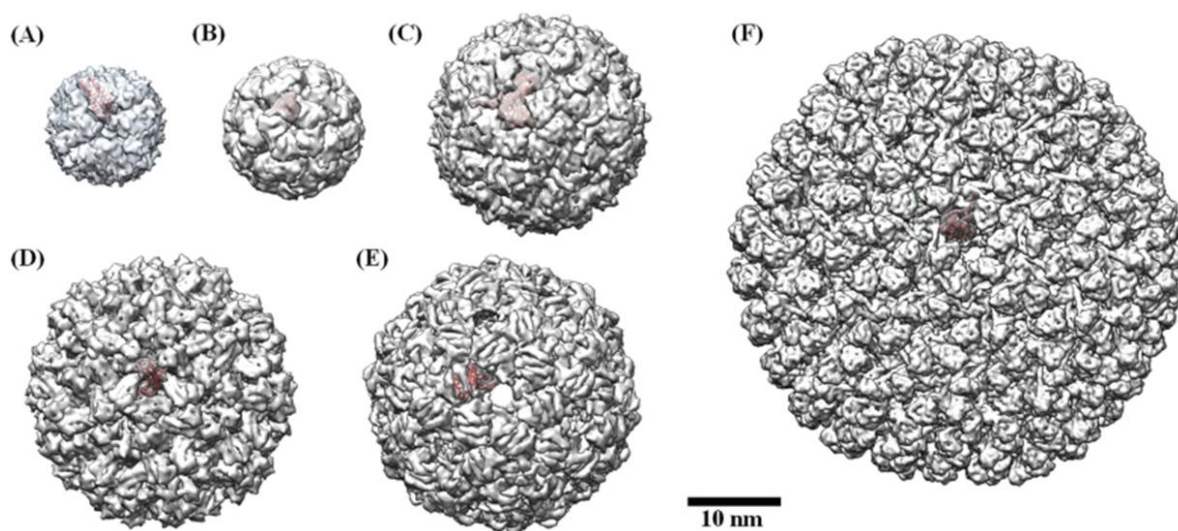


Figure 1.5 Surface diagram representations of various types of protein cage nanoparticles. (a) Ferritin (PDB:2JD6) (b) Lumazine synthase (PDB:1HQK) (c) Encapsuline (PDB:3DKT) (d) CCMV (PDB:1CWP) (e) bacteriophage Qβ (PDB: 1qbe) (f) bacteriophage P22 procapsid (PDB:3IYI)³⁶

1.2.2 Monomeric proteins

There are many types of monomeric proteins with their unique characteristics and functions (Figure 1.6). Recombinant fusion proteins could be genetically fused with two or more monomeric proteins by genetic engineering. They are applied in various biomedical research with high biocompatibility.

Fluorescent proteins for cancer cell imaging

Many fluorescent proteins were developed as reporter proteins to investigate protein localization and trafficking within the cells.³⁷ They have many advantages for biological researches. They are relatively small proteins, which can be easily fused to target proteins and do not interfere the function of target proteins. They are expressed without any toxicity in living cells. To visualize them, the light is only needed without the addition of exogenously added substrates. Green fluorescent protein (GFP) was first isolated from the jellyfish *Aequorea victoria*, and engineered to generate color mutants, such as blue fluorescent protein (BFP), cyan fluorescent protein (CFP), and yellow fluorescent proteins (YFP).

Scaffold proteins as the templates for chemical conjugation

Scaffold proteins play key roles in providing templates for chemical conjugation and complexation of them. Scaffold proteins have side chain to be covalently conjugated with chemical dye or ligands. Glutathione S-transferase (GST) has high affinity toward glutathione (GSH) and reactive cysteines which can form disulfide bonds with maleimide conjugated molecules through the maleimide – thiol reaction. On the other hand, scaffold proteins have a high affinity to its binder molecules. Monostreptavidin (mSA) has a high affinity for biotin and conjugates with biotinylated molecules.

Enzymes for signal amplification assay

Enzyme are proteins that accelerate chemical reactions with substrates. Heme peroxidases, such as ascorbate peroxidase-2 (APEX2), are well known as a powerful enzyme for proximity-labeling in biotechnology.³⁸ It can generate reactive singlet oxygens to activate dye molecules to label surrounding proteins. Proteomic mapping in live *Drosophila* tissues was established using an engineered ascorbate peroxidase.³⁹ Another useful enzyme is luciferase, which generates bright luminescence. Especially, nanoluciferase (Nanoluc) is a novel luciferase, which have enhanced stability, smaller size, and brighter luminescence intensity than other luciferases.⁴⁰

Affibody molecules for cancer cell targeting

In the late 90s and early 2000, advances in protein engineering technology resulted in the development of several non-antibody protein scaffold formats. Affibody molecules are monomeric

proteins consisting of three helical domains with small size of about 6.5 kDa. They can recognize their target molecules with high binding affinity and selectivity.⁴¹⁻⁴⁵ Since one of the first targets was HER2, which is overexpressed in the breast cancer cells,⁴¹ a variety of affibody molecules specific for target molecules have been generated by protein engineering. Compared to antibody, they have solubility and thermostability. They can also be produced in high yields in bacterial overexpression system, which means they can be genetically fused to any type of protein. These properties have contributed to promising antibody alternatives. Therefore, various recombinant fusion proteins with affibody have been applied in diagnostic and therapeutic studies.⁴³

Anti-IgG binding nanobody for primary antibody detection in signal amplification assay

Nanobody is also known as a camelid or shark-derived single-domain antibody, which composed of a single monomeric variable antibody domain. It is smaller in size compared to original antibody and has the potential to be produced as recombinant fusion proteins.⁴⁶⁻⁴⁸ It has also binding affinity to a specific target molecule. In particular, anti-IgG binding nanobodies were produced by phage display selections. They have binding affinity toward all mouse IgG subclasses and rabbit IgG and can be used as secondary antibody alternatives.⁴⁹

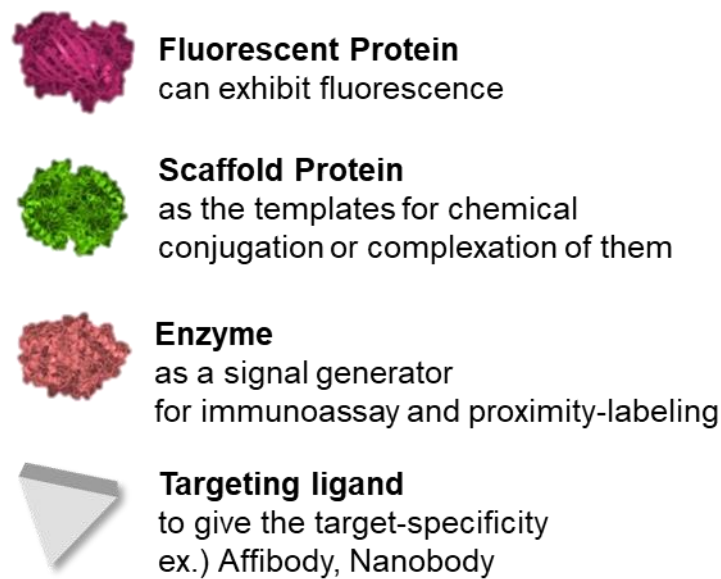


Figure 1.6 Schematic representation of various types of monomeric proteins.

1.2.3 Genetic Encoded Protein Tags

SpyTag/SpyCatcher (ST/SC) protein ligation system

Two different functional proteins can be physically linked by genetic engineering or post-translational ligation. As one of the post-translational ligation system, SpyTag/SpyCatcher protein ligation system was introduced as protein bioconjugation system.^{50, 51} SpyTag/SpyCatcher pair is derived by splitting the immunoglobulin-like collagen adhesion domain, so-called CnaB2, of *Streptococcus pyogenes*. SpyTag and SpyCatcher are 13 amino acid (AHIVMVDAYKPTK) polypeptide fragments and 15 kDa, respectively, and they spontaneously form a covalent isopeptide bond between residues Lys31 and Asp117 upon their recognition (Figure 1.7A). Ligation is reconstituted under a wide range of pH values, temperature, and in various detergents. SpyTag and SpyCatcher are reactive at the N-terminal, C-terminal and internal positions of a proteins. With this flexibility of SpyTag/SpyCatcher, SpyTag and SpyCatcher can be genetically fused to any type of protein and can be used *in vitro* and *in vivo* (Figure 1.7B).

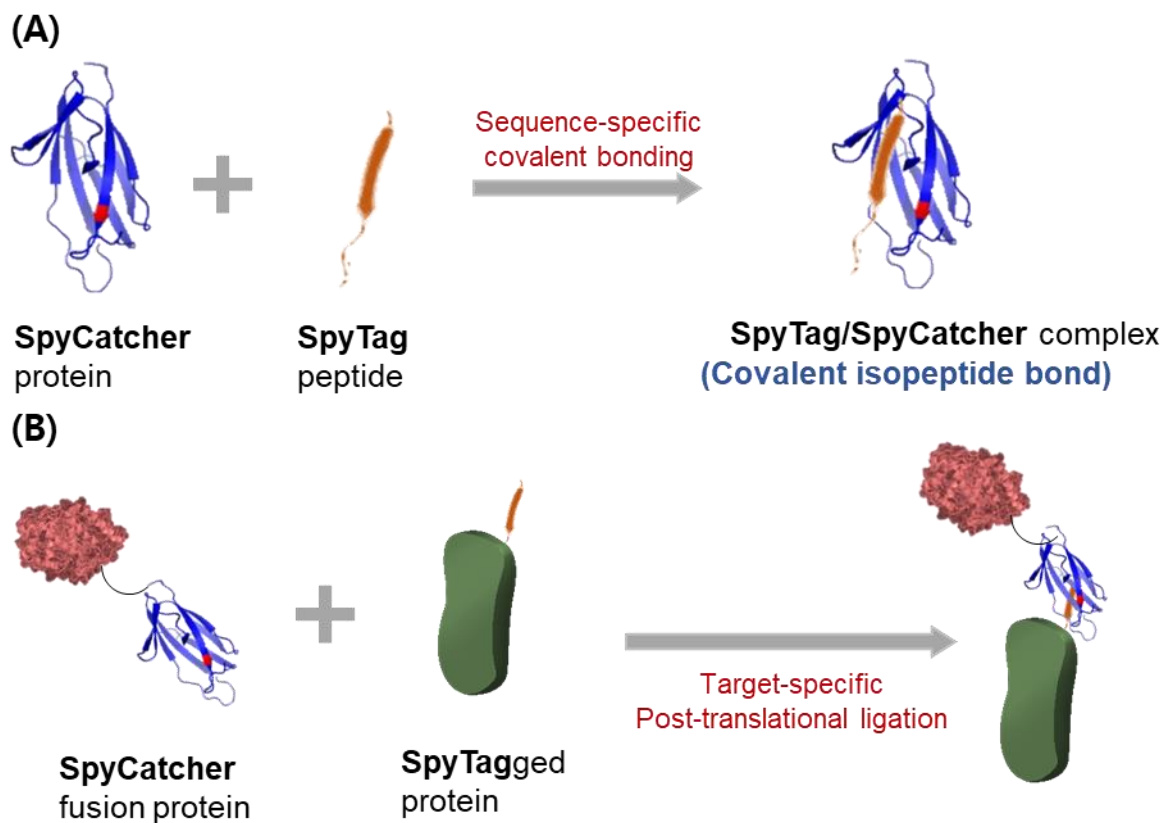


Figure 1.7 Cartoon of SpyTag/SpyCatcher protein ligation system. (A) Crystal structure of the SpyTag peptide, SpyCatcher protein and SpyTag/SpyCatcher complex.

1.3 Research Outline

1.3.1 Objective for the Thesis

In present research, many kinds of research suggest strategies to detect and visualize target molecules selectively. There are representative techniques in biomedical research. Fluorescence cell imaging is applied to visualize target molecules. Immunoassay is used to detect and quantify target molecules. These techniques are based on various types of molecules, which are fluorescent probes, labeling tag, and antibody.

The overall goal of this research thesis **is to develop target-specific labeling nanoplatfroms based on functional proteins for application in fluorescence cell imaging and immunoassay.** Protein-based labeling systems are recombinant proteins, which require low manufacturing costs and short preparation time with the *E.coli* overexpression system.

Lists of research project are followed:

- 1) Development of a target-specific fluorescent probes for fluorescence cell imaging
- 2) Development of a target-specific signal enhancer for immunoassays and TSA imaging.

1.3.2 Outline of the Thesis

The thesis begins with the introduction of the overall research in chapter 1. First of all, the importance of qualitative and quantitative analyses of target biomolecules in cells are explained. Next, various types of tools in current research were introduced for visualization or quantitation of target biomolecules. In addition, several advantages and application of functional proteins were discussed. With the objectives for the thesis, development of target-specific fluorescent probes for fluorescence cell imaging was described in chapter 2. Next, development of target-specific signal enhancer was described in chapter 3. Finally, summary and conclusions of this research thesis were proposed in chapter 4.

Chapter 2. Target-specific Fluorescent Probes for Fluorescence Cell Imaging based on Protein Cage Nanoparticles

2.1. Summary

Selective detection and effective visualization of specific target cells are essential but challenging. Fluorescence cell imaging with target-specific probes have been popularly utilized to visualize cell morphology and components and analyze cellular processes. Multi-displays of targeting ligands on a polyvalent single template could be applied as versatile multiplex fluorescent probes capable of individually visualizing two or more target cells without using separate individual probes. To implement this goal, one of protein cage nanoparticles, encapsulin, is used as a template and modified for dual targeting ability by displaying two different affibody molecules post-translationally. Encapsulin self-assembles in 60 identical subunits, forming a hollow and symmetric spherical structure of uniform size. SpyTag peptides were genetically fused to the surface of encapsulin, and a variety of proteins, such as fluorescent proteins and targeting affibody molecules, were genetically fused with SpyCatcher. Fluorescent proteins and affibody molecules were simultaneously labeled on a single encapsulin in a mixing-and-matching manner through bacterial superglue, SpyTag/SpyCatcher protein ligation system, post-translationally. We developed dual functional encapsulins as target-specific fluorescence cell imaging probes. We further established dual targeting protein cage nanoparticles by displaying two different affibodies onto encapsulin surface, which have been demonstrated to effectively recognize and bind to two individual targeting cells, visualizing them independently with selective colors on demand.

2.2. Introduction

Fluorescence cell imaging is typically applied to detect and visualize cell morphology and components and study cellular behaviors and responses derived from internal and/or external stimuli within biological systems.⁵² To precisely monitor the behaviors of specific cells, it is necessary to selectively label them with specific fluorescent probes. A wide range of target-specific fluorescent probes have been generated by combining fluorescent molecules with targeting ligands, including antibodies,⁵ targeting peptides,⁵³⁻⁵⁵ or affibody molecules.^{41, 42, 56, 57} Among them, affibody molecules are genetically engineered antibody mimics, which show high specificity and affinity for their targets. Affibody molecules have been applied for a wide range of biotechnology and therapeutic development in biomedicine with proven potential.^{42, 58-62} A combinatorial display of two or more affibody molecules on polyvalent platforms would allow for a dual or multiple targeting capabilities because each affibody molecule specifically recognizes and binds to its target cell. Protein cage nanoparticles are attractive polyvalent nanoplatforams for developing nanoscale bioimaging probes and biosensor components

because they have a well-defined symmetric hollow shell structure with uniform nanoscale particle sizes consisting of biomaterials, proteins.^{30, 63} They self-assemble in multiple copies of one or a few types of protein subunits in a precisely controlled manner. Their polyvalent characteristic often results in attachment of uniform multiple small ligands or chemicals to their surface genetically and/or chemically. Encapsulin (Encap) is a recently developed protein cage nanoparticle isolated from the thermophilic bacteria *Thermotoga maritima*.^{64, 65} We have previously developed Encaps as effective nanocarriers of antigenic peptides and therapeutic and/or diagnostic reagents using protein engineering.^{34, 66, 67} We have demonstrated that their genetic and chemical plasticity allows the simultaneous introduction of various oligopeptides genetically and diagnostic agents chemically at designated sites. Therefore, a single Encap can be given multiple functionalities simultaneously, such as targeting and probing functionalities. However, the genetic fusion of functional proteins onto protein cage nanoparticles often leads to misfolding of functional proteins and/or damage of self-assembly, and the chemical attachment of functional proteins to protein cage nanoparticles is only limited to tiny protein partners, and it is difficult to control their number and position.^{68, 69}

To circumvent these limitations, a recently developed bacterial superglue, the SpyTag/SpyCatcher (ST/SC) protein ligation system, was introduced in this research.⁵⁰ The protein ligation system covalently links two individually purified functional proteins together post-translationally by recognizing 15 kDa SC and 13 amino acid ST, which are genetically fused to corresponding partner proteins. SC and ST spontaneously form an irreversible isopeptide covalent bond upon recognition, and they can be genetically fused to any protein individually without a significant functional alteration of the fused proteins.^{70, 71}

In the current study, ST was genetically fused to the Encap surface loop region to construct tunable nanoplatfoms and simultaneously displayed multiple types of SC-fused functional proteins, either fluorescent proteins and affibody molecules or two different affibody molecules, in a mixing-and-matching manner (Figure 2.1). Using these tunable dual-functional Encap, we successfully demonstrated the targeting capability of dual-functional Encap with multiple combinations of targeting ligands and colors and the detecting ability of two different target cells with a single dual targeting Encap, which displays two different affibody molecules. Multiple display of functional proteins to polyvalent Encap was established using ST/SC in various ways on demand. These multiple functional Encap can simultaneously detect and visualize two or more target cells.

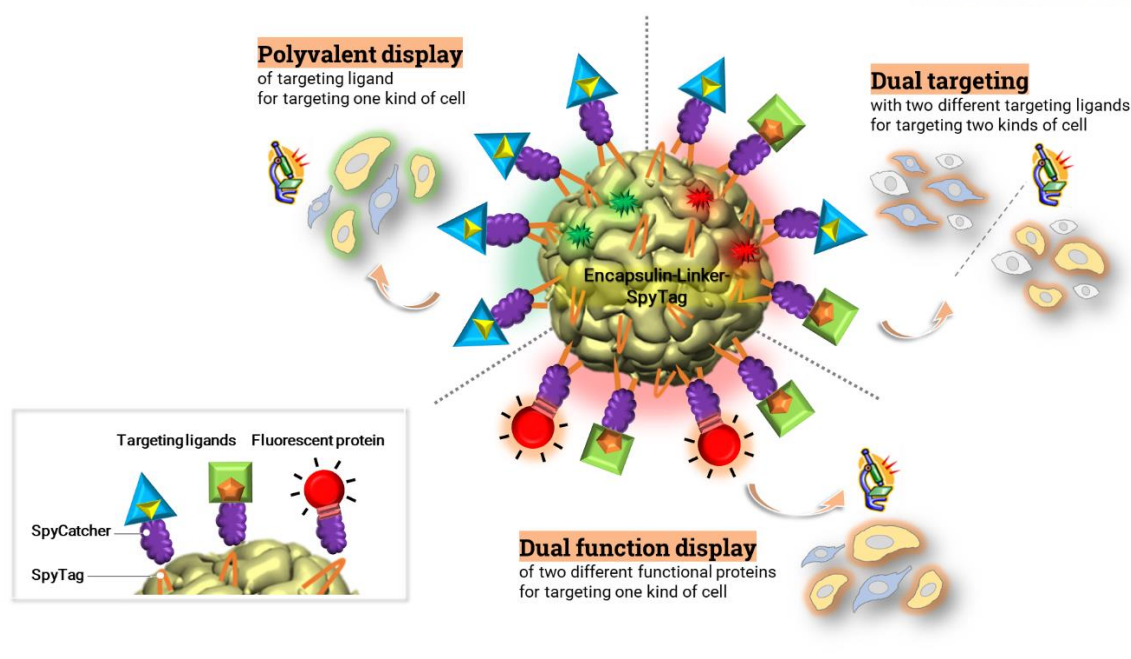


Figure 2.1 Schematic illustration of target-specific fluorescent probes. Functional proteins were multivalently displayed on Encapsulin post-translationally using bacterial glue to establish multiplex fluorescent cell imaging toolkits .

2.3. Materials and Methods

Genetic manipulation and purification of SC-fusion monomeric proteins and ST inserted Encap

SpyCatcher protein with extra amino acids was genetically fused to the C-termini of fluorescent proteins, mApple and eYFP (fluorescent proteins-SC), and N-termini of affibody molecules, HER2 and EGFR affibody molecules(SC-Afb), using established polymerase chain reaction (PCR) protocol with pETDuet based plasmids as a template.⁷⁰ The residues AHIVMVDAYKPTK with extra amino acids were genetically inserted between residues 138 and 139 (loop region) of encapsulin subunit by PCR with pET-30b based plasmids containing genes encoding encapsulin, which has only one exterior cysteine per subunit at position 123, as a template.³⁴ The amplified DNAs are transformed into competent *E. coli* strain BL21 (DE3), and the proteins were overexpressed. The *E. coli* cells containing resultant proteins were pelleted from 1.0 L of culture and were resuspended in 30 mL of phosphate buffer (50 mM sodium phosphate and 100 mM sodium chloride, pH 6.5). Lysozyme was added, and the solution was incubated for 30 min at 4°C. The suspension was sonicated for 10 min in 30 s intervals and subsequently centrifuged at 13000 g for 1 h at 4°C. SC fused monomeric proteins (fluorescent proteins-SC and SC-Afb) were purified with immobilized metal affinity chromatography (IMAC, 5 mL HisTrap FF column, GE HealthCare). SpyTag inserted encapsulin (Encap-L-ST) was purified with size exclusion chromatography (SEC) after heat precipitation for 20 min at 65°C.⁷²

Chemical conjugation of fluorescent dyes to Encap-L-ST

Thiol-reactive fluorescent dyes, such as fluorescein 5-maleimide (Thermo Scientific, 62245) and Alexa fluor 546 C5 maleimide (Thermo Scientific, A10258), were conjugated to Encap-L-ST, which has one outer cysteine per subunit.⁷³ Encap-L-ST was incubated with 5 mol equivalents of fluorescent dyes at room temperature with gentle shaking overnight. Free dyes were removed by dialysis with phosphate buffered saline (PBS) buffer overnight. The degree of fluorescent dye conjugation to Encap-L-ST was determined with UV/Vis spectrophotometer and ESI-TOF mass spectrometer. For mass analyses, each fluorescein-conjugated Encap (fEncap-L-ST and aEncap-L-ST) samples were loaded onto a MassPREP microdesalting column (Waters) and eluted with a gradient of 5-95% (v/v) acetonitrile containing 0.1% formic acid at a flow rate of 500 μ L/min.

Ligations of SC-proteins and Encap-L-ST

Concentrations of purified SC-proteins and Encap-L-ST were determined with either BCA assay or UV/Vis spectrophotometer. They were simply mixed with desired molar ratios and incubated for indicated time periods at room temperature with gentle shaking. Reaction resultants were analyzed with SDS-PAGE after adding SDS loading buffer and boiling at 110 °C. Ligations of SC-proteins and Encap-L-ST were further confirmed by measuring molecular masses of monomeric SC-Affibody molecules (SC-HER2Afb and SC-EGFRAfb) and reaction resultants (Encap:HER2Afb and Encap:EGFRAfb) with ESI-TOF mass spectrometer as described above. To characterize Encap protein cage architecture after ligations of SC-proteins, Encap ligated with a single type of SC-protein (Encap:HER2Afb, Encap:EGFRAfb, Encap:mApple and Encap:eYFP) and Encap with two different types of proteins (Encap:mApple:HER2Afb, Encap:mApple:EGFRAfb, Encap:eYFP:HER2Afb, and Encap:eYFP:EGFRAfb) were measured with size exclusion chromatography (SEC), dynamic light scattering (DLS), and transmission electron microscopy (TEM) analyses with the control sample.⁷⁴

Cell culture

SK-BR-3 was cultured in Dulbecco's modified Eagle's medium (DMEM) supplemented with 10% (v/v) fetal bovine serum (FBS) and 1% antibiotic-antimycotic. MCF-10A was cultured in DMEM/F12 (1:1) supplemented with 5% horse serum, 1% penicillin-streptomycin, hEGF (100ug/mL), hydrocortisone (1mg/mL) and insulin (10mg/mL). MDA-MB-468 was cultured in Leibovitz's L-15 medium with 10% (v/v) FBS, 1% antibiotic-antimycotic, 25mM HEPES and NaHCO₃. MCF-7 cells were cultured in RPMI-1640 supplemented with 5% FBS and 1% antibiotic-antimycotic. SK-BR-3, MCF-10A, MDA-MB-468 and MCF-7 cells were incubated in humidified atmosphere of 5% CO₂ and 95% air at 37 °C.

Fluorescent cell microscopic imaging

The cells (1×10^5 /well) were grown on microscope cover glass (18 mm Φ) in 12-well plate (SPL, 30012). Cells were fixed with 4% paraformaldehyde in PBS for 1 h and washed three times with PBS. To prevent non-specific binding of sample to the background, the blocking reagent (5% BSA, 5% FBS, and 0.5% Triton X-100 in PBS) was treated and incubated at room temperature for 1 h prior to sample treatment. After washing fixed cells three times with wash buffer (0.1% Triton X-100 in PBS), SC-ligated Encaps were added and they were incubated for 1 h at room temperature. Encaps without affibody molecules were also added separately as negative controls under the same condition. Before sealing, the cells were washed three times with wash buffer, and nuclei were stained with 4', 6-diamidino-2-phenylindole (DAPI). Images of samples were obtained by using Olympus Fluoview FV1000 fluorescent microscope (Olympus, UOBC).

2.4. Results and Discussion

ST Inserted Encap (Encap-L-ST) and SC-Fused Affibody molecules (SC-Afb) were constructed.

To polyvalently display affibody molecules as targeting ligands onto the Encap surface, we applied an ST/SC system.⁵⁰ A short and unfolded ST peptide (AHIVMVDAYKPTK) was genetically inserted into the surface loop region (at the position between subunit residues 138 and 139) of Encap-L-ST with extra residues (GGGGASASAS & ASASASGGGG) on both sides of each ST to provide conformational flexibility and to guarantee full access of their counterparts, SC-fused proteins. In the previously report, the loop regions are tolerable for peptide insertion of various lengths. As they are exposed on the Encap surface, they are accessible to other molecules.^{34, 67} On the other hand, SC is genetically fused to two different affibody molecules, EGFRfb and HER2fb, which selectively recognize and bind to epidermal growth factor receptor (SC-EGFRfb) and human epidermal growth factor receptor-2 (SC-HER2fb) on the surface of specific cancer cells, respectively.⁷⁰ SC-HER2fb and SC-EGFRfb were overexpressed in bacteria, purified with affinity chromatography, and their molecular masses were verified by an electrospray ionization time-of-flight mass spectrometer (ESI-TOF MS). The molecular masses of SC-HER2fb and SC-EGFRfb were measured at 21863.5 Da and 21704.0 Da, which correspond to the calculated molecular masses of each protein, 21864.6 Da and 21703.6 Da, respectively (Figure 2.2). Encap-L-ST has an external cysteine per subunit (60 cysteines per cage), and fluorescein-5-maleimide (F5M) was conjugated by a thiol-maleimide reaction and used as a fluorescent probe for fluorescent microscopic cell imaging.⁷⁵ Fluorescein conjugated Encap-L-ST (fEncap-L-ST) was examined by a mass spectrometer and a UV/Vis spectrophotometer. The molecular mass of the F5M treated Encap-L-ST subunit was measured at 33831.0 Da, which corresponds well to the sum (33833.2 Da) of the calculated Encap-L-ST subunit molecular masses (33405.8 Da) and F5M

(427.4 Da) (Figure 2.3). To quantify the molar ratio between the Encap subunit and F5M, a standard curve from the absorbance of different concentrations of free F5M molecules was acquired and the absorbance of fEncap-L-ST at 280 nm and 490 nm was measured, which represented the concentrations of the Encap subunit and F5M, respectively. The obtained molar concentrations translated to approximately 98% Encap subunits labeled with fluoresceins (Figure 2.3), indicating that almost every Encap-L-ST subunit was labeled with fluorescein.

Polyvalent fluorescently labeled Encap was ligated with affibody molecules using an ST/SC for target specific binding ability.

To investigate whether genetically fused SC-EGFRAfb or SC-HER2Afb can covalently attach to the surface of fEncap-L-ST through an SC/ST isopeptide bond formation, ST and SC were simply mixed and sampled at indicated times (Figure 2.4). Initially, either SC-EGFRAfb or SC-HER2Afb was mixed with fEncap-L-ST with the subunit ratio of 1:2 to consume all of the introduced SC-Afb (SC-EGFRAfb or SC-HER2Afb) and to avoid steric hindrance among ligated affibody molecules. A sodium dodecyl sulfate-polyacrylamide gel electrophoresis (SDS-PAGE) analyses of those reactions showed that the ligation between SC-Afb and fEncap-L-ST took almost 6 h to be completed (Figure 2.4), whereas that of monomeric SC-fused and ST-fused proteins was completed almost within 5 min in previous reports.^{70, 76} Previous studies suggested that the reactive aspartic acid of SC needs to be specifically aligned to facilitate ST with SC docking and to complete isopeptide formation²⁴. Therefore, the sheet formation of ST in the Encap loop region may be hindered and delayed quite a bit due to a steric constraint in the loop. ESI-TOF mass spectrometric analyses were performed to confirm isopeptide formation between SC and ST further. The molecular masses of the resulting ligation reactions were measured at 55678.0 Da (fEncap:HER2Afb) and 55516.5 Da (fEncap:EGFRAfb), respectively, which corresponded well to the calculated values of 55680.8 Da [21865.6 Da (SC-HER2Afb) + 33833.2 Da (fEncap-L-ST)–18 Da (H₂O)] and 55517.8 Da [21703.6 Da (SC-EGFRAfb) + 33833.2 Da (fEncap-L-ST)–18 Da (H₂O)] (Figure 2.2).

To evaluate the specific binding of each affibody molecule-ligated fEncap toward its target cells, we prepared two cancer cell lines, MDA-MB-468 and SK-BR-3 cells, which overexpressed EGFR and HER2 on their surfaces, respectively. We treated MDA-MB-468 and SK-BR-3 cells with fEncap:EGFRAfb and fEncap:HER2, respectively, and with fEncap-L-ST in parallel as negative controls and monitored them using fluorescent microscopy. Each ligated complex bound to their target cells efficiently (Figure 2.5, middle panels), whereas fEncap-L-ST without affibody molecules did not bind to either cell lines (Figure 2.5, top panels). Affibody molecule-ligated fEncap also did not bind to MCF-10A or MCF-7 cells, which do not overexpress HER2 and EGFR on their surfaces, respectively, (Figure 2.5, bottom panels), suggesting that fEncap-L-ST itself and the affibody molecule-ligated

fEncap do not bind to non-targeted cells significantly. These data indicated that polyvalently displayed affibody to Encaps effectively recognize their target cancer cells and selectively visualize them without any significant non-specific binding.

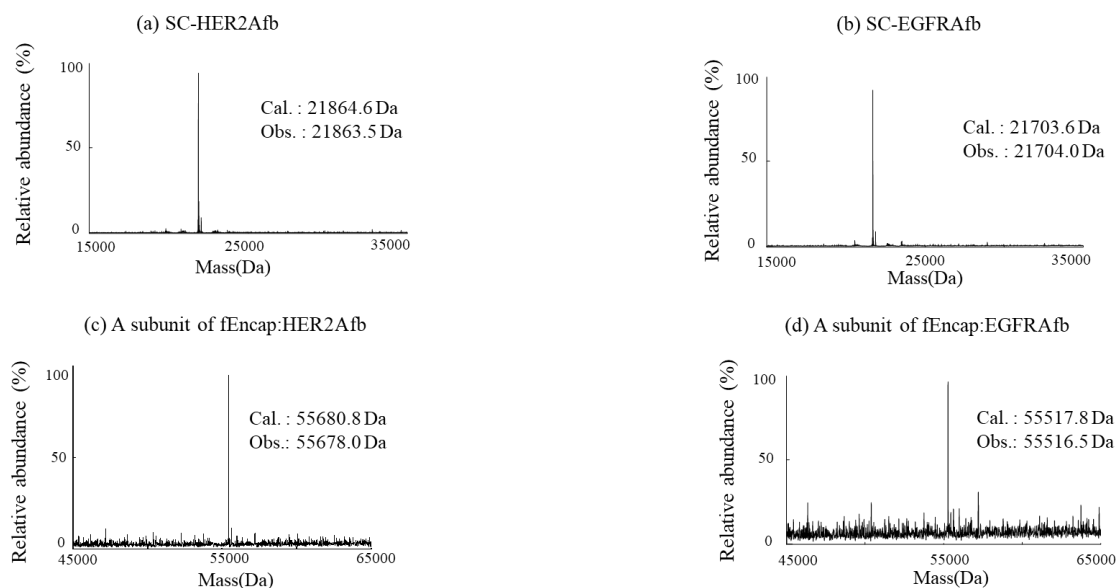


Figure 2.2 Molecular mass measurements of two different SC-Afbs. (a) SC-HER2Afb or (b) SC-EGFRAfb, and a subunit of reaction resultants of fEncap-L-ST and (c) SC-HER2Afb or (d) SC-EGFRAfb. Calculated and observed molecular masses are indicated.

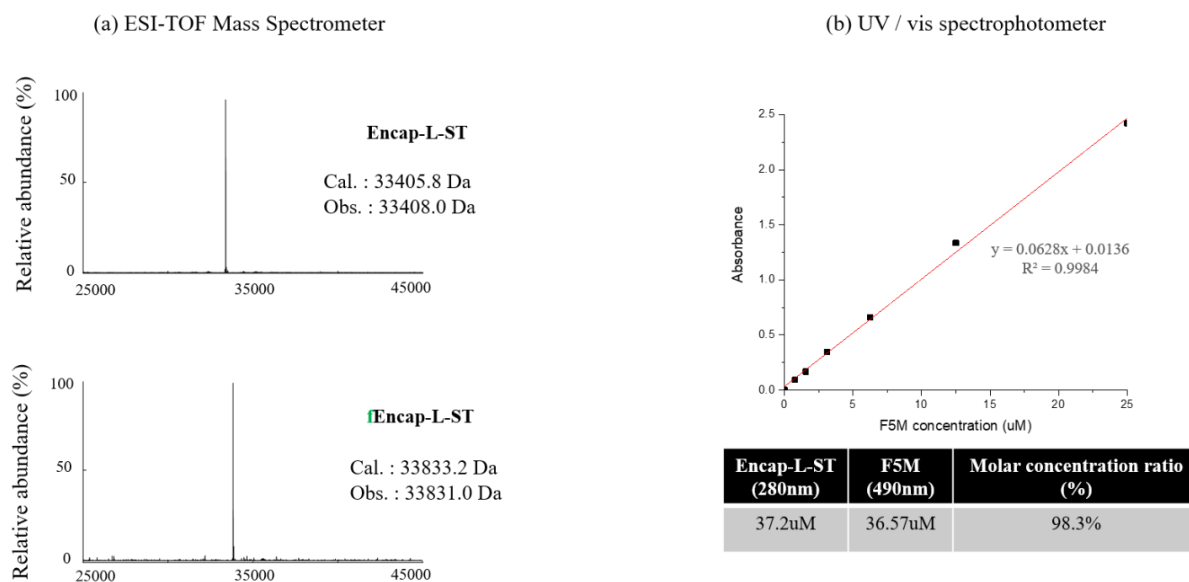


Figure 2.3 Characterization of fEncap-L-ST. (a) Molecular mass measurements of a subunit of Encap-L-ST (top) and fEncap-L-ST (bottom). Calculated and observed molecular masses are indicated. (b) The molar concentration ratio between Encap and fluorescein were measured by UV/ vis spectrophotometer.

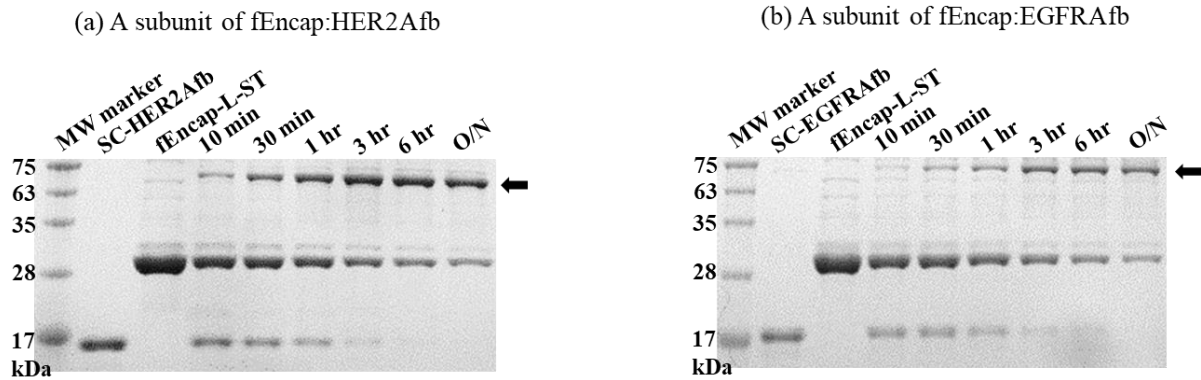


Figure 2.4 SDS-PAGE analyses of reaction results of SC-Afb and fEncap-L-ST. ST/SC ligation of (a) SC-HER2Afb and fEncap-L-ST and (b) SC-EGFRAfb and fEncap-L-ST was sampled at the indicated times, run on SDS-PAGE, and stained with Coomassie blue. Molecular weight markers were run together, and the apparent molecular weights are indicated (solid arrow indicates SC-Afb molecule-ligated fEncap (fEncap:HER2Afb or FEncap:EGFRAfb)).

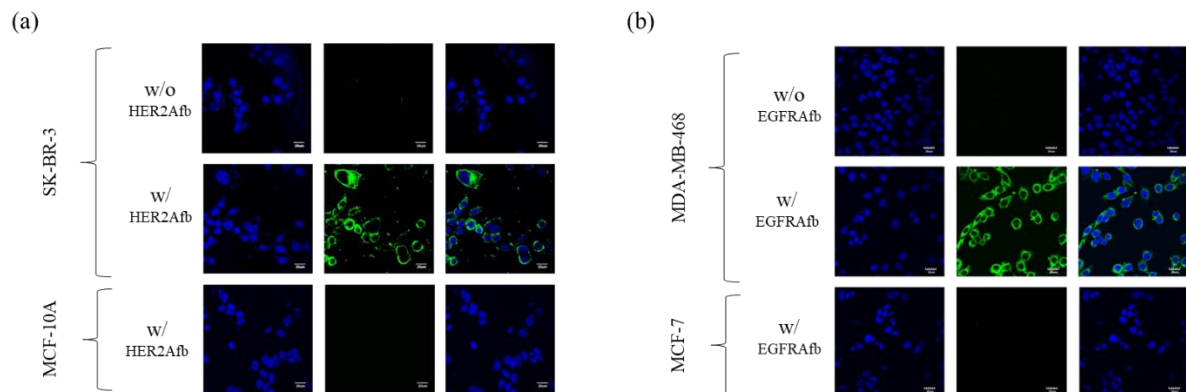
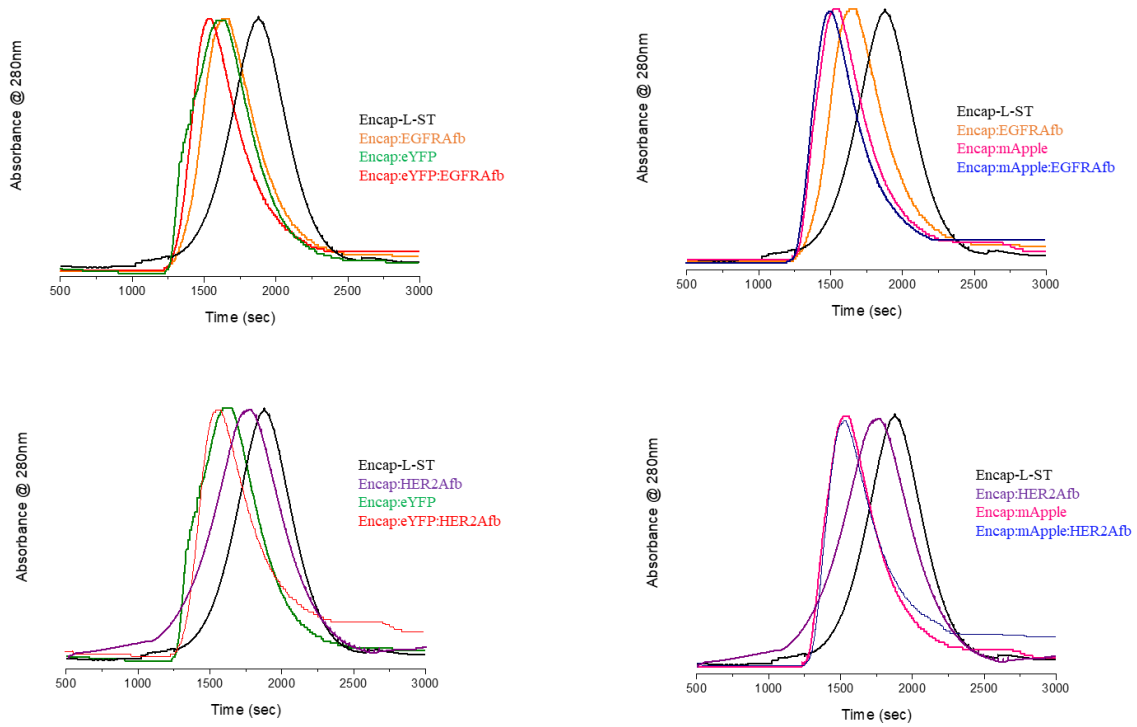


Figure 2.5 Fluorescent microscopic images with affibody molecule-ligated fEncap-L-ST. Various cancer cell lines are treated with (a) fEncap:HER2Afb and (b) fEncap:EGFRAfb. Cell lines and affibody molecules (with or without) are indicated on the left of the image panels. Nuclei are stained with DAPI (blue, left panels). Fluoresceins are visualized in green (middle panels). Scale bar = 20 μm .

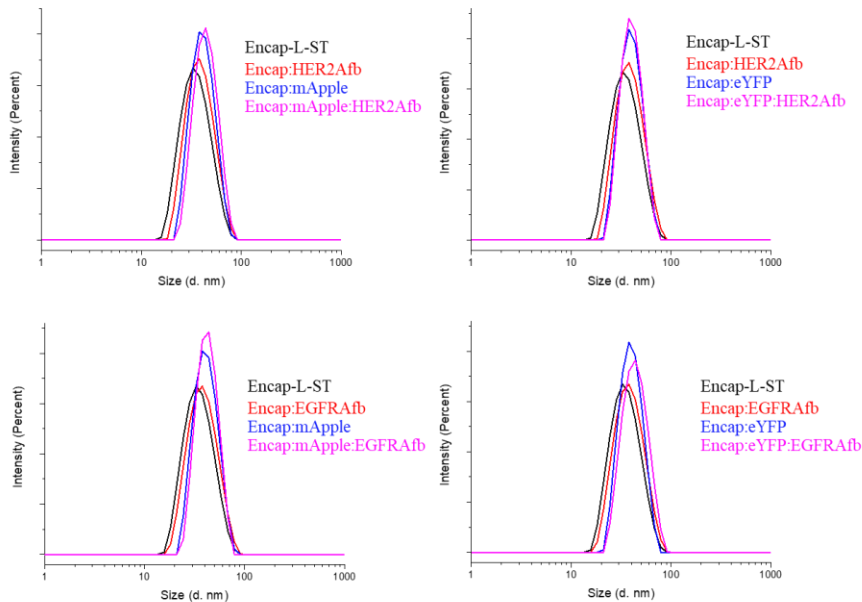
Multiple functional proteins were effectively displayed on the surface of Encap by ST/SC.

To investigate whether two different functional proteins can be displayed on the surface of Encap-L-ST, we selected two different fluorescent proteins, mApple and eYFP, as fluorescent probes. SC was genetically fused to the C-termini of fluorescent proteins mApple (mApple-SC) or eYFP (eYFP-SC) with extra amino acids as a linker. We previously demonstrated that SC-fused monomeric proteins could be easily ligated with ST-fused monomeric proteins.⁷⁰ To display both fluorescent proteins and affibody molecules simultaneously on the surface of Encap, we simply mixed the same amount of fluorescent protein-SC (mApple-SC or eYFP-SC) with the SC-Affibody molecule (SC-HER2Afb or SC-EGFRAfb) in a mixing-and-matching manner with Encap-L-ST. There are four combinations of multiple functional protein ligated Encap (Encap:mApple:HER2Afb, Encap:mApple:EGFRAfb, Encap:eYFP:HER2Afb, and Encap:eYFP:EGFRAfb, respectively). We performed size exclusion chromatography (SEC), dynamic light scattering, and transmission electron microscopy (TEM) analyses for characterization of functional protein ligated Encap. Encap ligated with a single protein type (Encap:HER2Afb, Encap:EGFRAfb, Encap:mApple and Encap:eYFP) or with two different types of proteins (Encap:mApple:HER2Afb, Encap:mApple:EGFRAfb, Encap:eYFP:HER2Afb and Encap:eYFP:EGFRAfb) were eluted slightly earlier than Encap-L-ST in SEC (Figure 2.6a), and their hydrodynamic diameters (36.68, 35.26, 39.12, 38.15, 42.26, 40.86, 38.69, and 41.50 nm, respectively) were also correspondingly larger than that of Encap-L-ST (32.59 nm) (Figure 2.6b). TEM images of negatively-stained SC-protein-ligated Encap confirmed their intact cage architecture and smudged extra densities at the exterior area, indicating that SC-proteins were well displayed on the Encap surface (Figure 2.6c). These results indicate that simultaneous ligations of fluorescent protein-SC and SC-Afb onto the surface of Encap-L-ST at defined ratios do not cause any significant alteration to the Encap protein cage architecture. To evaluate the tolerance of ligation amounts of SC-proteins to the surface of Encap-L-ST, we tested three different input ratios of SC-proteins to subunits of Encap-L-ST; 1:1:6 [10 fluorescent protein-SCs and 10 SC-affibody molecules per an Encap-L-ST (60 subunits per cage)] (Figure 2.7a, 2.7d, 2.7g, and 2.7j, Encap:mApple:HER2Afb, Encap:eYFP:HER2Afb, Encap:mApple:EGFRAfb, and Encap:eYFP:EGFRAfb, respectively), 2:2:6 (Figure 2.7b, 2.7e, 2.7h, and 2.7k), or 3:3:6 (Figure 2.7c, 2.7f, 2.7i, and 2.7l) and estimated the degree of covalent conjugations among them with SDS-PAGE (Figure 2.7). Most of the added SC-proteins were covalently attached to Encap-L-ST. However, reactions of 3:3:6 generated a noticeable amount of protein aggregation, probably due to the steric hindrance of ligated SC-proteins on the Encap surface. To avoid this aggregation issue but maximize functionality, we hereafter used the reaction results of 2:2:6 (Figure 2.8) for further studies. These data showed the maintenance of their integrity and function after the ST/SC ligation and approximately 20 affibody molecules and 20 fluorescent proteins per Encap can be sufficiently displayed for efficient targeting and fluorescence signals.

(a) SEC



(b) DLS



| | Z-Ave (d.nm) |
|----------------------|--------------|
| Encap-L-ST | 32.59 |
| Encap:HER2afb | 36.68 |
| Encap:EGFRafb | 35.26 |
| Encap:mApple | 39.12 |
| Encap:eYFP | 38.15 |
| Encap:mApple:HER2afb | 42.26 |
| Encap:mApple:EGFRafb | 40.86 |
| Encap:eYFP:HER2afb | 38.69 |
| Encap:eYFP:EGFRafb | 41.50 |

(c) TEM

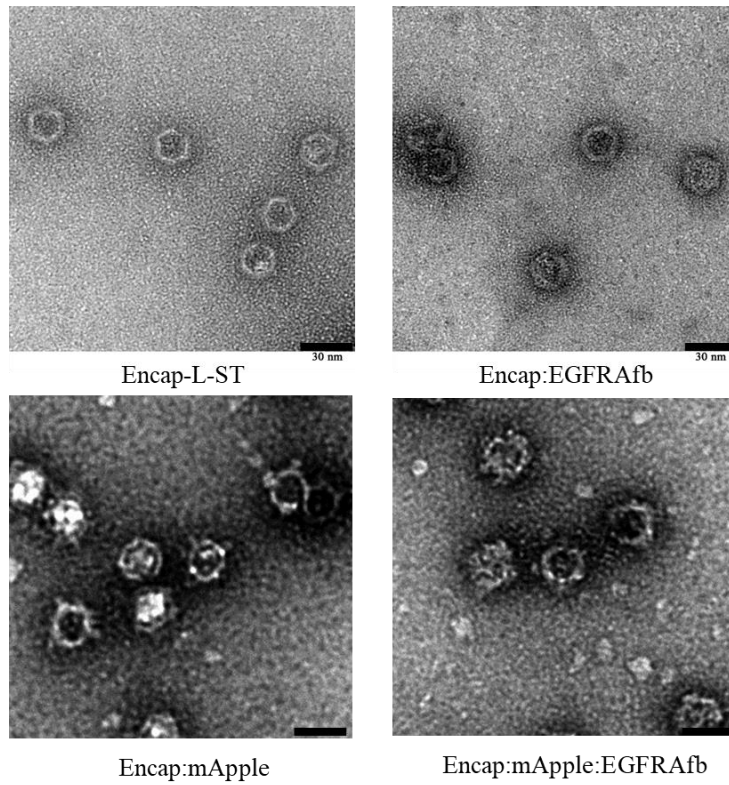


Figure 2.6 Characterizations of SC-proteins ligated Encap. (a) Size exclusion elution chromatographic profiles (b) dynamic light scattering measurements and (c) transmission electron microscopic images.

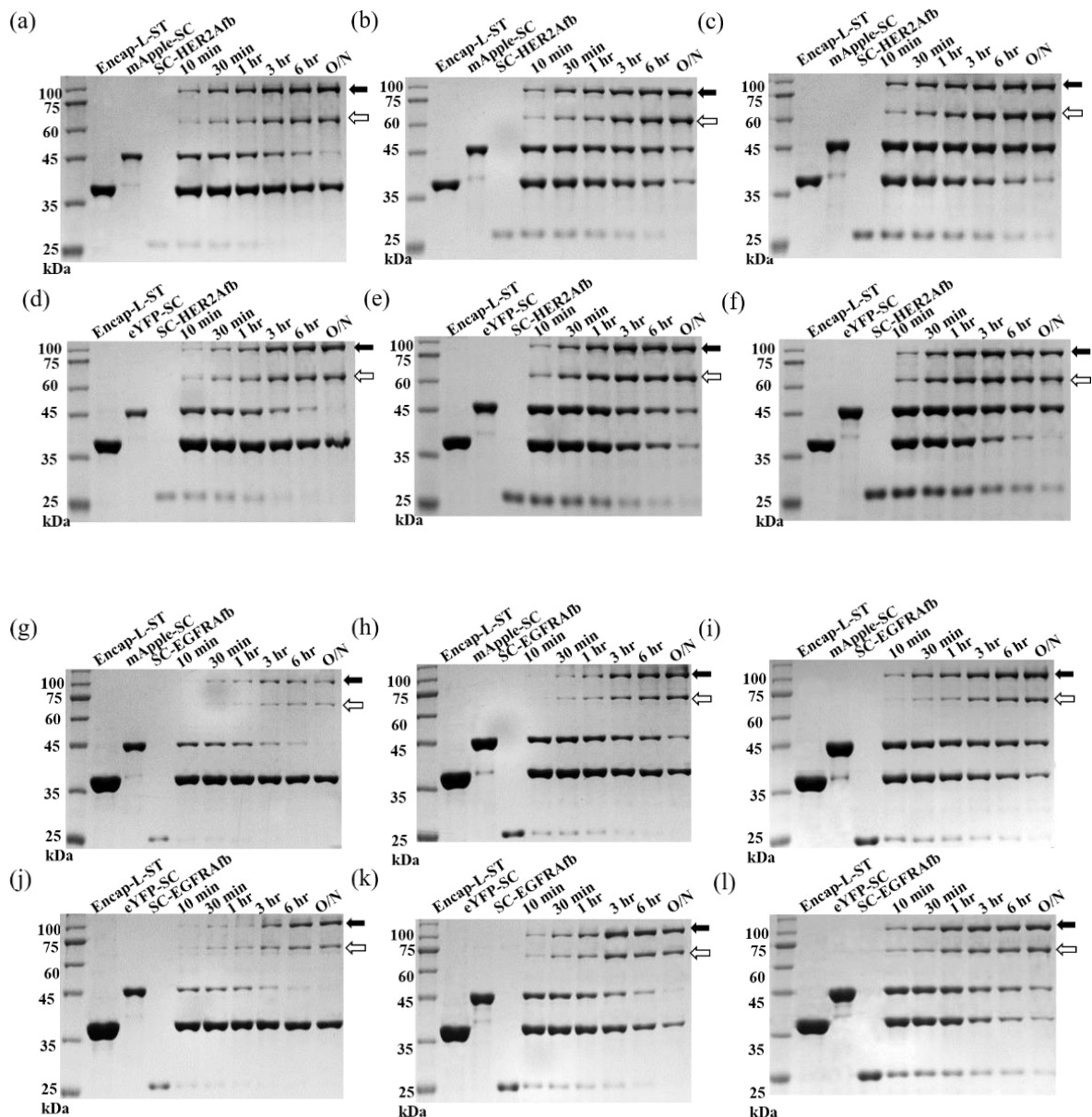


Figure 2.7 Optimization of input ratio of SC-proteins to subunit of Encap using SDS-PAGE. (a, d, g and j) 1:1:6 [10 fluorescent protein-SC and 10 SC-Afb molecule per an Encap-L-ST (60 subunits per cage), Encap:mApple:HER2Afb, Encap:eYFP:HER2Afb, Encap:mApple:EGFRAfb, and Encap:eYFP:EGFRAfb, respectively], (b, e, h and k) 2:2:6 (c, f, i and l) 3:3:6. Solid arrow indicates fluorescent protein-SC ligated Encap (Encap:mApple or Encap:eYFP). Blank arrow indicated SC-Afb molecule ligated Encap (Encap:HER2Afb or Encap:EGFRAfb). Reactions were sampled at indicated times, run on SDS-PAGE, and stained with Coomassie blue. Molecular weight markers were run together, and apparent molecular weights are indicated.

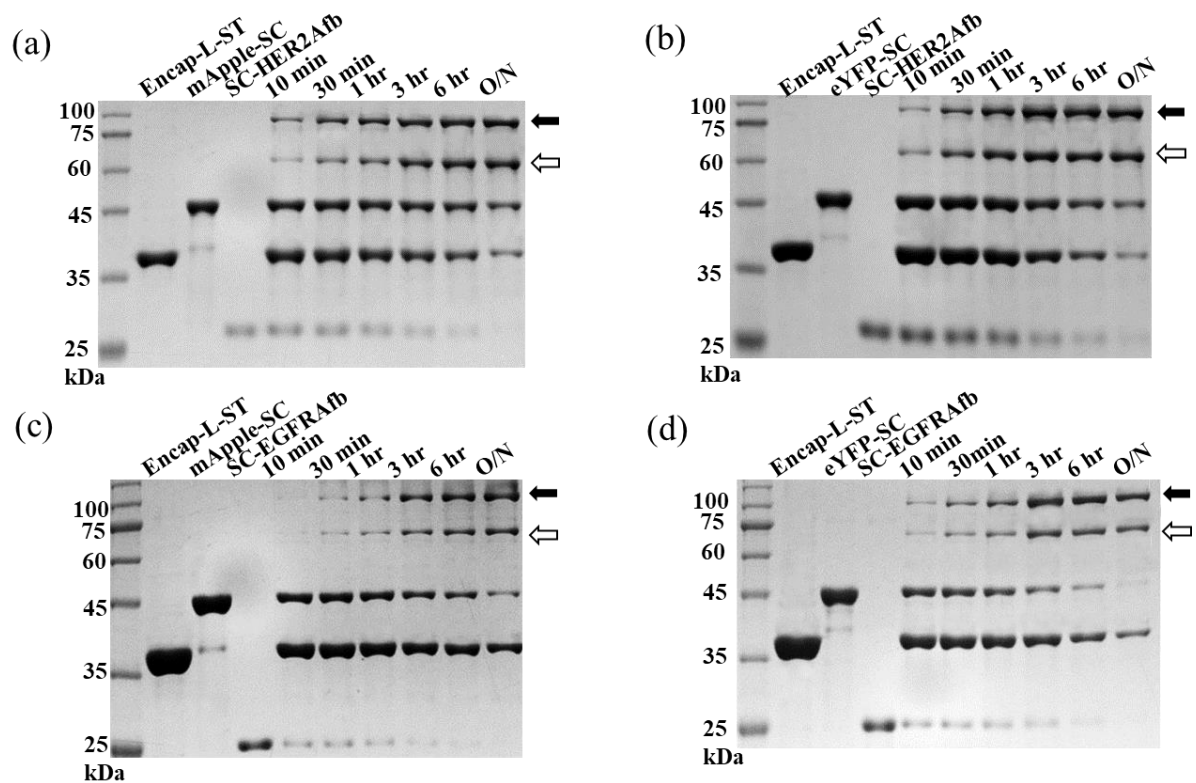


Figure 2.8 SDS-PAGE analyses of reaction results of SC-proteins and Encap. ST/SC ligation of (a) Encap:mApple:HER2Afb, (b) Encap:eYFP:HER2Afb, (c) Encap:mApple:EGFRAfb, and (d) Encap:eYFP:EGFRAfb. The input ratio of SC-protein to Encap is 2:2:6 [20 fluorescent protein-SC and 20 SC-affibody per Encap-L-ST (60 subunits per cage)]. Reactants were sampled at the indicated times, run on SDS-PAGE, and stained with Coomassie blue. Molecular weight markers were run together, and the apparent molecular weights are indicated (solid arrow indicates fluorescent protein-SC-ligated Encap (Encap:mApple or Encap:eYFP); blank arrow indicated SC-Afb molecule ligated Encap (Encap:HER2Afb or Encap:EGFRAfb)).

Dual functional Encap showed specific binding to their target cancer cells.

To evaluate the capability of targeted cell imaging of dual-functional Encap, we prepared two different target cancer cells, MDA-MA-468 and SK-BR-3, and treated four different combinations of dual-functional Encap (Encap:mApple:HER2Afb, Encap:eYFP:HER2Afb, Encap:eYFP:EGFRAfb, and Encap:eYFP:EGFRAfb) to them for fluorescence microscopic cell imaging, as previously described. SC-HER2Afb ligated dual functional Encap (Encap:mApple:HER2Afb and Encap:eYFP:HER2Afb) selectively bound to SK-BR-3 cells with red and yellow colors, respectively. Similarly, dual-functional Encaps with SC-EGFRAfb (Encap:mApple:EGFRAfb and Encap:eYFP:EGFRAfb) also selectively bound to their target, MDA-MB-468 cells, with corresponding fluorescent colors (Figure 2.9), whereas Encap without affibodies did not bind to target cancer cells, consistent with previous results (Figure 2.5). Furthermore, neither of the dual functional Encaps bound to HER2 negative MCF 7 cells or EGFR negative MCF 10A cells. These data indicate simultaneous targeting and visualizing with dual functional Encap with multiple combinations between desired targeting ligands and desired colors. This approach provides the opportunity for various Encap functionalities by ST/SC protein ligation on demand.

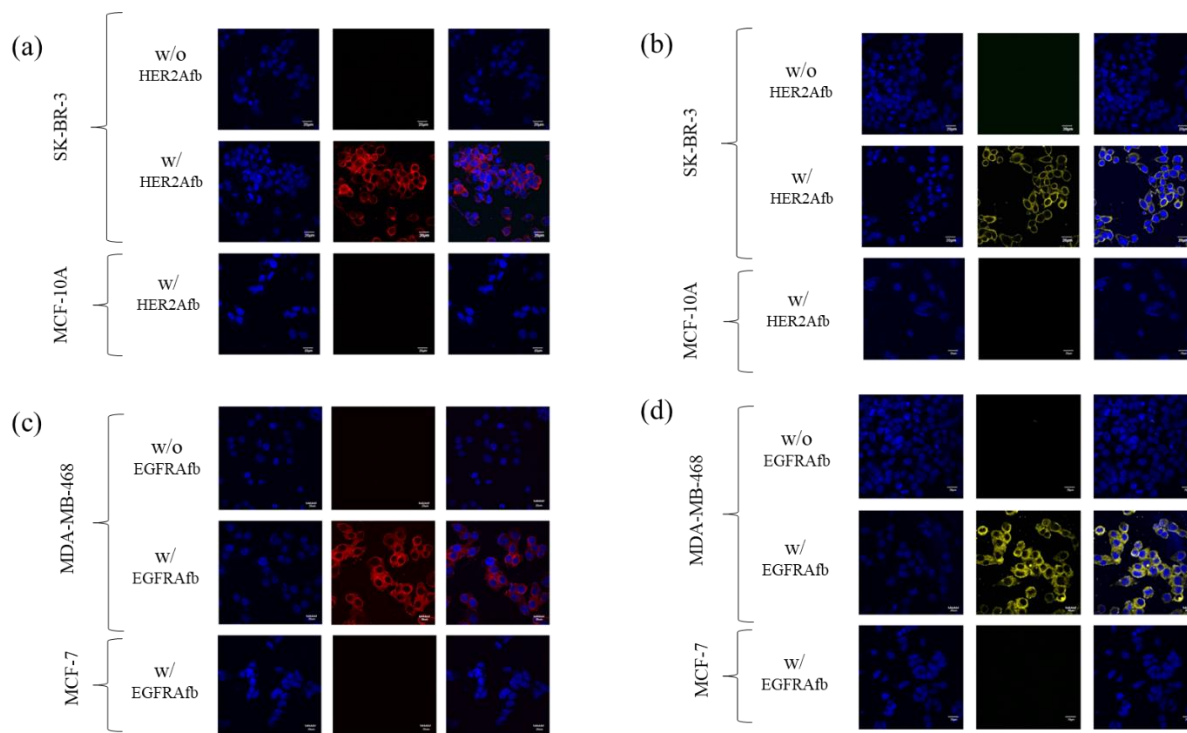


Figure 2.9 Fluorescent microscopic images of with dual functional Encap. Various cancer cell lines are treated with (a) Encap:mApple:HER2Afb, (b) Encap:eYFP:HER2Afb, (c) Encap:mApple:EGFRAfb, and (d) Encap:eYFP:EGFRAfb. Cell lines and affibody molecules used are indicated on the left of the image panels. Nuclei are stained with DAPI (blue, left panels). mApple and eYFP are visualized in red and yellow, respectively (middle panels). Scale bar = 20 μ m.

Two different targeting ligands ligated Encap was applied for dual targeting imaging.

Two different affibody molecules were polyvalently displayed to fluorescent dye-labeled Encap-L-ST. Before dual targeting imaging to give a dual-targeting capability to a single Encap probe. We checked the possibility of cross-targeting among affibody molecule-ligated Encap. First, we prepared either green fluorescent dye, F5M, or red fluorescent dye, Alexa fluor 546 maleimide to construct fluorescently labeled Encap-L-STs (fEncap-L-ST and aEncap-L-ST). Encap-L-ST was labeled with Alexa fluor 546 maleimide, and all Encap-L-ST subunits were also labeled with an Alexa fluor 546 maleimide (Figure 2.10), the same as those of F5M. fEncap-L-ST and aEncap-L-ST were subsequently ligated with SC-HER2Afb and SC-EGFRAfb, respectively, to form fEncap:HER2Afb and aEncap:EGFRAfb (Figure 2.11a). To check the cross-targeting possibility of fEncap:HER2Afb and aEncap:EGFRAfb, we treated SK-BR-3 and MDA-MB-468 cells with fEncap:HER2Afb and aEncap:EGFRAfb (Figure 2.12a and 2.12b), respectively, or aEncap:EGFRAfb and fEncap:HER2Afb (Figure 2.12c and 2.12d), respectively. As expected, green fluorescence only appeared in fEncap:HER2Afb-treated SK-BR-3 cells targeted by HER2Afb (Figure 2.12a), and red only appeared in aEncap:EGFRAfb-treated MDA-MB-468 cells, which are targeted by EGFRAfb (Figure 2.12b). These results imply that each affibody molecule-ligated Encap selectively recognizes its target cells and tightly binds them without any significant cross-targeting events.

For multiplex cell imaging, we treated fluorescently labeled Encap-L-ST with two different SC-Afbs (SC-HER2Afb and SC-EGFRAfb) to visualize two or more target cells (Figure 2.11b). Encap-L-ST chemically conjugated with one type of fluorescent dye (fEncap or aEncap) was ligated with both SC-HER2Afb and SC-EGFRAfb simultaneously as a master key to open multiple locks (to visualize multiple target cells with a fluorescent probe) (fEncap:HER2Afb:EGFRAfb or aEncap:HER2Afb:EGFRAfb). Each target cell was detected by the color corresponding to the labeled dye (Figure 2.12e and 2.12f) compared with the negative control cell line, HEK293T (Figure 2.13). Together, these results suggest that Encap-L-ST can serve as a multivalent template by efficiently displaying two or more different targeting ligands and can be used to detect two or more target cells simultaneously on demand by a novel protein ligation system, ST/SC.

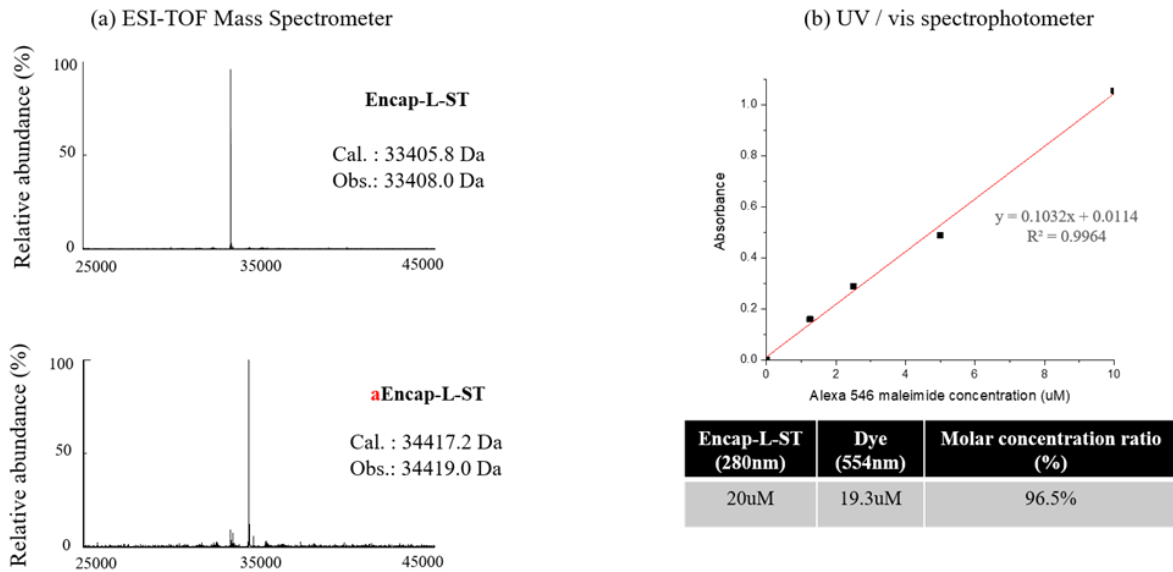


Figure 2.10 Characterization of aEncap-L-ST. (a) Molecular mass measurements of a subunit of Encap-L-ST (top) and aEncap-L-ST (bottom). Calculated and observed molecular masses are indicated. (b) The molar concentration ratio between Encap and fluorescein were measured by UV / vis spectrophotometer.

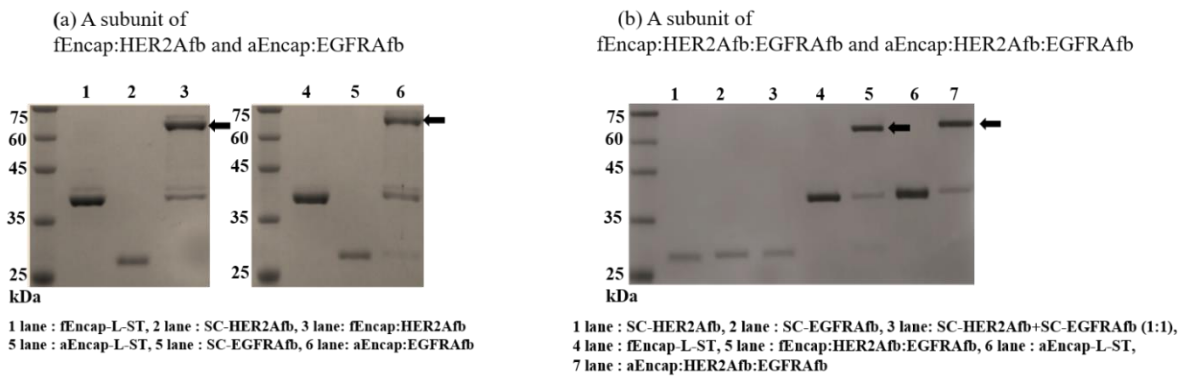


Figure 2.11 Characterization of reaction products for fluorescent microscopic images using SDS-PAGE. Solid arrows indicate (a) fEncap:HER2Afb for Figure 2.12a and 2.12c (left) and aEncap:EGFRAfb for Figure 2.12b and 2.12d (right). (b) fEncap:HER2Afb:EGFRAfb and aEncap:HER2Afb:EGFRAfb for Figure 2.12e and 2.12.

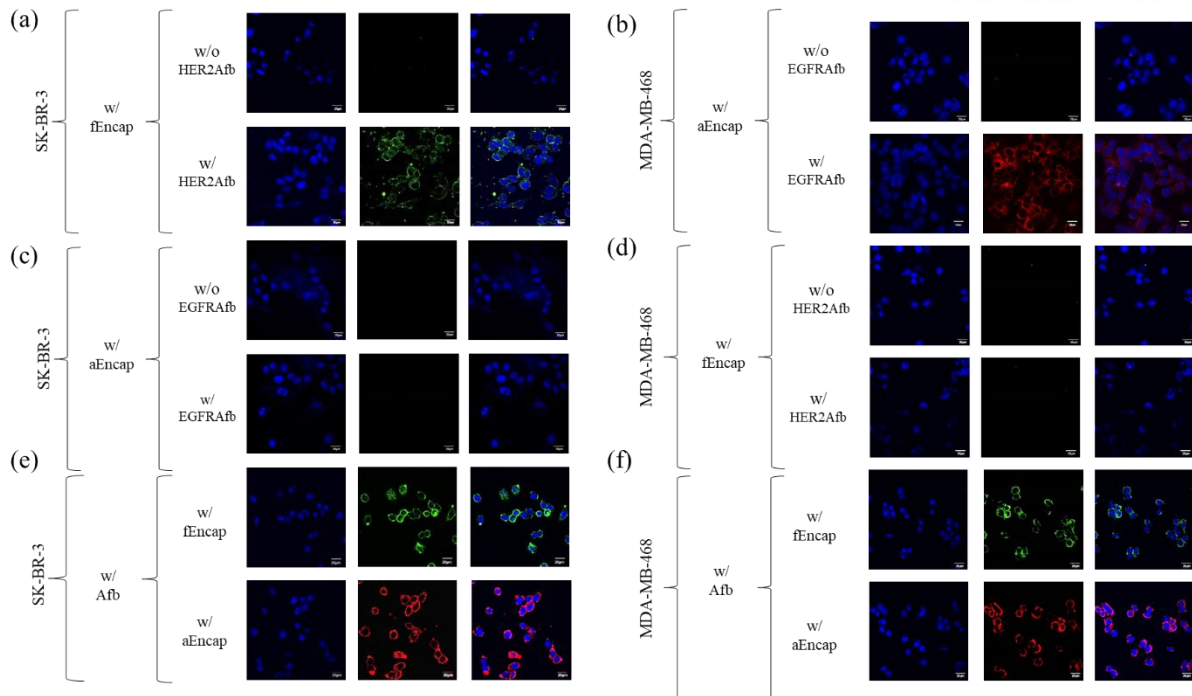


Figure 2.12. Fluorescent microscopic images with dual targeting Encap. Various cancer cell lines are treated with (a) fEncap:HER2Afb, (b) aEncap:EGFRAb, (c) aEncap:EGFRAb, (d) fEncap:HER2Afb (e and f) fEncap:HER2Afb:EGFRAb (top), and aEncap:HER2Afb:EGFRAb (bottom). Cell lines, affibody molecules, and fluorescently-labeled Encap are indicated on the left of the image panels. Nuclei are stained with DAPI (blue, left panels). Fluoresceins are visualized in green or red (middle panels). Scale bar = 20 μm .

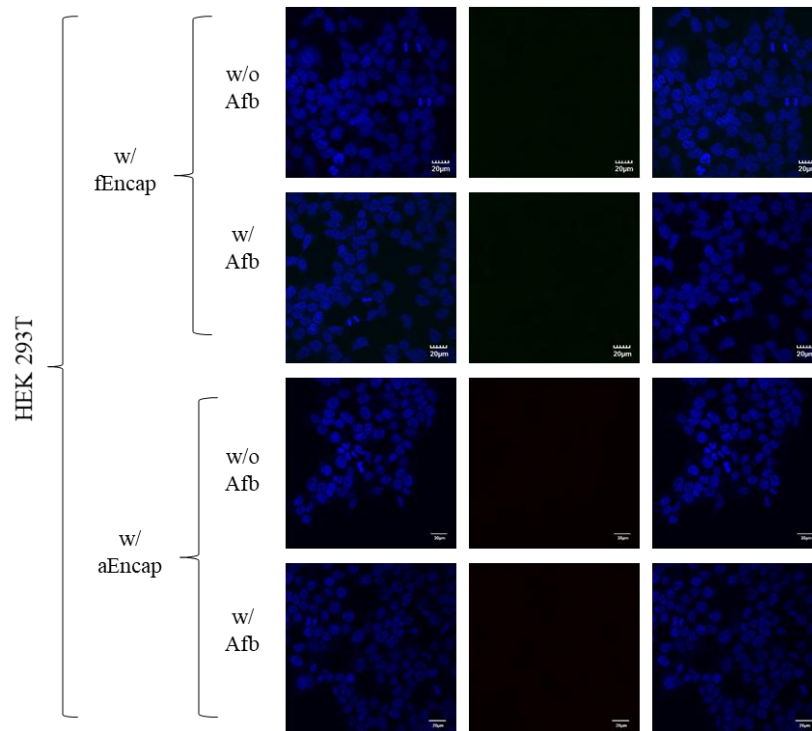


Figure 2.13. Fluorescent microscopic images of HEK293T cells treated with dual targeting Encap. Affibodies and fluorescein labeled Encap are indicated on the left of image panels. Nuclei are stained with DAPI (blue, left panels). Scale bar = 20 μm.

2.5. Conclusion

Here, a tunable dual-functional (targeting and probing or two different targetings) Encap protein cage nanoparticle was established using bacterial superglue, ST/SC, and its target-specific imaging capability was demonstrated with multiple combinations of targeting ligands and colors. Encap surface with symmetric cage structure was displayed with ST peptides polyvalently by genetic engineering. On the other hand, various fluorescent proteins and affibody molecules were genetically fused to SC-protein and prepared independently. SC-fused fluorescent proteins (mApple-SC or eYFP-SC) and affibody molecules (SC-EGFRAfb or SC-HER2Afb) were simultaneously displayed on the Encap-L-ST surface via a covalent isopeptide formation between ST and SC, and they were successfully demonstrated as combinatorial target-specific fluorescent probes. Dual targeting Encap probes were further constructed by displaying two different affibody molecules on their surface, and they visualized two target cells individually without using a set of individual probes. The polyvalent nature of Encap allowed us to display multiple functional proteins efficiently, and ST/SC bacterial glue made it possible to post-translationally display the desired functional proteins in a mixing-and-matching manner on demand. The approach we described here can be applied to other protein cage nanoparticles, protein oligomers, protein binding partners, and other functional proteins and may provide new opportunities to develop novel multifunctional delivery nanoplatforms and multifunctional complementary nanoscale building blocks for high-ordered functional nanostructures.

Chapter 3. Target-specific Signal Amplifiers for Immunoassays

3.1 Summary

Commercial secondary antibodies for immunoassays are usually produced by live animals or expensive mammalian cell culture systems. These antibodies are then conjugated with enzymes that amplify low-abundant target molecules' signal in a concentration-dependent manner, which repeatedly converts inactive substrates to signal-generating active products. In this study, we developed recombinant immunoglobulin G (IgG)-binding nanobody-based signal amplifiers using a well-established SpyTag/SpyCatcher protein ligation system. SpyCatcher as a scaffold protein was chemically conjugated with activated horseradish peroxidase (HRP), and SpyTag was genetically fused to two IgG-binding nanobodies specific for the Fc regions of mouse IgG1 and rabbit IgG, which is denoted as MG1Nb and RNb, respectively. We selectively ligated HRP-conjugated SpyCatcher with SpyTag-fused MG1Nb or RNb depending on the original species of primary antibodies and enhanced target molecules' signals in a plug-and-playable manner. We successfully demonstrated that HRP:MG1Nb and HRP:RNb selectively bind to target-bound mouse IgG1 or rabbit IgG, respectively, and perform as excellent target-specific signal amplifiers in various immunoassays such as western blot, enzyme-linked immunosorbent assay (ELISA), and multiplex tyramide signal amplification (TSA) cell and tissue imaging. These recombinant signal-amplifying IgG-binders can be simple and reliable alternatives to conventional secondary antibodies in various immunoassays.

3.2 Introduction

Qualitative and quantitative analysis of target biomolecules in cell, blood, and tissue samples are essential for early disease detection and prognosis of treatment in various biomedical research and clinical applications.⁷⁷⁻⁷⁹ Immunoassay is a biochemical methods that utilize antibodies to detect the presence and concentration of specific target molecules in biological component mixtures.⁸⁰ The immunoassay is based on antigen-antibody interaction and employs two different types of antibodies- primary antibody and secondary antibody. The primary antibody detects the target molecules with a high binding affinity for target-specific recognition and selection, thus ensuring the accuracy and precision of the assay. However, the secondary antibody's purpose is to recognize and bind to the target-bound primary antibody, regardless of the target molecule. And then, they generate signals that high enough for detection. Secondary antibodies are generally conjugated with horseradish peroxidases (HRP), which repeatedly convert inactive substrates to signal-generating active products. As a result, they can generate considerable amplification of low primary signals in a concentration-dependent manner. Amplified signals can be quantified via colorimetric, fluorescent, and chemiluminescent measurements. Therefore, low-abundance biomolecules in biological samples are selectively detected

and quantified by immunoassays. Although enzyme-conjugated secondary antibodies are widely used for signal amplification, their production requires live animals or mammalian cell culture systems with high manufacturing costs, long preparation time, and animal welfare and ethical issues compared to recombinant protein production with bacterial overexpression systems. Therefore, there is a high demand for the development of immunoglobulin G (IgG)-binding recombinant signal amplifiers, which have primary antibody-binding ability and generate signals of significant intensities.

We tried to develop IgG-binding recombinant signal amplifiers, we have previously introduced the antibody binding domain (ABD) derived from *Staphylococcus aureus* protein A as a universal non-immunoglobulin IgG binder which has a high binding affinity to and specificity for the Fc region of various IgGs.^{38, 81} For signal amplification, we fused the ABD to glutathione-*S*-transferase (GST) to create a scaffolding protein for conjugation to multiple activated HRPs. The HRP-GST-ABD bound to the Fc region of target-bound primary antibodies derived from various species, and amplified target-specific signals in both enzyme-linked immunosorbent assays (ELISA) and immunohistochemistry. However, HRP-GST-ABD lacked species-selectivity, binding to the Fc region of various IgGs regardless of the origin of the primary antibody.⁷³ In a similar approach, Jeong *et al.* developed IgG binder molecules, Repebody, composed of leucine-rich repeat modules and specific to IgG from different species, by phage display. Repebody was further labeled with various signal generators such as HRP, a fluorescent dye, and quantum dots for use in immunoassays and imaging as an alternative to conventional secondary antibodies.⁸² Meanwhile, single-domain antibodies, also known as nanobodies, are commonly used as scaffolding proteins to screen high affinity binders against specific target molecules for diagnostic and therapeutic purposes.^{47, 48, 83-85} Nanobodies derived from camelids or sharks are highly stable in a wide temperature range and easily used as recombinant fusion proteins with various functional proteins due to their small size and high stability in bacterial overexpression systems. Recently, anti-IgG nanobodies against various mouse IgG subclasses and rabbit IgGs were screened and generated by phage display. High quantities of these nanobodies were produced in bacterial overexpression systems and directly labeled with fluorophores or enzymes for signal enhancement in various immunoassays and immunostaining.⁴⁹

In this study, we prepared two species-specific IgG-binding nanobodies specific for Fc regions of mouse IgG1 and rabbit IgG, denoted as MG1Nb and RNb, respectively. To establish plug-and-playable modular IgG-binding signal amplifier, we used the well-established SpyTag/SpyCatcher protein ligation system, which allowed us to covalently ligate above two individual functional modules post-translationally. Each MG1Nb and RNb were genetically fused with a SpyTag peptide and the activated HRP was chemically conjugated to SpyCatcher. HRP-conjugated SpyCatcher was efficiently ligated to each SpyTag-fused IgG-binding nanobody in a plug-and-playable manner. Target-specific signal amplification was evaluated in western blot, ELISA, and multiplex TSA cell and tissue imaging (Figure

3.1).

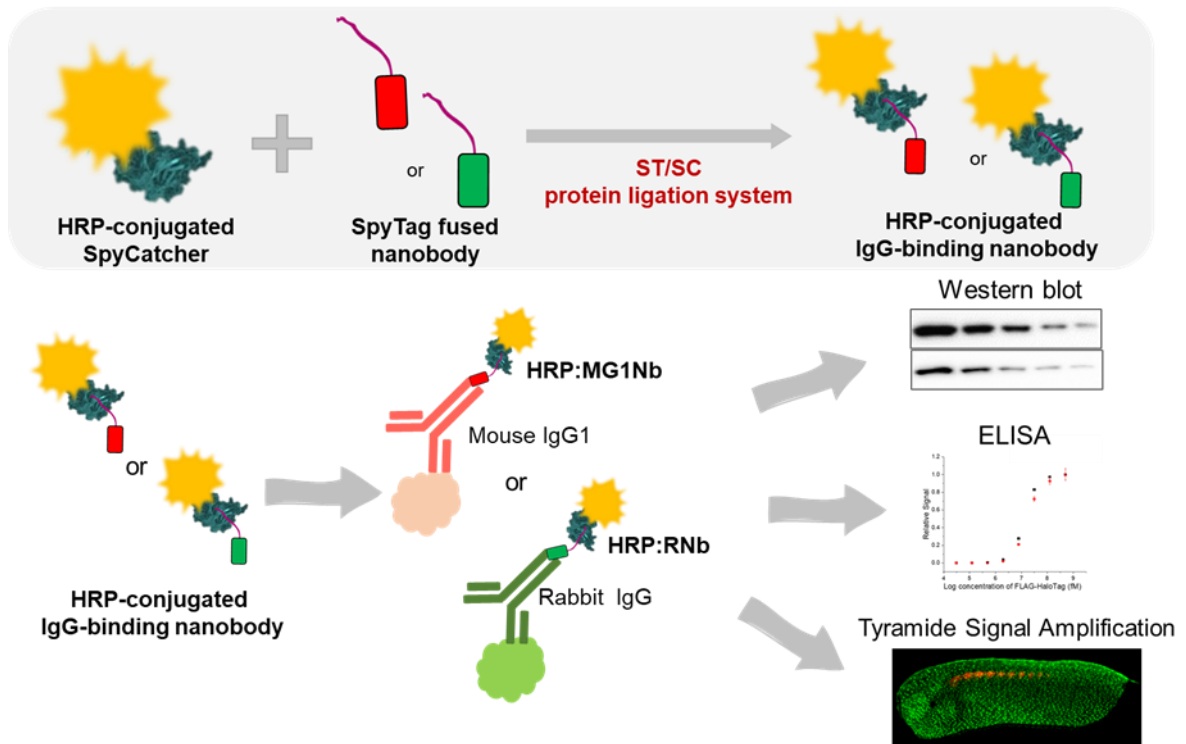


Figure 3.1 Schematic illustration of target-specific signal amplifiers.

3.3 Materials and Methods

Genetic modification and purification of SpyCatcher-S10C and SpyTag fused nanobodies

Serine residue at position 10 of SpyCatcher protein was substituted with cysteine using established polymerase chain reaction (PCR) protocol with pETDuet based plasmids as a template.⁷¹ TP1107 with an additional cysteine in pTP1112 and TP897 with three additional cysteines in pTP955 were gifts from Dirk Görlich (Addgene plasmids #104158 and #104164, respectively).⁴⁹ SpyTag (AHIVMVDAYKPTK) was genetically inserted to the N-termini of anti-mouse IgG1 nanobody (TP1107) and anti-rabbit IgG nanobody (TP1897) with an extra flexible linker by PCR with pETDuet based plasmids as a template. Recombinant DNAs were transformed into competent *E. coli* strain BL21(DE3), and cells were grown in 1.0 L of Luria-Bertani (LB) medium containing 10 mg/L of ampicillin, induced with 0.5 mM of isopropyl β -D-1-thiogalactopyranoside (IPTG), and harvested by centrifugation at 13000 g. The *E. coli* cells containing resultant proteins were resuspended in 30 mL of lysis buffer (50 mM sodium phosphate, 100 mM sodium chloride, and 15 mg/L of lysozyme, pH 7.4) and incubated for 30 min at 4°C. The suspension was sonicated for 10 min in 30 s intervals and subsequently centrifuged at 13000 g for 1 h at 4°C. Each protein was purified with batch type of Ni²⁺-NTA affinity chromatography.

Chemical conjugation of horseradish peroxidase (HRP) or fluorescent dyes to SC_{S10C}

EZ-Link Maleimide Activated Horseradish Peroxidase (Mal-HRP, Thermo Fisher) was conjugated to SC_{S10C} (HRP-SC). SC_{S10C} was incubated with 5 mol equivalents of Mal-HRP at 4°C with gently shaking overnight. Unconjugated SC_{S10C} and Mal-HRP were removed by using Ni²⁺-NTA affinity chromatography and centrifugal filter (Millipore, MWCO: 50 kDa) sequentially. Thiol-reactive fluorescent dyes such as fluorescein 5-maleimide (F5M) (Thermo Fisher) and Alexa fluor 647 C2 maleimide (Invitrogen) were independently conjugated to SC_{S10C}. SC_{S10C} was incubated with 3 mol equivalents of fluorescent dyes at 4°C with gently shaking overnight. Free dyes were removed by centrifugal filter (Millipore, MWCO: 10 kDa).

Construction of HRP:Nbs or fluorescent dye conjugated Nbs using SpyTag/SpyCatcher ligation

For HRP:Nbs or fluorescent dye conjugated Nbs, HRP-SC, F5M-SC, Alexa647-SC and two different SpyTag fused nanobodies (MG1Nb-ST and RNb-ST) were mixed with the molar ratio of 1:1.5 to use up all available HRP-SC, F5M-SC, or Alexa647-SC. They were incubated at indicated times (10, 30 min, 1, 3, 6 h, and overnight) at room temperature with gentle shaking. Reaction resultants were analyzed with SDS-PAGE after adding SDS loading buffer and boiling at 110°C. We removed unligated free MG1Nb-ST or RNb-ST using centrifugal filter and quantitated the molar ratio between the HRP or fluorescent dye and Nbs (MG1Nb or RNb) by UV/Vis spectrophotometer.

Surface plasmon resonance (SPR) analysis

SPR experiments were performed with carboxyl dextran CM5 gold chips on a Biacore 3000 device (Biacore AB, Sweden) at 25 °C using both HBS-EP buffer as an immobilization solution and PBS buffer as a running solution. Each mouse IgG1 or rabbit IgG was immobilized onto the surface of CM5 sensor chips by standard amine-coupling chemistry.^{86, 87} Briefly, a mixture of EDC (50 mg/ml) and NHS (50 mg/ml) was injected onto the chip at a flow rate of 10 µL/min to activate carboxyl groups on the sensor chip surface and subsequently 0.1 mg/ml of mouse IgG1 or rabbit IgG were added into two different channels at the same flow rate. Excess reactive groups were blocked with 1 M ethanolamine (pH 8.0). Subsequently, MG1Nb-ST, RNb-ST, HRP:MG1Nb, or HRP:RNb (PBS, pH 7.4) were introduced with various concentration to monolayers of mouse IgG1 or rabbit IgG immobilized CM5 sensor chips at a flow rate of 10 µL/min. The associating and dissociating parameters of them to either mouse IgG1 or rabbit IgG were analyzed by fitting the SPR data with Biaevaluation software using the 1:1 Langmuir binding model.⁸⁸

Western blot

The concentration of purified FLAG-HaloTag protein and cell lysates of HEK293T transiently transfected with gene of FLAG-HaloTag were determined by BCA assay. Each diluted protein sample was denatured and separated on SDS-PAGE (Bio-Rad). The separated proteins were transferred from the gel to a polyvinylidene fluoride (PVDF) membranes using Bolt® Mini Blot Module (Invitrogen, 20V, 1 h) and the membranes were blocked with 5% (w/v) skim milk in TBST for 1 h at RT. Anti-FLAG mouse IgG1 (Abcam) and anti-FLAG rabbit IgG (Thermo Fisher) were used as primary antibodies for selective detection. The blocked membranes were then incubated overnight at 4 °C with each diluted primary antibody according to manufacturer's protocol. After three washes in TBST, membranes were incubated for 1 h at RT with anti-mouse or anti-rabbit HRP-conjugated secondary antibodies (Jackson ImmunoResearch Inc.) or HRP:Nbs (HRP:MG1Nb or HRP:RNb). The concentration of HRP:Nbs was determined by UV/vis photospectrometer and diluted to corresponding concentration of HRP-conjugated secondary antibodies. After three washes in TBST, the membranes were further incubated with the enhanced chemiluminescence (ECL) western blotting substrate solutions (Thermo Fisher) for the purpose of the signal development and enhancement.

Simple Indirect ELISA

The experiments were conducted with transparent Immuno MicroWell 96-well plates (Nunc Maxisorp, flat-bottom) according to the use of HRP-conjugated secondary antibodies. Purified FLAG-HaloTag protein and EpCAM (Sino Biological Inc.) were serially diluted with PBS buffer. Each protein solution was loaded into the wells and incubated at 4 °C overnight to immobilize the target proteins on

the surface of the plate through physical adsorption.⁷³ At the next day, each well was washed four times with PBS buffer containing 0.1% Tween-20 (PBST). The blocking buffer (5% goat serum in PBST) was loaded and incubated with gently shaking for 4 h at RT. After blocking, each well was washed four times with PBST and the solutions of diluted primary antibodies against FLAG (anti-FLAG mouse IgG1 (Abcam) and anti-FLAG rabbit IgG (Thermo-Fisher)) and EpCAM (anti-EpCAM mouse IgG1 and anti-EpCAM rabbit IgG (Sino Biological Inc.)) were loaded in the wells of the target analyte (FLAG-HaloTag protein or EpCAM)-immobilized plates and incubated with gently shaking for 1 h at RT. Each well was washed four times with PBST. Subsequently, corresponding anti-mouse or anti-rabbit HRP-conjugated secondary antibodies (Jackson ImmunoResearch Inc.) or HRP:Nbs were added to wells and incubated with gently shaking for 1 h at RT, and then washed five times with PBST. The substrate 3,3',5,5'-tetramethylbenzidine (TMB) solution (Thermo Fisher) was loaded into each well. The reaction solutions were incubated for 2 min at RT and 2 N H₂SO₄ solution was added immediately into each well to stop the reaction. The absorbance of each well was monitored at 450 nm with a microplate reader, SpectraMAX 190 (Molecular Devices). All the experiments were conducted three times independently and plotted with errors.

Cell culture for TSA-based immunohistochemistry

NIH3T6.7 and A431 cells were cultured in DMEM supplemented with 10% (v/v) FBS and 1% antibiotic-antimycotic. MCF-7 cells were cultured in RPMI-1640 supplemented with 5% FBS and 1% antibiotic-antimycotic. All cells were incubated in humidified atmosphere of 5% CO₂ and 95% air at 37 °C.

Preparation and analysis of fluorescence cell microscopy and TSA-based cell immunohistochemistry

The NIH3T6.7, A431, and MCF-7 cells (1×10^5 /well) were grown on microscope cover glass (18 mm Φ) in 12-well plate (SPL). Cells were fixed with 4% paraformaldehyde in PBS for 20 min at 4 °C and washed three times with PBS. To prevent non-specific binding of sample to the background, the blocking reagent (5% BSA, 5% FBS, and 0.5% Triton X-100 in PBS) was treated and incubated at room temperature for 1 h prior to sample treatment and rinsed with wash buffer (0.1% Triton X-100 in PBS). The fixed NIH3T6.7 and A431 cells were treated with diluted anti-HER2 mouse IgG1 and anti-EGFR rabbit IgG, respectively, for 2 h at RT. The negative MCF-7 cells were treated in parallel with diluted anti-HER2 mouse IgG1 or anti-EGFR rabbit IgG for 2 h at RT.

For fluorescence cell imaging, Alexa647:MG1Nb and F5M:RNb were incubated with NIH3T6.7 cells and A431 cells, respectively, for 2 h at RT after washing fixed cell three times with wash buffer. The MCF-7 cells were also treated with Alexa:647:MG1Nb or F5M:RNb. Before sealing, the cells were washed three times with wash buffer and nuclei were stained with DAPI. Images of samples were

obtained by using Olympus Fluoview FV1000 fluorescent microscope (Olympus, UOBC).

For the TSA assays, the anti-mouse HRP-conjugated secondary antibodies, HRP:MG1Nb, or HRP:RNb were incubated with NIH3T6.7 cells pre-incubated with anti-HER2 mouse IgG1 for 2 h at RT. The anti-rabbit HRP-conjugated secondary antibodies, HRP:MG1Nb or HRP:RNb were incubated with A431 cells pretreated with anti-EGFR rabbit IgG for 2 h at RT. Tyramide working solution was freshly prepared by diluting the tyramide stock solution 1:100 in amplification buffer with 0.0015% H₂O₂ just before the reactions and 100 μL was added to each sample. The reaction mixtures were incubated at RT for 10 min and rinsed with PBST. The nuclei of the cells were also stained with DAPI. Fluorescence cell images were obtained using an Olympus Fluoview FV1000 confocal microscope (Olympus, UOBC).

Xenopus embryo sample preparation

Adult *Xenopus laevis* female were ovulated by human chorionic gonadotropin (hCG) injection. Eggs were *in vitro* fertilized and dejellied with 3% cysteine in 1/3X MMR (Marc's Modified Ringers) solution (pH 7.9). Fertilized eggs and embryos were grown up in 1/3X MMR. To confirm the function of each HRP:MG1Nb or HRP:RNb in TSA-based immunohistochemistry at tissue-based samples, we fixed embryos between stage 24 and 26 with MEMFA fixation solution (MEM salts and 4% formaldehyde) for 2 h at RT or overnight at 4°C. Then, fixed embryos were used for TSA-based immunohistochemistry.

TSA-based immunohistochemistry of whole embryos

Xenopus embryos were incubated in blocking solution (10% FBS, 2% DMSO in TBS + 0.1% Triton X-100) for 30 min at RT to inhibit nonspecific binding before immunohistochemistry. For labeling α-tubulin or skeletal muscle fiber, each anti-α-tubulin rabbit IgG (abcam) or anti-skeletal muscle fiber mouse IgG1 (12/101, DSHB) were diluted according to manufacturer's protocol and incubated overnight at 4°C. After washing three times, the diluted HRP-conjugated secondary antibodies (Sigma-Aldrich) or HRP:Nbs were incubated for 2 h at RT. For the tyramide labeling, all embryo samples were incubated with Alexa-488 tyramide or Alexa-647 tyramide in amplification buffer according to manufacturer's protocol to accumulate tyramide solution in tissues for 30 min, then 0.0015% of H₂O₂ was added and incubated additional 30 min for signal amplification. Images were captured using a confocal fluorescent microscope with Z-stack and tile-scanning process (LSM780, Zeiss).

3.4 Results and Discussion

Horseradish peroxidase (HRP) is conjugated to SpyCatcher, and IgG-binding nanobodies are genetically fused to SpyTag

Horseradish peroxidase (HRP) is one of the most usually conjugated enzymes with secondary antibodies because it is highly stable and produces enough signals in immunoassays for detecting low-abundance target molecules. We used the SpyTag/SpyCatcher (ST/SC) system to construct HRP-conjugated IgG-binding nanobodies as signal amplifiers. We selected the SC protein as our scaffold protein and substituted the serine residue at position 10 of SC with a cysteine (SC_{S10C}) to conjugate EZ-Link maleimide activated horseradish peroxidase (Mal-HRP).⁷¹ Meanwhile, we prepared two recently developed nanobodies, mouse IgG1-binding nanobody (MG1Nb) and rabbit IgG-binding nanobody (RNb), and genetically introduced a SpyTag peptide (AHIVMVDAYKPTK) with an extra flexible linker to each C-terminus. SC_{S10C} and the SpyTag-fused nanobodies (Nb-STs; MG1Nb-ST and RNb-ST) were overexpressed in bacteria and purified with one-step Ni-NTA agarose column chromatography.⁴⁹ The purity and apparent molecular mass of SC_{S10C}, MG1Nb-ST, and RNb-ST were confirmed with SDS-PAGE (Figure 3.2A). HRP-conjugated SC (HRP-SC) was obtained by reacting SC_{S10C} with excess amounts of Mal-HRP, followed by removing the unreacted Mal-HRP and SC (Figure 3.2B). The majority of HRP conjugated with one SC_{S10C}, and 15 % of HRP conjugated with two SC_{S10C}, which corresponds to bands at approximately 65 kDa and 78 kDa, respectively (Figure 3.2C).

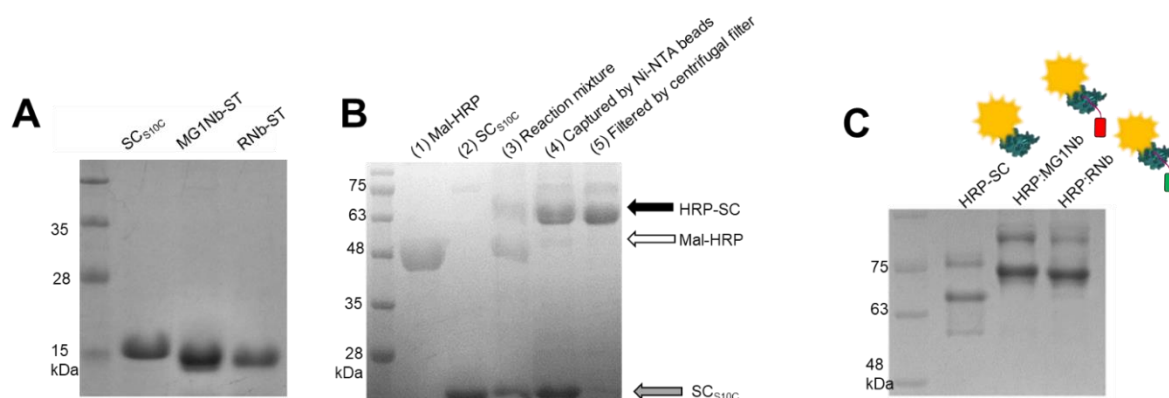


Figure 3.2 Characterization of purified proteins and reaction proteins using SDS-PAGE. (A) SDS-PAGE analysis of purified SC_{S10C} and Nb-STs (MG1Nb-ST and RNb-ST). (B) SDS-PAGE analysis of (3) reaction products obtained from (1) SC_{S10C} and (2) the EZ-Link maleimide-activated horseradish peroxidase (Mal-HRP) and reaction products purified with Ni-NTA beads (4) and centrifugal filter (5). (C) SDS-PAGE analysis of IgG-binding signal amplifiers, HRP:MG1Nb and HRP:RNb.

SpyTag-fused IgG-binding nanobodies (Nb-STs) are ligated with HRP-SC to produce IgG-binding signal amplifiers, HRP:MG1Nb and HRP:RNb

To construct HRP-conjugated IgG-binders, we first optimized the reaction time and ratio of MG1Nb-ST or RNb-ST to HRP-SC. We mixed HRP-SC with MG1Nb-ST or RNb-ST at the molar ratio of 1:1.5 to use all available HRP-SC. The ligation reaction between the Nb-STs and HRP-SC occurred in about 10 min, consuming all the HRP-SC (Figure 3.3) in consistent with previous reports.^{70, 76} To quantify the molar ratios of HRP and nanobody (MG1Nb or RNb) in each HRP:Nb, we acquired the absorbances of each HRP:Nb at 280 and 403 nm, indicating the presence of protein and heme, respectively, and calculated the molar concentration using the molar extinction coefficients (ϵ_{molar}) for each (Figure 3.4A). The UV/Vis absorption spectra revealed that each MG1Nb-ST or RNb-ST was ligated to HRP-SC at 1:1 molecular ratio through an isopeptide bond between the ST and SC (Figure 3.4B). In addition, each protein's elution profiles were checked with that of a protein standard mixture to confirm whether they form any high ordered oligomers or contain any contaminants (Figure 3.4C). These results imply that the cysteine mutation in SC and subsequent HRP conjugation did not disturb the ligation reaction and that HRP:MG1Nb and HRP:RNb were successfully established.

To investigate the binding behaviors of HRP:MG1Nb and HRP:RNb to mouse IgG1 and rabbit IgG, respectively, we performed surface plasmon resonance (SPR) analysis (Figure 3.5),⁷³ We first immobilized either mouse IgG1 (anti-FLAG mouse IgG1) or rabbit IgG (anti-FLAG rabbit IgG) on the surfaces of SPR CM5 chips and then introduced MG1Nb-ST and RNb-ST alone, not ligated to HRP-SC, to the corresponding mouse IgG1- or rabbit IgG-immobilized CM5 chip. We observed rapid increases of SPR response units (RU) upon the introduction of Nb-ST concentrations from 62.5 nM to 500 nM and slow decreases of RU upon washing with buffers (Figure 3.5A and 3.5C). In contrast, no apparent change was observed upon the introduction of MG1Nb-ST (Figure 3.5E) or RNb-ST (Figure 3.5G) to mismatched rabbit IgG- or mouse IgG1-immobilized CM5 chips, respectively, suggesting that there is no detectable cross-binding between them. MG1Nb-ST and RNb-ST exhibited strong binding to their corresponding immunoglobulins with dissociation constants (K_d) of 0.37 nM and 2.61 nM, respectively (Figure 3.5E). Besides, when HRP:MG1Nb and HRP:RNb were introduced upon ligation to the corresponding mouse IgG1- and rabbit IgG-immobilized CM5 chips, they showed high binding affinity as well (Figure 3.5B and 3.5D), with dissociation constants (K_d) of 12 nM and 1.77 nM, respectively (Figure 3.5E). HRP-SC ligation to nanobodies may have a slight effect on binding behavior to antibodies. However, HRP:MG1Nb and HRP:RNb can still selectively and strongly bind to IgGs derived from mouse or rabbit, respectively.

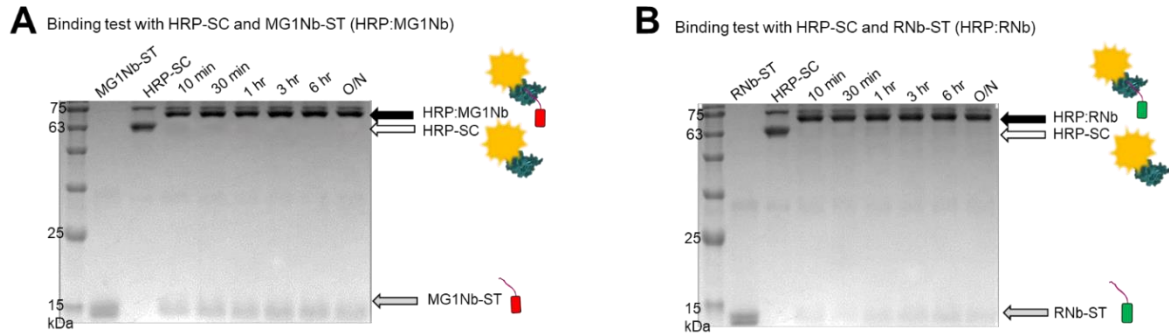


Fig. 3.3 SDS-PAGE analysis of reaction results of HRP-SC and Nb-STs. Reaction results of (A) MG1Nb-ST with HRP-SC and (B) RNb-ST with HRP-SC. Reactions were sampled at the indicated times, run on SDS-PAGE, and stained with Coomassie blue. Molecular weight markers were run together, and the apparent molecular weights are indicated (solid arrow indicates IgG-binding signal amplifiers, HRP:MG1Nb and HRP:RNb, respectively).

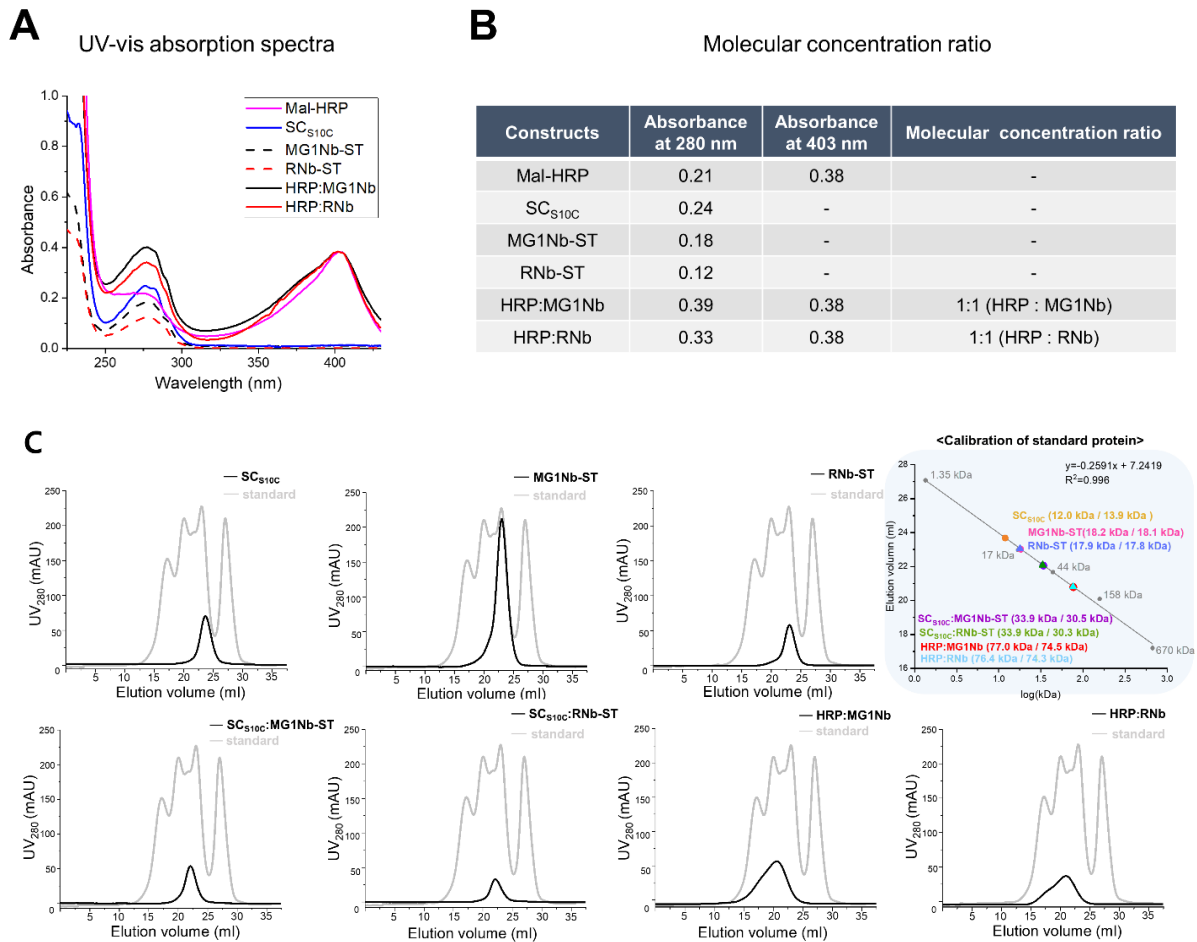


Figure 3.4 Characterization of purified proteins and reaction proteins using analytical methods. (A) UV-vis absorption spectra and (B) molecular concentration ratio of SC_{S10C}, Mal-HRP, HRP:MG1Nb and HRP:RNb determined by measuring with UV-vis spectrophotometer. (C) The gel filtration elution

profiles of used proteins in this study. All experiments were performed on a Superose 6 column (GE Healthcare). The calibration of the gel filtration was used to estimate molecular mass based on the protein's elution volume. The values between brackets indicate the estimated versus the theoretical molecular weight of the samples.

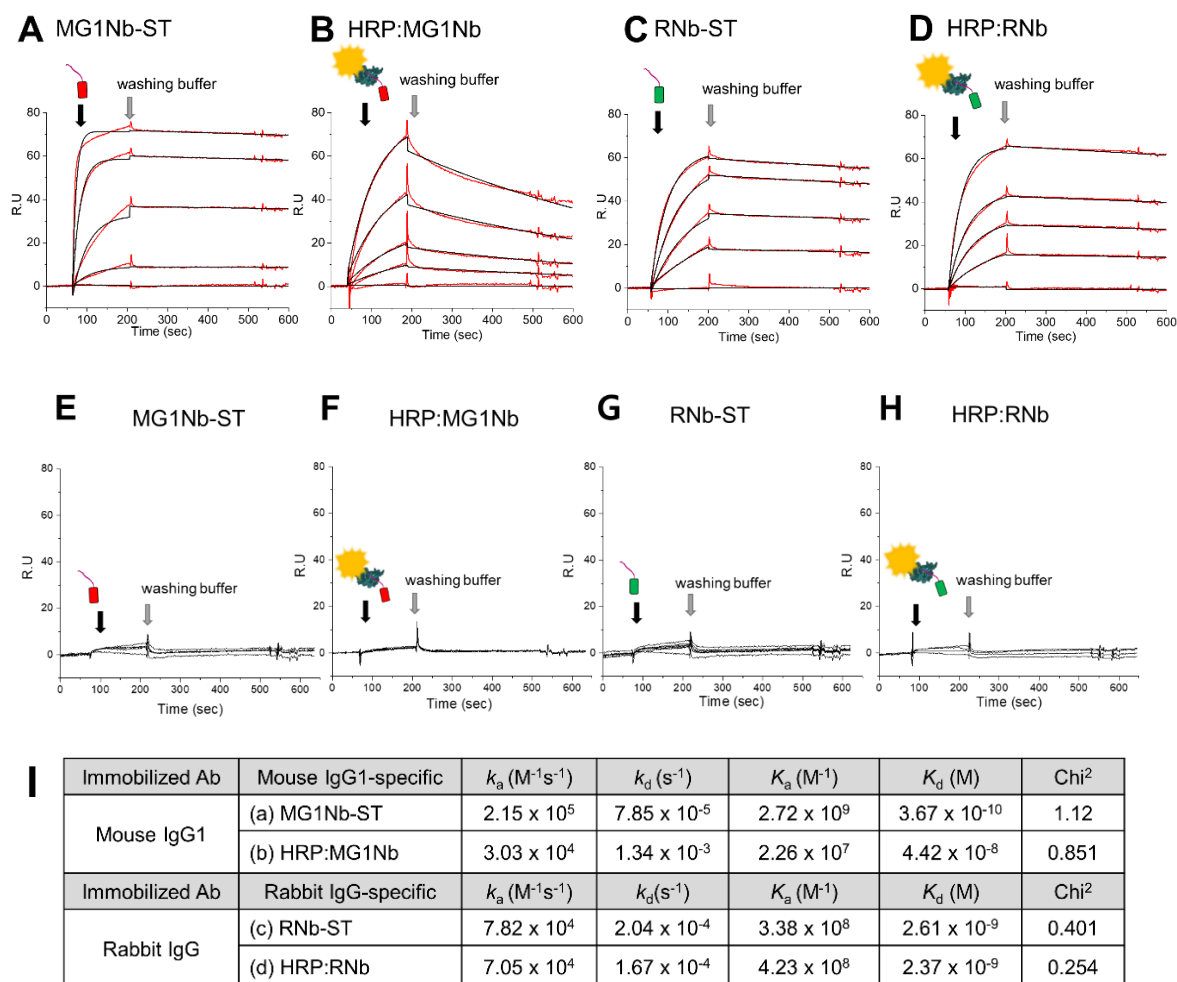


Figure 3.5 SPR sensorgrams of Nb-STs and HRP:Nbs. (A) MG1Nb-ST or (B) HRP:MG1Nb binding to mouse IgG1-immobilized CM5 chip (black lines) and (C) RNb-ST or (D) HRP:RNb binding to rabbit IgG-immobilized CM5 chip (black lines) and the fitting curves (red lines). (E) MG1Nb-ST or (F) HRP:MG1Nb binding to rabbit IgG-immobilized CM5 chip (black lines) and (G) RNb-ST or (H) HRP:RNb binding to mouse IgG1-immobilized CM5 chip. The time points at which samples or washing buffers are introduced are indicated as black and gray arrows, respectively. (I) The binding parameters for the interactions of MG1Nb and mouse IgG1 or RNb and rabbit IgG by SPR analysis (k_a ; association rate constant, k_d ; dissociation rate constant, K_a ; association constant, K_d ; dissociation constant).

HRP:MG1Nb and HRP:RNb serve as signal amplifiers specific to primary antibodies in western blots

Biological samples contain many proteins with similar size and properties that are not dominant enough to be detected with simple fluorescence dye-labeled antibodies or affinity reagents.^{5,89} Therefore, it is often necessary to quantitatively amplify original signals to detect specific low abundant target molecules. Western blot is generally used to detect specific low abundant target proteins in complex biological samples and quantify them. We investigated whether HRP:MG1Nb and HRP:RNb can selectively bind to target-bound mouse IgG1 or rabbit IgG, respectively, and quantitatively amplify signals in western blots. We first performed western blots with purified samples of known concentration to examine whether HRP:Nbs can quantitatively amplify original signals according to the concentrations applied. We purified FLAG-tag fused HaloTag protein (FLAG-HaloTag), serially diluted the protein from 10 to 160 ng, ran the dilutions out in an SDS-PAGE, and transferred them onto the polyvinylidene difluoride (PVDF) membrane. After blocking with 5% skimmed milk, membranes were probed with either anti-FLAG mouse IgG1 or anti-FLAG rabbit IgG. We then treated the membranes with either anti-mouse and anti-rabbit conventional HRP-conjugated secondary antibodies or HRP:MG1Nb and HRP:RNb, respectively, and subsequently added enhanced chemiluminescence (ECL) western blotting substrate solution. Anti-mouse HRP-conjugated secondary antibody (Figure 3.6A) and HRP:MG1Nb (Figure 3.6B) probed with anti-FLAG mouse IgG1 generated similar series of concentration-dependent signals for purified FLAG-HaloTag without significant background noise (Figure 3.6A and 3.6B). The signal intensities gradually increased as the concentrations of FLAG-HaloTag increased. Almost identical results were also obtained with anti-rabbit HRP-conjugated secondary antibody (Figure 3.6C) and HRP:RNb (Figure 3.6D) when FLAG-HaloTag was probed with anti-FLAG rabbit IgG (Figure 3.6C and 3.6D). For quantitative analysis, band intensity was plotted against protein input concentration using ImageJ program (Figure 3.7). Both HRP:MG1Nb and HRP:RNb showed linear signal enhancement patterns correlating with the sample concentrations and generated signal intensities at each concentration highly similar to those of conventional HRP-conjugated secondary antibodies (Figure 3.7A and 3.7B).

Western blot can quantitatively detect target molecules in complex biological samples. We next performed western blots with lysates from HEK293T cells, which were transiently transfected with FLAG-HaloTag genes. A serial dilutes of cell lysates (0.65 to 10 μ g in total protein concentration) were applied to SDS-PAGE. The samples transferred to a PVDF membrane, processed as a western blot, and probed as described above. Both anti-mouse HRP-conjugated secondary antibody (Figure 3.6E) and HRP:MG1Nb (Figure 3.6F) probed with anti-FLAG mouse IgG1 successfully amplified the series of concentration-dependent signals of cell lysates at the expected locations without significant background (Figure 3.6E and 3.6F). Similar results were obtained with anti-rabbit HRP-conjugated secondary

antibody (Figure 3.6G) and HRP:RNb (Figure 3.6H) in combination with anti-FLAG rabbit IgG (Figure 3.6G and 3.6H). Besides, there was no band signal generated with HRP:MG1Nb and HRP:RNb when anti-FLAG rabbit IgG and anti-FLAG mouse IgG1 were used as primary antibodies, respectively, (Figure 3.6B, 3.6D, 3.6F, and 3.6H), confirming that there is no detectable cross-binding reactivity in consistence with SPR data. HRP:MG1Nb and HRP:RNb exhibited linear signal amplification patterns dependent on target molecule concentration in a complex cell lysate, and the HRP:Nb patterns corresponded well to those of conventional HRP-conjugated secondary antibodies (Figure 3.7C and 3.7D). These results indicate that HRP:MG1Nb and HRP:RNb can specifically recognize target-bound mouse IgG1 and rabbit IgG, respectively, without cross-reaction and quantitatively amplify the signals of target analytes in western blots effectively. These HRP:Nbs present an opportunity to substitute conventional HRP-conjugated secondary antibodies with recombinant signal amplifiers.

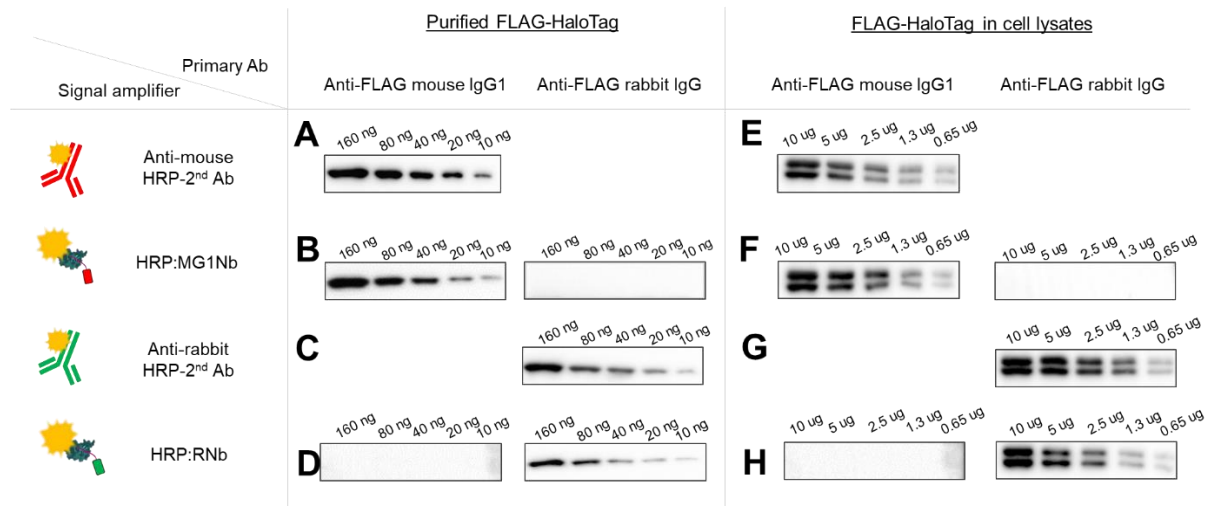


Figure 3.6 Western blots. Various concentrations of (A–D) purified FLAG-HaloTag proteins and (E–H) FLAG-HaloTag gene-transfected cell lysates were loaded on SDS-PAGE, transferred to a membrane, and probed with either anti-FLAG mouse IgG1 or anti-FLAG rabbit IgG. Next, membranes were treated with (A, E) anti-mouse HRP-conjugated secondary antibody and (B, F) HRP:MG1Nb or anti-rabbit HRP-conjugated secondary antibody and (D, H) HRP:RNb, respectively. All bands were developed with ECL western blotting substrate solution.

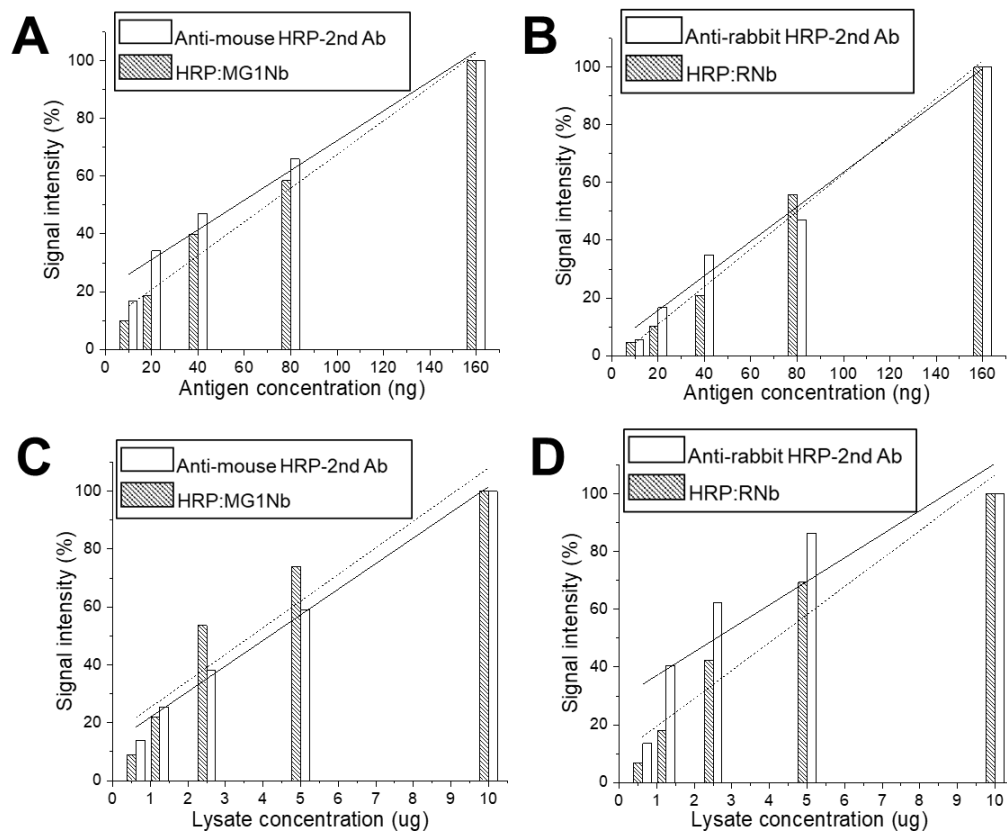


Figure 3.7 Quantitative analyses of signal enhancement of western blots. Band signal intensities of (A and B) purified FLAG-HaloTag proteins and (C and D) FLAG-HaloTag gene-transfected cell lysates were probed with (A and C) anti-FLAG mouse IgG1 and treated with anti-mouse HRP-conjugated secondary antibody and HRP:MG1Nb or probed with (B and D) anti-FLAG rabbit IgG and treated with anti-rabbit HRP-conjugated secondary antibody and HRP:RNb.

HRP:MG1Nb and HRP:RNb are utilized as primary antibody-specific, but target analyte-independent signal-amplifiers in indirect ELISA

To investigate the application of HRP:Nbs in another immunoassay, we performed indirect ELISA to detect target analytes present in a solid surface using antibodies. First, via physical adsorption, we immobilized various concentrations of the previously mentioned purified FLAG-HaloTag protein as a model protein on the surface of an ELISA plate, followed by treatment with blocking buffer. We applied either anti-FLAG mouse IgG1 or anti-FLAG rabbit IgG to the immobilized FLAG-HaloTag. After extensive washing, we loaded the corresponding HRP-conjugated secondary antibodies or HRP:Nbs. Next, we added tetramethylbenzidine (TMB) substrate solution onto the plates and measured the absorption at 450 nm. When we applied anti-FLAG mouse IgG1 with anti-mouse HRP-conjugated secondary antibody and HRP:MG1Nb as signal amplifiers, we obtained similar representative sigmoidal curves for each HRP construct between the linear absorbance range of 2 to 125 nM for the FLAG-HaloTag proteins (Figure 3.8A). We also obtained comparable sigmoidal curves between the linear absorbance range of 0.488 to 125 nM using anti-rabbit HRP-conjugated secondary antibody and HRP:RNb in combination with anti-FLAG rabbit IgG (Figure 3.8B). To demonstrate target analyte independency, we performed the same assay with another target biomolecule, epithelial cell adhesion molecule (EpCAM), a biomarker for circulating tumor cells.⁹⁰ EpCAM showed almost identical sigmoidal detection curves to both HRP:Nbs and HRP-conjugated secondary antibodies (Figure 3.8C and 3.8D) with about the same linear response range. These data suggest that HRP:MG1Nb and HRP:RNb can individually recognize and bind to their corresponding target-bound primary antibodies in indirect ELISA. The HRP:Nbs can target independently and amplify signals comparably to conventional HRP-conjugated secondary antibodies.

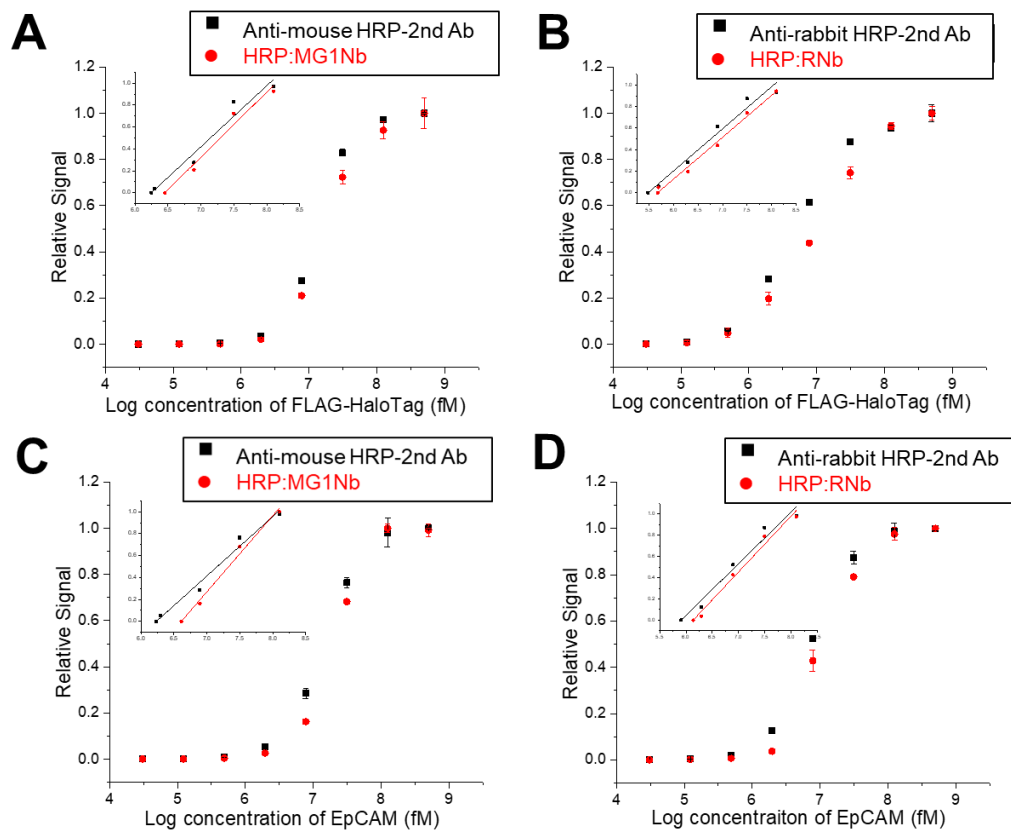


Figure 3.8 Indirect ELISA. Various concentrations of (A and B) purified FLAG-HaloTag proteins and EpCAM (C and D) were immobilized on 96 well plates and probed with either (A and C) anti-FLAG mouse IgG1 or (B and D) anti-FLAG rabbit IgG to capture target molecules. Next, plates were treated with (A and C) anti-mouse HRP-conjugated secondary antibody and HRP:MG1Nb or (B and D) anti-rabbit HRP-conjugated secondary antibody and HRP:RNb with the TMB substrate solution for signal enhancement. Signal responses were plotted and linear signal responses were observed at medium concentrations of target analytes (insets).

Simultaneous HRP:MG1Nb and HRP:RNb enhance fluorescence signal intensities of two different target molecules in cell-based TSA assays

The tyramide signal amplification (TSA) assay is an antibody-based proximity labeling assay that provides enhanced sensitivity in cell and tissue applications.^{15,91} Upon binding to target-bound primary antibodies, HRP-conjugated secondary antibodies locally activate fluorescent dye-conjugated tyramide derivatives to label adjacent localized proteins, resulting in the significant enhancement of the fluorescence signal. In this study, we examined if HRP:Nbs activates the fluorescent dye-conjugated tyramide derivatives in a TSA assay to enhance the fluorescent signal at a target site.

To directly compare fluorescent signals generated by a single fluorescent dye to TSA, we conjugated SC_{S10C} with Alexa Fluor 647 maleimide or fluorescein-5-maleimide (Alexa647-SC or F5M-SC) via thiol-maleimide Michael-type addition. After removing unreacted dyes, Alexa647-SC and F5M-SC were mixed with excess amounts of MG1Nb-ST and RNb-ST to form Alexa647:MG1Nb (Figure 3.9A) and F5M:RNb (Figure 3.9B), respectively, and free Nb-ST was removed using a centrifugal filter.

HER2-overexpressing NIH3T6.7 cells and EGFR-overexpressing A431 cells were prepared and initially imaged with Alexa647:MG1Nb and F5M:RNb in combination with anti-HER2 mouse IgG1 and anti-EGFR rabbit IgG, respectively. Relatively weak red and green fluorescence signals appeared in Alexa647:MG1Nb-treated NIH3T6.7 cells with anti-HER2 mouse IgG1 (Figure 3.10A, top panel) and F5M:RNb-treated A431 cells with anti-EGFR rabbit IgG, respectively (Figure 3.10B, top panel). In contrast, neither of the dye-conjugated antibody-binding nanobodies bound to MCF-7 cells, which do not overexpress HER2 or EGFR (Figure 3.11A and 3.11E). For TSA, we employed same cell line/primary antibody pairs with conventional HRP-conjugated secondary antibodies or HRP:Nbs instead of dye-conjugated nanobodies and further treated them with a TSA reagent (a mixture Alexa 647 tyramide and 0.0015 % of H₂O₂) for 10 min. When anti-mouse HRP-conjugated secondary antibody and HRP:MG1Nb were selectively bound to target NIH3T6.7 cells via anti-HER2 mouse IgG1, the fluorescence microscopic images revealed extremely high red fluorescence signals (Figure 3.10A, second and third panels, respectively). Use of HRP:RNb in place of HRP:MG1Nb did not generate any fluorescence signal (Figure 3.10A, bottom panel). Similarly, dramatically enhanced green fluorescence signals were observed in anti-rabbit HRP-conjugated secondary antibody or HRP:RNb-treated A431 cells with Alexa 488-conjugated tyrimide (Figure 3.10B, second and bottom panels, respectively), and use of HRP:MG1Nb in place of HRP:RNb did not produce any fluorescence signals (Figure 3.10B, third panel). Fluorescence signal intensity plots revealed that TSA with HRP-conjugated secondary antibody or HRP:Nbs generated 5 times more fluorescence signal than that of fluorescently labeled antibodies (Figure 3.10C and 3.10D). Also, HRP:Nbs showed enhanced signal with comparable sensitivity to that of conventional secondary antibodies. We also confirmed that there was no fluorescence signal generated in similarly treated HER2 and EGFR double negative MCF-7 cells

(Figure 3.11), suggesting minimal apparent non-specific binding of HRP-conjugated secondary antibody or HRP:Nbs to the cells.

In addition to pre-existing surface markers, we presented target proteins on the surface of the cells by transiently transfecting HEK293T cells with the FLAG-HaloTag gene, which translates as an integral membrane protein that presents FLAG-tag on the plasma membrane. We then selectively imaged these cells with TSA. We first treated the transfected HEK293T cells with Oregon green 488-HaloTag ligands to confirm the expression of FLAG-HaloTag proteins on the surface of the HEK293T cells. We further incubated the cells with anti-FLAG mouse IgG1 or anti-FLAG rabbit IgG and processed them with the corresponding HRP-conjugated secondary antibodies or HRP:Nbs, along with TSA reagents (a mixture Alexa 647 tyramide and 0.0015 % of H₂O₂) as described above. The fluorescence signals of Oregon green 488 and Alexa 647 overlapped, indicating that only the transiently transfected cells were selectively detected, and their signals are amplified (Figure 3.12).

Because HRP:MG1Nb and HRP:RNb selectively bind without cross-reaction to mouse IgG1 and rabbit IgG, respectively, it is possible for them to be used simultaneously to detect two different target molecules in a sample using two different primary antibodies. To demonstrate the simultaneous detection of two different targets in the same sample with HRP:MG1Nb and HRP:RNb, we selected two different target proteins (α -tubulin and EGFR) in A431 cells and treated the cells with both anti- α -tubulin mouse IgG1 and anti-EGFR rabbit IgG. To avoid the cross-catalytic activity of previously bound HRP-conjugated secondary antibody or HRP:Nb, we performed the TSA assays sequentially. First, we treated them with either HRP-conjugated anti-mouse IgG1 antibody or HRP:MG1Nb, followed by incubation in an Alexa 647 tyramide and 0.0015% H₂O₂ mixture for 10 min to amplify specific signals of α -tubulin. Next, we inactivated the previously associated HRPs with 3% H₂O₂. Further, we treated the cells again with either HRP-conjugated anti-rabbit IgG antibody or HRP:RNb, followed by incubation in an Alexa 488 tyramide and 0.0015% H₂O₂ mixture for 10 min to amplify specific signals of EGFR. In both the HRP-conjugated secondary antibody-treated and HRP:Nb-treated A431 cells, α -tubulin and EGFR were individually visualized with red and green colors, respectively, in single cells (Figure 3.10E and 3.10G). A fluorescence intensity correlation using line scan analysis in microscopy was performed to characterize the degree of overlap between two channels in an image (α -tubulin-red and EGFR-green channels). The merged images and plots showed no significant overlap of α -tubulin and EGFR, located in cell cytosol and surface, respectively (Figure 3.10F and 3.10H). These data indicate that HRP:Nbs can bind species-specifically to target-bound primary antibodies and perform signal enhancement of two different targets without cross-reactivity in TSA-based immunohistochemistry.

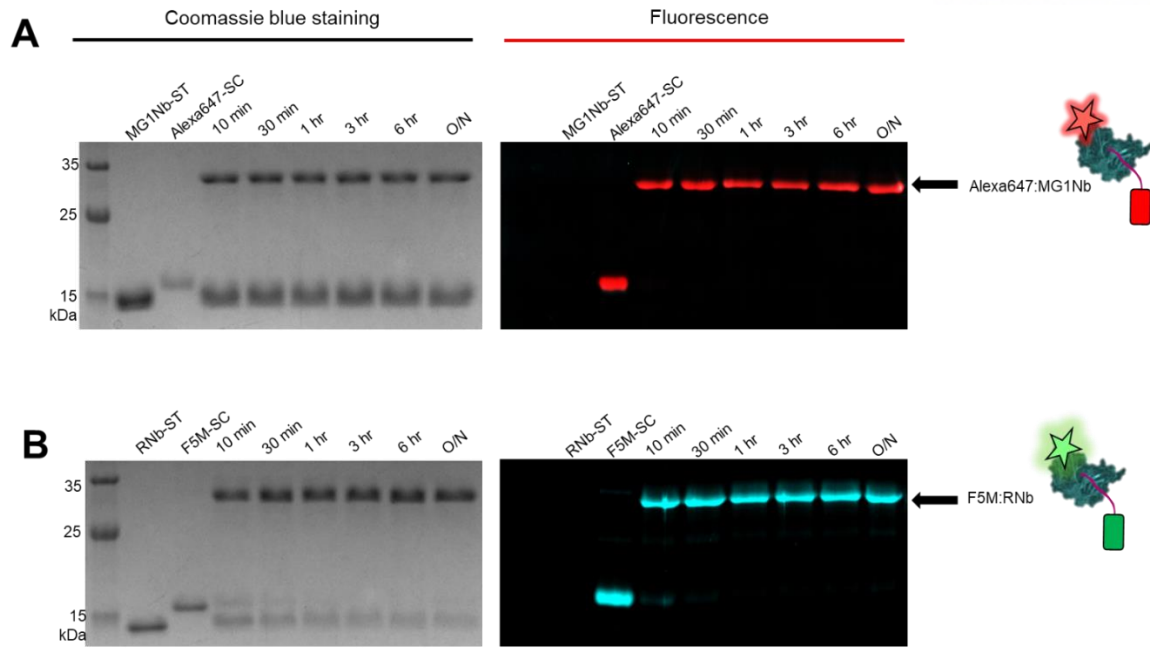


Figure 3.9 SDS-PAGE analysis of reaction results of dye conjugated SCs and Nb-STs. Reaction results of (A) MG1Nb-ST with Alexa647-SC and (B) RNb-ST with F5M-SC. Reactions were sampled at the indicated times, run on SDS-PAGE, stained with Coomassie blue, and imaged them with white light (left panels) and fluorescence (right panels). Molecular weight markers were run together, and the apparent molecular weights are indicated (solid arrow indicates fluorescent dye conjugated nanobodies, Alexa647:MG1Nb and F5M:RNb)

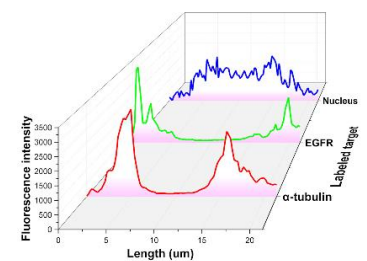
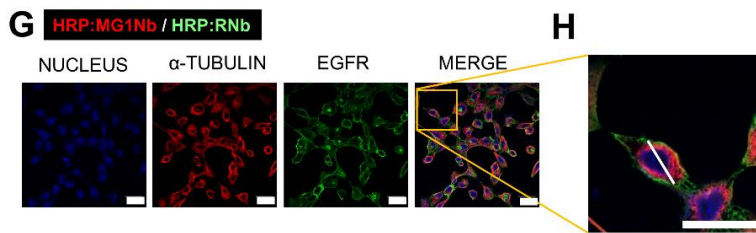
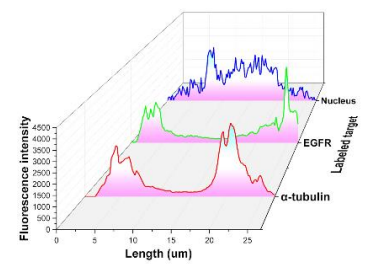
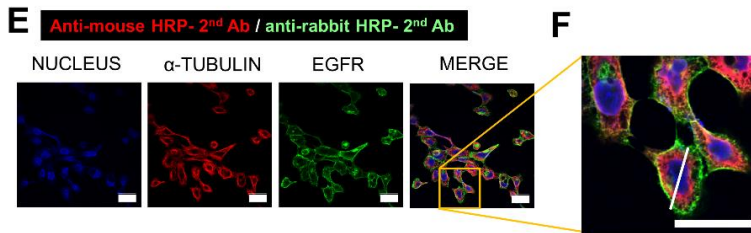
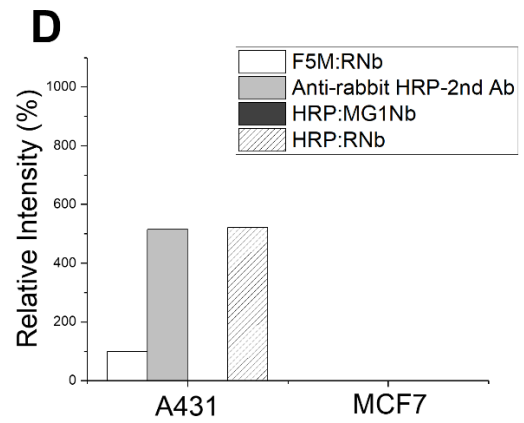
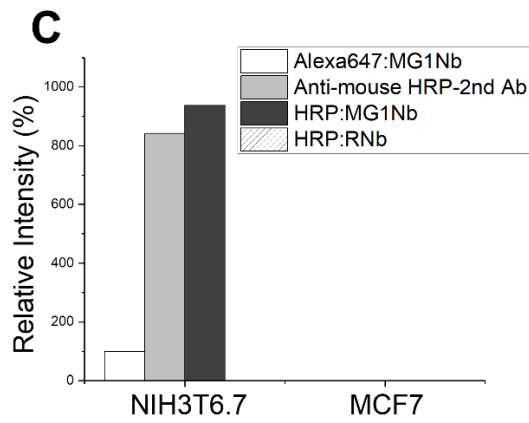
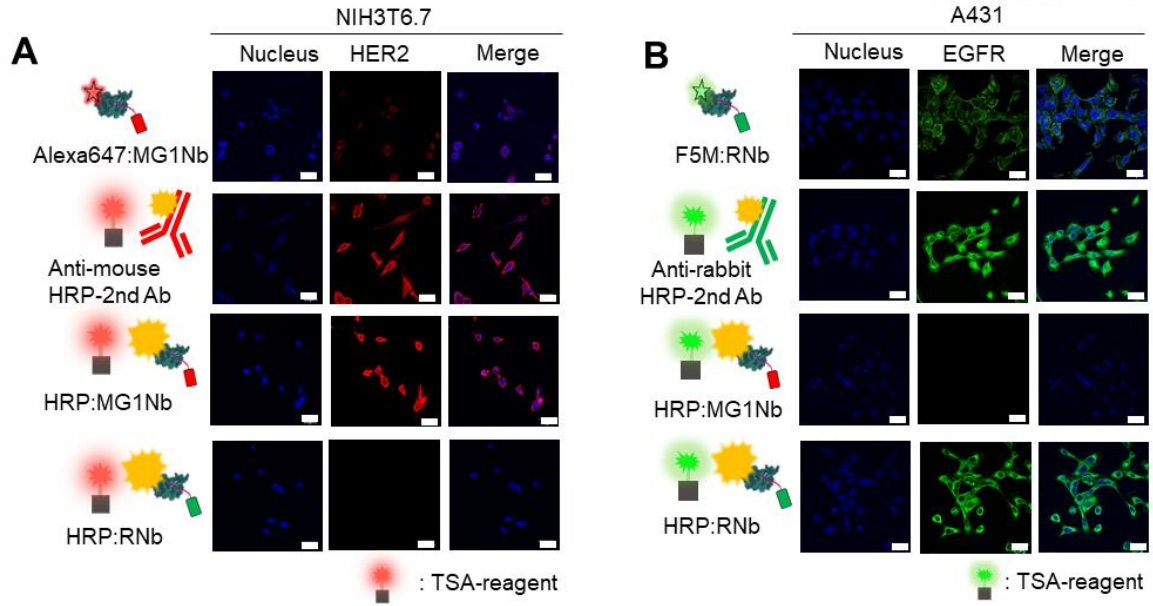


Figure 3.10 Fluorescent cell imaging and tyramide signal amplification (TSA) assays. (A) HER2 overexpressing NIH3T6.7 cells and (B) EGFR overexpressing A431 cells were probed with anti-HER2 mouse IgG1 and anti-EGFR rabbit IgG, respectively, and subsequently incubated with (A, top panels) Alexa647:MG1Nb or (B, top panels) F5M:RNb, or treated with (second panels) HRP-conjugated secondary antibodies, (third panels) HRP:MG1Nb, or (bottom panels) HRP:RNb in the presence of TSA reagent. Relative fluorescence intensity of dye-conjugated and TSA resultants in (C) NIH3T6.7 cells and (D) A431 cells were plotted. (E and G) A431 cells were probed with anti- α -tubulin mouse IgG1 and anti-EGFR rabbit IgG, simultaneously, and then incubated with (E) anti-mouse HRP-conjugated secondary antibody or (G) HRP:MG1Nb. Subsequently, previously bound signal amplifiers were inactivated with 3% H₂O₂ and (E) anti-rabbit HRP-conjugated secondary antibody or (G) HRP:RNb were then added. The fluorescence intensity correlations generated by (F) HRP-conjugated secondary antibodies and (H) HRP:Nbs were plotted by line scan analysis. (Scale bars: 30 μ m)

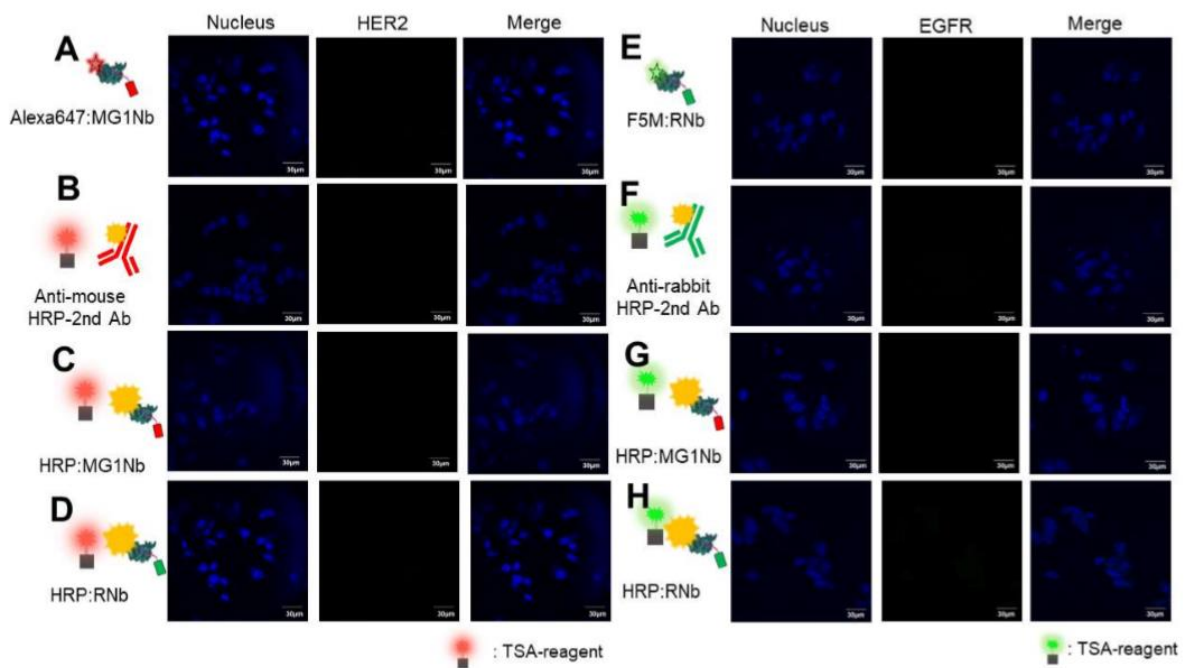


Figure 3.11 Tyramide signal amplification (TSA) assays with negative cells. HER2 and EGFR double negative MCF-7 cells were probed with (A – D) anti-HER2 mouse IgG1 and (E – H) anti-EGFR rabbit IgG, respectively, and subsequently incubated with (A) Alexa647-conjugated MG1Nb and (E) F5M-conjugated RNb, (B, F) HRP-conjugated secondary antibodies, (C, G) HRP:MG1Nb, or (D, H) HRP:RNb. For signal amplification, TSA reagents (Alexa 647 and Alexa 488 tyramides) were treated with HRP-conjugated secondary antibodies or HRP:Nbs incubated samples.

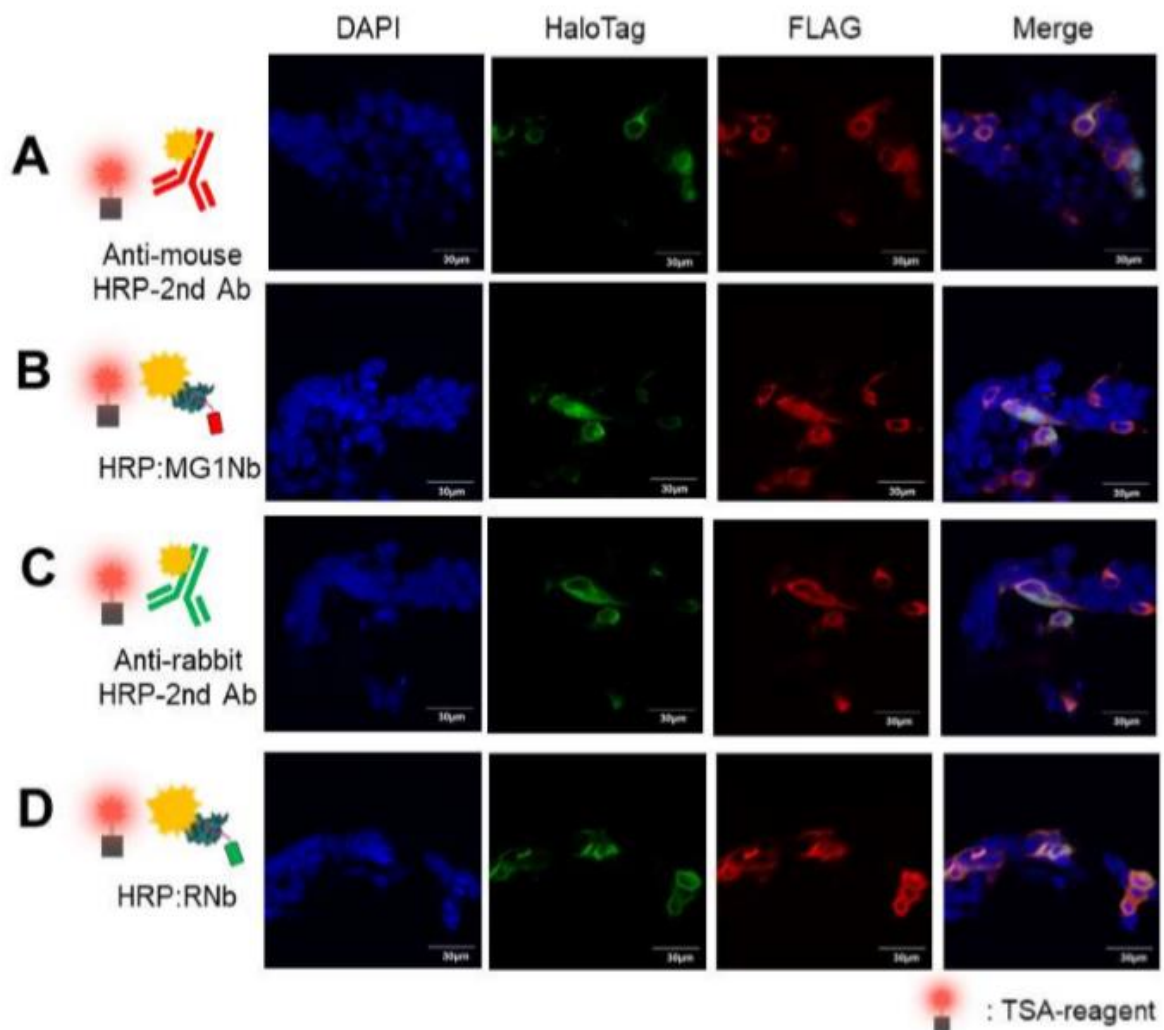


Figure 3.12 Tyramide signal amplification (TSA) assays in FLAG-HaloTag gene-transfected HEK293T cells. Transfected HEK293T cells were treated with HaloTag Oregon Green Ligands to confirm the expression of FLAG-HaloTag on the surface of cells, then probed with (A and B) anti-FLAG mouse IgG1 and (C and D) anti-FLAG rabbit IgG, respectively. For signal amplification, they were subsequently incubated with (A) anti-mouse HRP-conjugated secondary antibody, (B) HRP:MG1Nb, (C) anti-rabbit HRP-conjugated secondary antibody or (D) HRP:RNb in presence of TSA reagents.

HRP:MG1Nb and HRP:RNb efficiently penetrate *Xenopus* whole embryos and successfully amplify target protein signal in TSA assays

To investigate whether HRP:Nbs can be used in more complex and heterogeneous tissue TSA assays, we prepared *Xenopus laevis* whole embryos and performed TSA-based immunostaining with HRP:Nbs.^{92, 93} We tested several tissue-specific primary antibodies such as anti-skeletal muscle fiber mouse IgG1 (12/101)⁹⁴ and anti- α -tubulin rabbit IgG to visualize the muscle and the cilia, respectively, and then incubated the samples with either HRP-conjugated secondary antibodies or HRP:Nbs followed by a TSA assay. The fluorescence imaging analysis revealed that the HRP-conjugated secondary antibody and HRP:Nb selectively bound to the primary antibody (Figure 3.13A; top and middle panels, 3.13B; top and bottom panels), resulting in high target-specific signal amplification for whole embryo samples, whereas mismatched HRP:Nbs did not (Figure 3.13A; bottom panel, 3.13B; middle panel). These data imply that HRP:Nbs can efficiently penetrate tissue samples and selectively bind to the target-bound primary antibodies, resulting in high target-specific signal amplification. To demonstrate simultaneous detections of two different target molecules in the same sample with HRP:MG1Nb and HRP:RNb, we labeled two different targets (skeletal muscle fiber and α -tubulin) in the same whole embryo mount sample (Figure 3.13C and 3.13D). We treated the sample with two different primary antibodies as described above. Next, we performed a TSA assay with either HRP-conjugated secondary antibodies (Figure 3.13C) or HRP:Nbs (Figure 3.13D), which resulted in target-specific dual-color labeling. These data suggest that HRP:Nbs can be applied as dual-labeling reagents in localization studies of multiple target proteins combined with primary mouse and rabbit IgGs, even in thick and complex whole embryos.

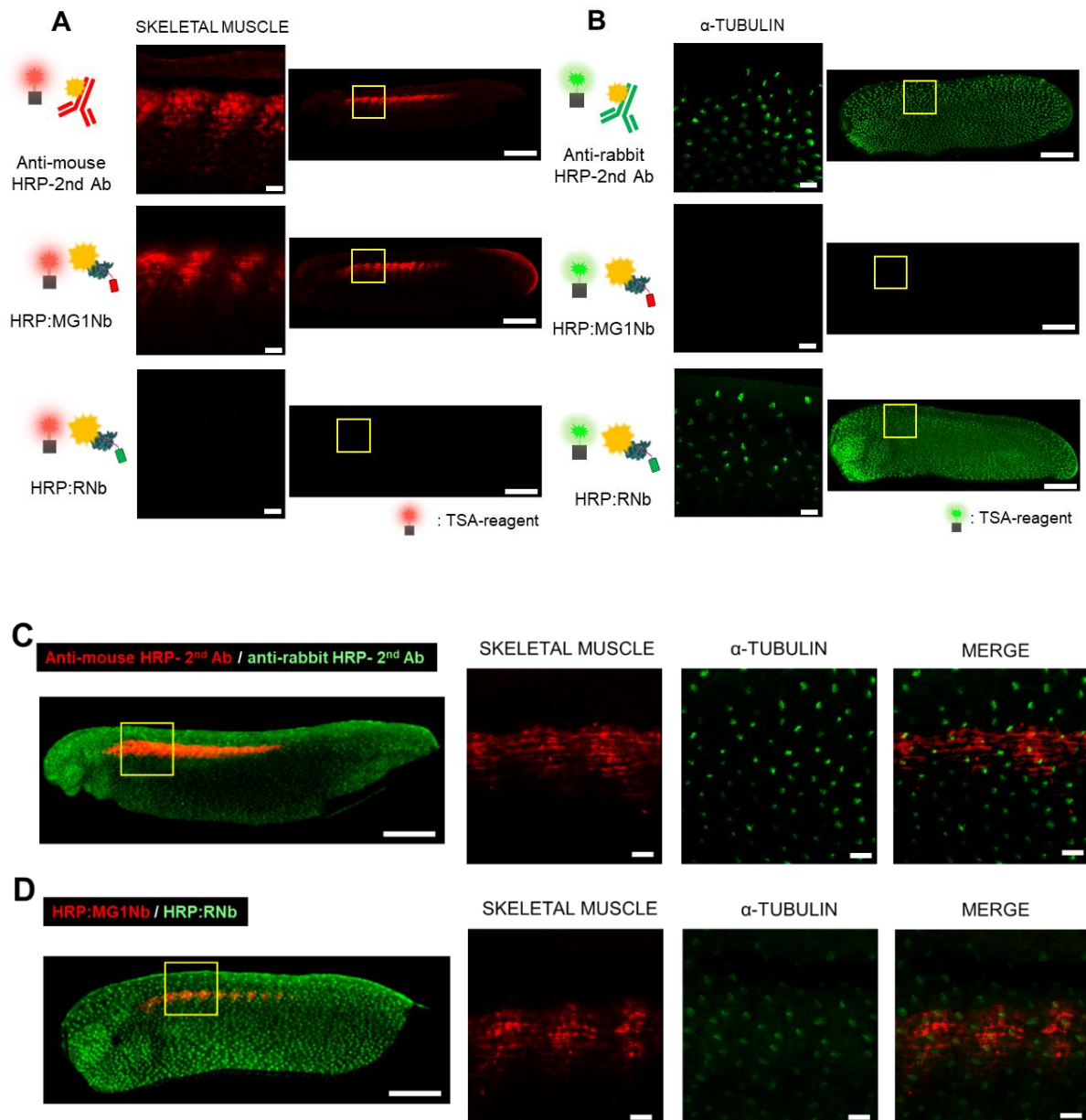


Figure 3.13 Tyramide signal amplification (TSA) assays in *Xenopus* whole embryos. *Xenopus* samples were probed with (A) anti-skeletal muscle fiber mouse IgG1 and (B) anti- α -tubulin rabbit IgG and then incubated with HRP-conjugated secondary antibodies (top panel), HRP:MG1Nb (middle panel) or HRP:RNb (bottom panel) in the presence of TSA reagents. (C and D) Samples were probed with anti-skeletal muscle fiber mouse IgG1 and anti- α -tubulin rabbit IgG, simultaneously, and then incubated with (C) anti-mouse HRP-conjugated secondary antibody or (D) HRP:MG1Nb in the presence of TSA reagents. After inactivation of previously bound HRP, (C) anti-rabbit HRP-conjugated secondary antibody or (D) HRP:RNb were added with fresh TSA reagent. Scale bars: 50 μ m (whole embryos sample: 500 μ m).

3.5 Conclusion

Here we established plug-and-playable HRP-conjugated recombinant IgG-binding signal enhancers with an excellent high binding affinity for mouse IgG1 and rabbit IgG, respectively, based on ST/SC protein ligation system. HRP was conjugated to an SC scaffold protein via a thiol-maleimide reaction, whereas two species-specific mouse IgG1-binding (MG1Nb) and rabbit IgG-binding nanobodies (RNb) were genetically fused to an ST peptide. The HRP-conjugated SCs were ligated to the individual ST-fused nanobodies, via a covalent isopeptide formation between ST and SC in a plug-and-playable manner, and we performed various types of immunoassays to verify their species-specific IgG-binding and signal amplification capabilities. In western blots and ELISA, both HRP-conjugated nanobodies (HRP:Nbs) specifically recognized target-bound mouse IgG1 and rabbit IgG, respectively, without detectable cross-reactivity. We obtained linear signal enhancement patterns correlating to the sample concentrations with HRP:Nbs using purified and complex cell lysate samples. HRP:Nbs generated signal intensities depending on each concentration, which is comparable to those of conventional HRP-conjugated secondary antibodies. They had species-specificity toward their corresponding IgGs and were applied for the simultaneous detection and visualization of two different target molecules within a single cell in TSA-based immunohistochemistry. Furthermore, HRP:Nbs penetrated the thick and complicated whole embryos as well as conventional HRP-conjugated secondary antibodies and could selectively label two different target molecules in a single whole embryo mount sample, allowing localization studies of multiple target proteins in a single cell or embryo. Although secondary antibodies possess very high specificity and affinity to primary antibodies, the production of secondary antibodies comes with high manufacturing costs and long preparation time due to live animals or mammalian cell culture systems. In contrast, IgG-binding nanobodies, inexpensively produced in large quantities in *E. coli*, do not require live animal production and can be conjugated to enzymes via the ST/SC system in a plug-and-playable manner. The recombinant signal-amplifying IgG-binders we have developed in this study may be reliable alternatives to conventional secondary antibodies in various immunoassays.

Chapter 4. Concluding Remarks

4.1 Summary and Conclusions

As stated in Chapter 1, I explained why qualitative and quantitative analyses of target biomolecules are important in cells. I then discussed various types of detecting tools in current research for visualization or quantitation of target biomolecules with several advantages and disadvantages. To apply functional proteins, functional proteins were suggested, and their background information was described.

My doctoral research thesis is to develop target-specific labeling nanoplatfoms based on functional proteins for application in fluorescence cell imaging and immunoassay.

In Chapter 2, I developed a tunable dual-functional (targeting and probing or two different targetings) Encap probes using bacterial glue, the ST/SC protein ligation system. I demonstrated its target-specific imaging capability with multiple combinations of targeting ligands and colors. I have prepared three types of tunable dual-functional Encap protein cage nanoparticles. Polyvalent affibody-conjugated Encap probes effectively recognize their target cancer cells visualizing specific target cancer cells. Dual functional Encap probes targeted and visualized their target cancer cells with multiple combinations between desired targeting ligands and desired colors. Besides, dual targeting Encap probes visualized two target cells individually without using a set of individual probes. This study suggests that the polyvalent nature of Encap allows us to display multiple functional proteins efficiently, and ST/SC bacterial glue makes it possible to post-translationally display the desired functional proteins in a mixing-and-matching manner on demand.

Lastly, in Chapter 3, I developed a target-specific signal enhancer to be applied in various immunoassays. HRP was conjugated to two different recombinant IgG binding nanobodies, respectively, using ST/SC protein ligation system, and their excellent high binding affinity was demonstrated. In western blots and ELISA, HRP conjugated nanobodies specifically recognized target-bound primary antibodies without cross-reactivity and exhibited linear signal amplification patterns correlating to the sample concentrations. Their species-specificity toward primary antibody allowed the simultaneous detection and visualization of two different target molecules within a single sample derived from cells and whole embryos. This study suggests that recombinant signal-amplifying IgG-binders perform as reliable alternatives to conventional secondary antibodies in various immunoassays.

References

1. Ueno, T.; Nagano, T., Fluorescent probes for sensing and imaging. *Nat Methods* **2011**, *8* (8), 642-5.
2. Terai, T.; Nagano, T., Fluorescent probes for bioimaging applications. *Curr Opin Chem Biol* **2008**, *12* (5), 515-21.
3. Zhu, H.; Fan, J.; Du, J.; Peng, X., Fluorescent Probes for Sensing and Imaging within Specific Cellular Organelles. *Acc Chem Res* **2016**, *49* (10), 2115-2126.
4. Becker, A.; Riefke, B.; Ebert, B.; Sukowski, U.; Rinneberg, H.; Semmler, W.; Licha, K., Macromolecular contrast agents for optical imaging of tumors: comparison of indotricarbocyanine-labeled human serum albumin and transferrin. *Photochem Photobiol* **2000**, *72* (2), 234-41.
5. Ogawa, M.; Kosaka, N.; Choyke, P. L.; Kobayashi, H., In vivo molecular imaging of cancer with a quenching near-infrared fluorescent probe using conjugates of monoclonal antibodies and indocyanine green. *Cancer Res* **2009**, *69* (4), 1268-1272.
6. Wei, W.; Li, D.; Cai, X.; Liu, Z.; Bai, Z.; Xiao, J., Highly specific recognition of denatured collagen by fluorescent peptide probes with the repetitive Gly-Pro-Pro and Gly-Hyp-Hyp sequences. *J Mater Chem B* **2020**.
7. Pleijhuis, R.; Crane, L.; van Oosten, M.; van Dam, G.; Ntziachristos, V., Optical Imaging Applications in Cancer Research and Treatment. *Cancer-Cares, Treatments and Preventions* **2014**.
8. Liss, V.; Barlag, B.; Nietschke, M.; Hensel, M., Self-labelling enzymes as universal tags for fluorescence microscopy, super-resolution microscopy and electron microscopy. *Sci Rep* **2015**, *5*, 17740.
9. Hoelzel, C. A.; Zhang, X., Visualizing and Manipulating Biological Processes by Using HaloTag and SNAP-Tag Technologies. *Chembiochem* **2020**, *21* (14), 1935-1946.
10. Brun, M. A.; Tan, K. T.; Nakata, E.; Hinner, M. J.; Johnsson, K., Semisynthetic Fluorescent Sensor Proteins Based on Self-Labeling Protein Tags. *Journal of the American Chemical Society* **2009**, *131* (16), 5873-5884.
11. Choi, H.; Liao, Y. C.; Lavis, L.; Young, Y. J.; Lippincott-Schwartz, J., Probing Dynamics of Proteins via Self-Labeling Tags. *Biophys J* **2018**, *114* (3), 667a-667a.
12. Gautier, A.; Nakata, E.; Lukinavicius, G.; Tan, K. T.; Johnsson, K., Selective Cross-Linking of Interacting Proteins Using Self-Labeling Tags. *Journal of the American Chemical Society* **2009**, *131* (49), 17954-17962.
13. Los, G. V.; Encell, L. P.; McDougall, M. G.; Hartzell, D. D.; Karassina, N.; Zimprich, C.; Wood, M. G.; Learish, R.; Ohana, R. F.; Urh, M.; Simpson, D.; Mendez, J.; Zimmerman, K.; Otto, P.; Vidugiris, G.; Zhu, J.; Darzins, A.; Klaubert, D. H.; Bulleit, R. F.; Wood, K. V., HaloTag: a novel protein labeling technology for cell imaging and protein analysis. *ACS*

Chem Biol **2008**, *3* (6), 373-82.

14. Charubin, K.; Streett, H.; Papoutsakis, E. T., Development of Strong Anaerobic Fluorescent Reporters for *Clostridium acetobutylicum* and *Clostridium ljungdahlii* Using HaloTag and SNAP-tag Proteins. *Appl Environ Microbiol* **2020**, *86* (20).
15. Wang, G. J.; Achim, C. L.; Hamilton, R. L.; Wiley, C. A.; Soontornniyomkij, V., Tyramide signal amplification method in multiple-label immunofluorescence confocal microscopy. *Methods* **1999**, *18* (4), 459-464.
16. Schonhuber, W.; Fuchs, B.; Juretschko, S.; Amann, R., Improved sensitivity of whole-cell hybridization by the combination of horseradish peroxidase-labeled oligonucleotides and tyramide signal amplification. *Appl Environ Microbiol* **1997**, *63* (8), 3268-73.
17. Li, J.; Wang, Y.; Chiu, S. L.; Cline, H. T., Membrane targeted horseradish peroxidase as a marker for correlative fluorescence and electron microscopy studies. *Front Neural Circuits* **2010**, *4*, 6.
18. Hopkins, C.; Gibson, A.; Stinchcombe, J.; Futter, C., Chimeric molecules employing horseradish peroxidase as reporter enzyme for protein localization in the electron microscope. *Methods Enzymol* **2000**, *327*, 35-45.
19. Gao, W.; Hu, C. M.; Fang, R. H.; Zhang, L., Liposome-like Nanostructures for Drug Delivery. *J Mater Chem B* **2013**, *1* (48).
20. Geers, B.; De Wever, O.; Demeester, J.; Bracke, M.; De Smedt, S. C.; Lentacker, I., Targeted liposome-loaded microbubbles for cell-specific ultrasound-triggered drug delivery. *Small* **2013**, *9* (23), 4027-35.
21. Jhaveri, A. M.; Torchilin, V. P., Multifunctional polymeric micelles for delivery of drugs and siRNA. *Front Pharmacol* **2014**, *5*, 77.
22. Zhang, W.; Shi, Y.; Chen, Y.; Ye, J.; Sha, X.; Fang, X., Multifunctional Pluronic P123/F127 mixed polymeric micelles loaded with paclitaxel for the treatment of multidrug resistant tumors. *Biomaterials* **2011**, *32* (11), 2894-906.
23. Han, G.; Ghosh, P.; Rotello, V. M., Functionalized gold nanoparticles for drug delivery. *Nanomedicine-Uk* **2007**, *2* (1), 113-123.
24. Han, G.; Ghosh, P.; Rotello, V. M., Multi-functional gold nanoparticles for drug delivery. *Bio-Applications of Nanoparticles* **2007**, *620*, 48-56.
25. Rosenholm, J. M.; Sahlgren, C.; Linden, M., Towards multifunctional, targeted drug delivery systems using mesoporous silica nanoparticles - opportunities & challenges. *Nanoscale* **2010**, *2* (10), 1870-1883.
26. Lima-Tenorio, M. K.; Pineda, E. A. G.; Ahmad, N. M.; Fessi, H.; Elaissari, A., Magnetic nanoparticles: In vivo cancer diagnosis and therapy. *Int J Pharmaceut* **2015**, *493* (1-2), 313-327.
27. Brigger, I.; Dubernet, C.; Couvreur, P., Nanoparticles in cancer therapy and diagnosis.

Advanced Drug Delivery Reviews **2002**, *54* (5), 631-651.

28. Uchida, M.; Klem, M. T.; Allen, M.; Suci, P.; Flenniken, M.; Gillitzer, E.; Varpness, Z.; Liepold, L. O.; Young, M.; Douglas, T., Biological containers: Protein cages as multifunctional nanoplatfoms. *Adv Mater* **2007**, *19* (8), 1025-1042.

29. Zdanowicz, M.; Chroboczek, J., Virus-like particles as drug delivery vectors. *Acta Biochim Pol* **2016**, *63* (3), 469-73.

30. Ma, Y.; Nolte, R. J.; Cornelissen, J. J., Virus-based nanocarriers for drug delivery. *Advanced drug delivery reviews* **2012**, *64* (9), 811-825.

31. Min, J.; Moon, H.; Yang, H. J.; Shin, H. H.; Hong, S. Y.; Kang, S., Development of P22 Viral Capsid Nanocomposites as Anti-Cancer Drug, Bortezomib (BTZ), Delivery Nanoplatfoms. *Macromol Biosci* **2014**, *14* (4), 557-564.

32. Wang, J. G.; Fang, T.; Li, M.; Zhang, W. J.; Zhang, Z. P.; Zhang, X. E.; Li, F., Intracellular delivery of peptide drugs using viral nanoparticles of bacteriophage P22: covalent loading and cleavable release. *Journal of Materials Chemistry B* **2018**, *6* (22), 3716-3726.

33. Ra, J. S.; Shin, H. H.; Kang, S.; Do, Y., Lumazine synthase protein cage nanoparticles as antigen delivery nanoplatfoms for dendritic cell-based vaccine development. *Clin Exp Vaccine Res* **2014**, *3* (2), 227-34.

34. Moon, H.; Lee, J.; Min, J.; Kang, S., Developing genetically engineered encapsulin protein cage nanoparticles as a targeted delivery nanoplatfom. *Biomacromolecules* **2014**, *15* (10), 3794-3801.

35. Jones, J. A.; Giessen, T. W., Advances in encapsulin nanocompartment biology and engineering. *Biotechnol Bioeng* **2020**.

36. Choi, B.; Kim, H.; Choi, H.; Kang, S., Protein Cage Nanoparticles as Delivery Nanoplatfoms. *Biomimetic Medical Materials: From Nanotechnology to 3d Bioprinting* **2018**, *1064*, 27-43.

37. Kremers, G. J.; Gilbert, S. G.; Cranfill, P. J.; Davidson, M. W.; Piston, D. W., Fluorescent proteins at a glance. *J Cell Sci* **2011**, *124* (Pt 2), 157-60.

38. Lee, J.; Song, E. K.; Bae, Y.; Min, J.; Rhee, H. W.; Park, T. J.; Kim, M.; Kang, S., An enhanced ascorbate peroxidase 2/antibody-binding domain fusion protein (APEX2-ABD) as a recombinant target-specific signal amplifier. *Chem Commun* **2015**, *51* (54), 10945-10948.

39. Chen, C. L.; Hu, Y. H.; Udeshi, N. D.; Lau, T. Y.; Wirtz-Peitz, F.; He, L.; Ting, A. Y.; Carr, S. A.; Perrimon, N., Proteomic mapping in live *Drosophila* tissues using an engineered ascorbate peroxidase. *P Natl Acad Sci USA* **2015**, *112* (39), 12093-12098.

40. England, C. G.; Ehlerding, E. B.; Cai, W., NanoLuc: A Small Luciferase Is Brightening Up the Field of Bioluminescence. *Bioconjug Chem* **2016**, *27* (5), 1175-1187.

41. Gao, J.; Chen, K.; Miao, Z.; Ren, G.; Chen, X.; Gambhir, S. S.; Cheng, Z., Affibody-

- based nanoprobe for HER2-expressing cell and tumor imaging. *Biomaterials* **2011**, 32 (8), 2141-2148.
42. Löfblom, J.; Feldwisch, J.; Tolmachev, V.; Carlsson, J.; Ståhl, S.; Frejd, F. Y., Affibody molecules: engineered proteins for therapeutic, diagnostic and biotechnological applications. *FEBS letters* **2010**, 584 (12), 2670-2680.
 43. Stahl, S.; Graslund, T.; Eriksson Karlstrom, A.; Frejd, F. Y.; Nygren, P. A.; Lofblom, J., Affibody Molecules in Biotechnological and Medical Applications. *Trends Biotechnol* **2017**, 35 (8), 691-712.
 44. De, A.; Kuppusamy, G.; Karri, V., Affibody molecules for molecular imaging and targeted drug delivery in the management of breast cancer. *Int J Biol Macromol* **2018**, 107 (Pt A), 906-919.
 45. Frejd, F. Y.; Kim, K. T., Affibody molecules as engineered protein drugs. *Exp Mol Med* **2017**, 49 (3), e306.
 46. Siontorou, C. G., Nanobodies as novel agents for disease diagnosis and therapy. *Int J Nanomed* **2013**, 8, 4215-4227.
 47. Cortez-Retamozo, V.; Backmann, N.; Senter, P. D.; Wernery, U.; De Baetselier, P.; Muyldermans, S.; Revets, H., Efficient cancer therapy with a nanobody-based conjugate. *Cancer Res* **2004**, 64 (8), 2853-2857.
 48. Muyldermans, S.; Baral, T. N.; Retarnozzo, V. C.; De Baetselier, P.; De Genst, E.; Kinne, J.; Leonhardt, H.; Magez, S.; Nguyen, V. K.; Revets, H.; Rothbauer, U.; Stijemans, B.; Tillib, S.; Wernery, U.; Wyns, L.; Hassanzadeh-Ghassabeh, G.; Saerens, D., Camelid immunoglobulins and nanobody technology. *Vet Immunol Immunop* **2009**, 128 (1-3), 178-183.
 49. Pleiner, T.; Bates, M.; Gorlich, D., A toolbox of anti-mouse and anti-rabbit IgG secondary nanobodies. *J Cell Biol* **2018**, 217 (3), 1143-1154.
 50. Zakeri, B.; Fierer, J. O.; Celik, E.; Chittock, E. C.; Schwarz-Linek, U.; Moy, V. T.; Howarth, M., Peptide tag forming a rapid covalent bond to a protein, through engineering a bacterial adhesin. *P Natl Acad Sci USA* **2012**, 109 (12), E690-E697.
 51. Reddington, S. C.; Howarth, M., Secrets of a covalent interaction for biomaterials and biotechnology: SpyTag and SpyCatcher. *Curr Opin Chem Biol* **2015**, 29, 94-9.
 52. Enterina, J. R.; Wu, L.; Campbell, R. E., Emerging fluorescent protein technologies. *Current opinion in chemical biology* **2015**, 27, 10-17.
 53. Komatsu, T.; Johnsson, K.; Okuno, H.; Bito, H.; Inoue, T.; Nagano, T.; Urano, Y., Real-time measurements of protein dynamics using fluorescence activation-coupled protein labeling method. *Journal of the American Chemical Society* **2011**, 133 (17), 6745-6751.
 54. Wang, R. E.; Niu, Y.; Wu, H.; Amin, M. N.; Cai, J., Development of NGR peptide-based agents for tumor imaging. *American journal of nuclear medicine and molecular imaging* **2011**, 1 (1), 36.

55. Olson, E. S.; Jiang, T.; Aguilera, T. A.; Nguyen, Q. T.; Ellies, L. G.; Scadeng, M.; Tsien, R. Y., Activatable cell penetrating peptides linked to nanoparticles as dual probes for in vivo fluorescence and MR imaging of proteases. *Proceedings of the National Academy of Sciences* **2010**, *107* (9), 4311-4316.
56. Lyakhov, I.; Zielinski, R.; Kuban, M.; Kramer-Marek, G.; Fisher, R.; Chertov, O.; Bindu, L.; Capala, J., HER2-and EGFR-Specific Affiprobe: Novel Recombinant Optical Probes for Cell Imaging. *Chembiochem* **2010**, *11* (3), 345-350.
57. Ardeshipour, Y.; Chernomordik, V.; Zielinski, R.; Capala, J.; Griffiths, G.; Vasalatiy, O.; Smirnov, A. V.; Knutson, J. R.; Lyakhov, I.; Achilefu, S.; Amir, G.; Moinuddin, H., In vivo fluorescence lifetime imaging monitors binding of specific probes to cancer biomarkers. *PloS one* **2012**, *7* (2), e31881.
58. Han, J.-A.; Kang, Y. J.; Shin, C.; Ra, J.-S.; Shin, H.-H.; Hong, S. Y.; Do, Y.; Kang, S., Ferritin protein cage nanoparticles as versatile antigen delivery nanoplatforams for dendritic cell (DC)-based vaccine development. *Nanomedicine: Nanotechnology, Biology and Medicine* **2014**, *10* (3), 561-569.
59. Lucon, J.; Qazi, S.; Uchida, M.; Bedwell, G. J.; LaFrance, B.; Prevelige Jr, P. E.; Douglas, T., Use of the interior cavity of the P22 capsid for site-specific initiation of atom-transfer radical polymerization with high-density cargo loading. *Nature chemistry* **2012**, *4* (10), 781.
60. Patterson, D. P.; Rynda-Apple, A.; Harmsen, A. L.; Harmsen, A. G.; Douglas, T., Biomimetic antigenic nanoparticles elicit controlled protective immune response to influenza. *ACS nano* **2013**, *7* (4), 3036-3044.
61. Kang, Y. J.; Park, D. C.; Shin, H.-H.; Park, J.; Kang, S., Incorporation of thrombin cleavage peptide into a protein cage for constructing a protease-responsive multifunctional delivery nanoplatforam. *Biomacromolecules* **2012**, *13* (12), 4057-4064.
62. Banerjee, D.; Liu, A. P.; Voss, N. R.; Schmid, S. L.; Finn, M., Multivalent display and receptor-mediated endocytosis of transferrin on virus-like particles. *Chembiochem* **2010**, *11* (9), 1273-1279.
63. Rurup, W. F.; Snijder, J.; Koay, M. S.; Heck, A. J.; Cornelissen, J. J., Self-sorting of foreign proteins in a bacterial nanocompartment. *Journal of the American Chemical Society* **2014**, *136* (10), 3828-3832.
64. Sutter, M.; Boehringer, D.; Gutmann, S.; Günther, S.; Prangishvili, D.; Loessner, M. J.; Stetter, K. O.; Weber-Ban, E.; Ban, N., Structural basis of enzyme encapsulation into a bacterial nanocompartment. *Nature Structural and Molecular Biology* **2008**, *15* (9), 939.
65. Hicks, P. M.; Rinker, K. D.; Baker, J. R.; Kelly, R. M., Homomultimeric protease in the hyperthermophilic bacterium *Thermotoga maritima* has structural and amino acid sequence homology

to bacteriocins in mesophilic bacteria. *FEBS letters* **1998**, *440* (3), 393-398.

66. Choi, B.; Moon, H.; Hong, S. J.; Shin, C.; Do, Y.; Ryu, S.; Kang, S., Effective Delivery of Antigen-Encapsulin Nanoparticle Fusions to Dendritic Cells Leads to Antigen-Specific Cytotoxic T Cell Activation and Tumor Rejection. *ACS Nano* **2016**, *10* (8), 7339-50.

67. Moon, H.; Lee, J.; Kim, H.; Heo, S.; Min, J.; Kang, S., Genetically engineering encapsulin protein cage nanoparticle as a SCC-7 cell targeting optical nanoprobe. *Biomaterials research* **2014**, *18* (1), 21.

68. Smith, M. L.; Lindbo, J. A.; Dillard-Telm, S.; Brosio, P. M.; Lasnik, A. B.; McCormick, A. A.; Nguyen, L. V.; Palmer, K. E., Modified tobacco mosaic virus particles as scaffolds for display of protein antigens for vaccine applications. *Virology* **2006**, *348* (2), 475-88.

69. Zhou, H. X., Loops, linkages, rings, catenanes, cages, and crowders: entropy-based strategies for stabilizing proteins. *Acc Chem Res* **2004**, *37* (2), 123-30.

70. Moon, H.; Bae, Y.; Kim, H.; Kang, S., Plug-and-playable fluorescent cell imaging modular toolkits using the bacterial superglue, SpyTag/SpyCatcher. *Chem Commun* **2016**, *52* (97), 14051-14054.

71. Pessino, V.; Citron, Y. R.; Feng, S. Y.; Huang, B., Covalent Protein Labeling by SpyTag-SpyCatcher in Fixed Cells for Super-Resolution Microscopy. *Chembiochem* **2017**, *18* (15), 1492-1495.

72. Moon, H.; Kim, W. G.; Lim, S.; Kang, Y. J.; Shin, H.-H.; Ko, H.; Hong, S. Y.; Kang, S., Fabrication of uniform layer-by-layer assemblies with complementary protein cage nanobuilding blocks via simple His-tag/metal recognition. *Journal of Materials Chemistry B* **2013**, *1* (35), 4504-4510.

73. Min, J.; Song, E. K.; Kim, H.; Kim, K. T.; Park, T. J.; Kang, S., A Recombinant Secondary Antibody Mimic as a Target-specific Signal Amplifier and an Antibody Immobilizer in Immunoassays. *Sci Rep-Uk* **2016**, *6*, 1-10.

74. Kang, H. J.; Kang, Y. J.; Lee, Y.-M.; Shin, H.-H.; Chung, S. J.; Kang, S., Developing an antibody-binding protein cage as a molecular recognition drug modular nanoplatform. *Biomaterials* **2012**, *33* (21), 5423-5430.

75. Nair, D. P.; Podgórski, M.; Chatani, S.; Gong, T.; Xi, W.; Fenoli, C. R.; Bowman, C. N., The thiol-Michael addition click reaction: a powerful and widely used tool in materials chemistry. *Chemistry of Materials* **2013**, *26* (1), 724-744.

76. Schoene, C.; Fierer, J. O.; Bennett, S. P.; Howarth, M., SpyTag/SpyCatcher Cyclization Confers Resilience to Boiling on a Mesophilic Enzyme. *Angew Chem Int Edit* **2014**, *53* (24), 6101-6104.

77. Shang, J.; Zrazhevskiy, P.; Postupna, N.; Keene, C. D.; Montine, T. J.; Gao, X. H., Multiplexed In-cell Immunoassay for Same-sample Protein Expression Profiling. *Sci Rep-Uk* **2015**, *5*, 1-12.

78. Carter, P., Improving the efficacy of antibody-based cancer therapies. *Nat Rev Cancer* **2001**, *1*

(2), 118-129.

79. Grandi, A.; Parri, M.; Campagnoli, S.; Nogarotto, R.; De Camilli, E.; Naldi, I.; Cinti, C.; Sarmientos, P.; Grandi, G.; Terracciano, L.; Viale, G.; Pileri, P.; Grifantini, R. M., Novel targets and monoclonal antibodies for cancer therapy. *Cancer Res* **2013**, *73* (8), 5533.

80. von Mehren, M.; Adams, G. P.; Weiner, L. M., Monoclonal antibody therapy for cancer. *Annu Rev Med* **2003**, *54*, 343-369.

81. Braisted, A. C.; Wells, J. A., Minimizing a binding domain from protein A. *P Natl Acad Sci USA* **1996**, *93* (12), 5688-5692.

82. Jeong, S.; Heu, W.; Kim, J. W.; Kim, H. S., Protein Binders Specific for Immunoglobulin G from Different Species for Immunoassays and Multiplex Imaging. *Anal Chem* **2016**, *88* (23), 11938-11945.

83. Ferrari, D.; Garrapa, V.; Locatelli, M.; Bolchi, A., A Novel Nanobody Scaffold Optimized for Bacterial Expression and Suitable for the Construction of Ribosome Display Libraries. *Mol Biotechnol* **2019**, 43-55.

84. Tijink, B. M.; Laeremans, T.; Budde, M.; Walsum, M. S. V.; Dreier, T.; de Haard, H. J.; Leemans, C. R.; van Dongen, G. A. M. S., Improved tumor targeting of anti-epidermal growth factor receptor Nanobodies through albumin binding: taking advantage of modular Nanobody technology. *Mol Cancer Ther* **2008**, *7* (8), 2288-2297.

85. Vincke, C.; Loris, R.; Saerens, D.; Martinez-Rodriguez, S.; Muyldermans, S.; Conrath, K., General Strategy to Humanize a Camelid Single-domain Antibody and Identification of a Universal Humanized Nanobody Scaffold. *J Biol Chem* **2009**, *284* (5), 3273-3284.

86. Kim, H.; Kang, Y. J.; Min, J.; Choi, H.; Kang, S., Development of an antibody-binding modular nanoplatfor for antibody-guided targeted cell imaging and delivery. *Rsc Adv* **2016**, *6* (23), 19208-19213.

87. Vashist, S. K.; Dixit, C. K.; MacCraith, B. D.; O'Kennedy, R., Effect of antibody immobilization strategies on the analytical performance of a surface plasmon resonance-based immunoassay. *Analyst* **2011**, *136* (21), 4431-4436.

88. Jung, Y. W.; Kang, H. J.; Lee, J. M.; Jung, S. O.; Yun, W. S.; Chung, S. J.; Chung, B. H., Controlled antibody immobilization onto immunoanalytical platforms by synthetic peptide. *Anal Biochem* **2008**, *374* (1), 99-105.

89. Leslie, B. J.; Hergenrother, P. J., Identification of the cellular targets of bioactive small organic molecules using affinity reagents. *Chem Soc Rev* **2008**, *37* (7), 1347-1360.

90. Spizzo, G.; Went, P.; Dirnhofer, S.; Obrist, P.; Moch, H.; Baeuerle, P. A.; Mueller-Holzner, E.; Marth, C.; Gastl, G.; Zeimet, A. G., Overexpression of epithelial cell adhesion molecule (Ep-CAM) is an independent prognostic marker for reduced survival of patients with

epithelial ovarian cancer. *Gynecol Oncol* **2006**, *103* (2), 483-488.

91. Bobrow, M. N.; Litt, G. J.; Shaughnessy, K. J.; Mayer, P. C.; Conlon, J., The Use of Catalyzed Reporter Deposition as a Means of Signal Amplification in a Variety of Formats. *J Immunol Methods* **1992**, *150* (1-2), 145-149.

92. Kieserman, E. K.; Lee, C.; Gray, R. S.; Park, T. J.; Wallingford, J. B., High-magnification in vivo imaging of *Xenopus* embryos for cell and developmental biology. *Cold Spring Harb Protoc* **2010**, *2010* (5), pdb-prot5427.

93. Lee, C.; Kieserman, E.; Gray, R. S.; Park, T. J.; Wallingford, J., Whole-mount fluorescence immunocytochemistry on *Xenopus* embryos. *CSH Protoc* **2008**, *2008*, pdb-prot4957.

94. Kintner, C. R.; Brockes, J. P., Monoclonal-Antibodies Identify Blastemal Cells Derived from Dedifferentiating Muscle in Newt Limb Regeneration. *Nature* **1984**, *308* (5954), 67-69.

Acknowledgements

가장 먼저, 지난 5년 6개월 간 박사 과정을 무탈하게 마칠 수 있게 많은 도움 주신 강세병 교수님께 진심으로 감사합니다. 교수님의 뜻 깊은 조언으로 의미 있는 성과를 낼 수 있었습니다. 또한, 바쁘신 와중에 1, 2차 committee meeting 과 최종 논문 심사를 위해 시간 내주시고 많은 코멘트 주신 박태주 교수님, 박찬영 교수님, 채영찬 교수님, 박종남 교수님께 진심으로 감사드립니다.

함께 동거 동락한 실험실 멤버들에게도 감사의 인사를 전합니다. 먼저, 졸업하신 선배님들이 닦아 놓은 길 위에서 편하게 연구할 수 있어서 감사합니다. 그리고 오랫동안 함께 했던 선배인 김한솔 박사님! 우리 실험실 분위기 메이커로서, 모두들 즐겁게 잘 지낼 수 있게 도움 주셔서 감사합니다. 미국에 가서 많은 경험과 실적 쌓아서 돌아오길 바랍니다. 대학원 동기인 최혁준 오빠! 연구 분야는 달랐지만, 필요할 때 코멘트 잘 해줘서 감사합니다. 차기 랩장으로서, 실험실 잘 이끌어가고 마지막까지 정리 잘해서 졸업 잘하길 바랍니다. 그리고, 너무 엉뚱해서 당황스럽지만 이제는 어느정도 인간미가 보이는 박성국! 논문 빨리 내고 졸업 잘해서 시골 촌동네를 벗어나길 바랍니다. 엄살 잘 부리는 찡찌이 엄수민! 남은 기간동안 잘 버티고 잘 헤쳐 나가서 원하는 사이언스 저널에 논문을 내도록 노력하십시오. 좋은 성과로 졸업하길 기원합니다. 그리고 우리 실험실에서 유일하게 외향적인 전희진! 소심하고 모자란 오빠들을 데리고 즐거운 실험실 생활이 될 수 있도록 기원하고 좋은 성과로 졸업하길 바랍니다. 그 동안 모두들 저의 잔소리를 잘 들어줘서 감사합니다. 모든 것들이 연구하는데 큰 도움이 되길 바랍니다. 필요한 것들이 있으면 언제든지 연락하십시오.

또한, 힘들지만 즐겁게 인생을 살아가는 우리 가족에게 감사드립니다. 항상 인생을 긍정적으로 바라볼 수 있도록 많은 사랑 주신 부모님께 감사합니다. 앞으로 받은 만큼 베풀 수 있는 사람이 되도록 노력하겠습니다. 하나 밖에 없는 여동생 윤현아, 나이 차이는 많이 나지만 오히려 언니처럼 든든하게 옆에 있어줘서 많은 의지가 되었다. 앞으로 하고 싶은 일 하면서 즐겁게 살길 바란다. 우리집 막내 한경아, 즐겁게 공부하고 원하는 꿈을 이룰 수 있길 바란다.

마지막으로, 11년이라는 긴 기간 동안 제 옆을 지켜준 경룡이에게 감사드립니다. 제가 항상 의지할 수 있고 마음 편하게 연구할 수 있는 데 큰 힘이 되어 주어서 고마워. 앞으로 즐거운 인생 함께 살아가도록 노력하자.

이 외에도 제가 살아오는 동안 크고 작은 도움을 주신 모든 분들께 감사드리며, 모두들 행복한 인생을 살아가길 바랍니다.

2020.11.25

배윤지 드림

Appendix A
Microperoxidase study

A. Microperoxidase study

A.1 Introduction

Microperoxidases are introduced as one of the signal-generating enzymes. Microperoxidase is biosynthetic heme-peptide conjugates employed as models for heme protein active sites and catalysts and for charge-transfer chromophores with potential applications biosensors and electron carriers.^{1, 2} Heme is covalently attached to the peptide via thioether bonds to two cysteine residues within a Cys-X-X-Cys-His (CXXCH) motif. Microperoxidases with different amino acid sequences are derived from various organisms containing cytochrome *c* and produced by proteolytic digestion.^{3, 4} The *E. coli* cytochrome *c* maturation (*Ccm*) proteins are required to attach the heme to CXXCH motif.^{5, 6} Heme and the apoprotein are synthesized in the *E. coli* cytoplasm, and both are translocated to the periplasm, where the protein's signal sequence is cleaved.⁷ The resulting proteins have heme (Figure A1). For further study, microperoxidase fusion proteins were established and purified to be applied in enzyme-mediated signal enhancement.

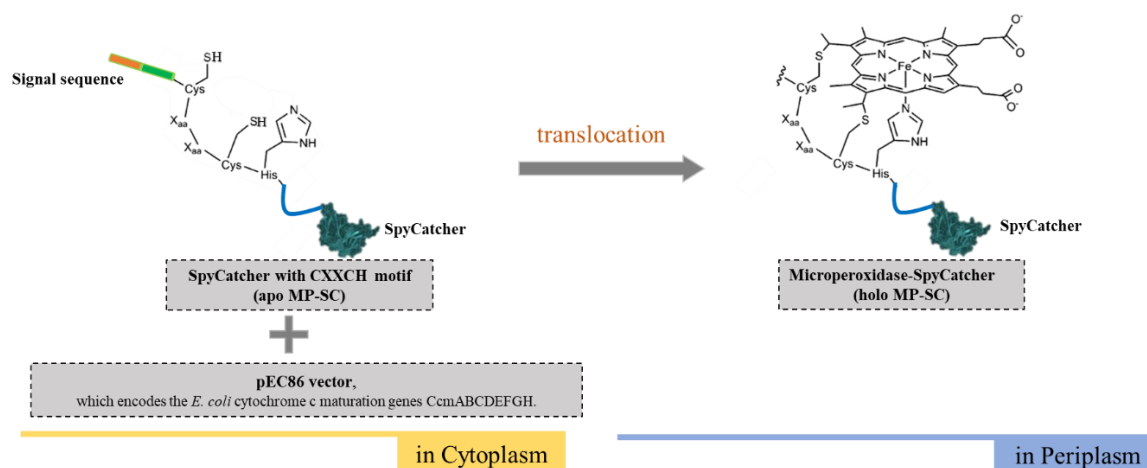


Figure A1. Schematic representation of the heme attachment process mediated by the Ccm system

A.2 Purification of microperoxidase fusion proteins

Microperoxidase was fused to SpyCatcher (MP-SC), and its activity was validated through an enzyme activity test. MP-SC was inserted into the pETDuet plasmid with an additional signal sequence, which is essential for translocation to the periplasm.⁸ Initially, as a proof of concept, the pETDuet plasmid encoding holo MP-SC with or without signal sequence was co-transformed with or without pEC86 vector encoding the *E. coli* cytochrome *c* maturation genes *CcmABCDEFGH* (Figure A2). All constructs had HisTag at the C-terminus of MP-SC for purification. They were well overexpressed and purified at a high concentration using Ni-NTA chromatography.⁹ When MP-SCs were overexpressed together with pEC86 vector and signal sequence, they only showed a dark red colored pellet. As

expected, both signal sequence and *CcmABCDEFGHIH* are essential for heme maturation to CXXCH motif.

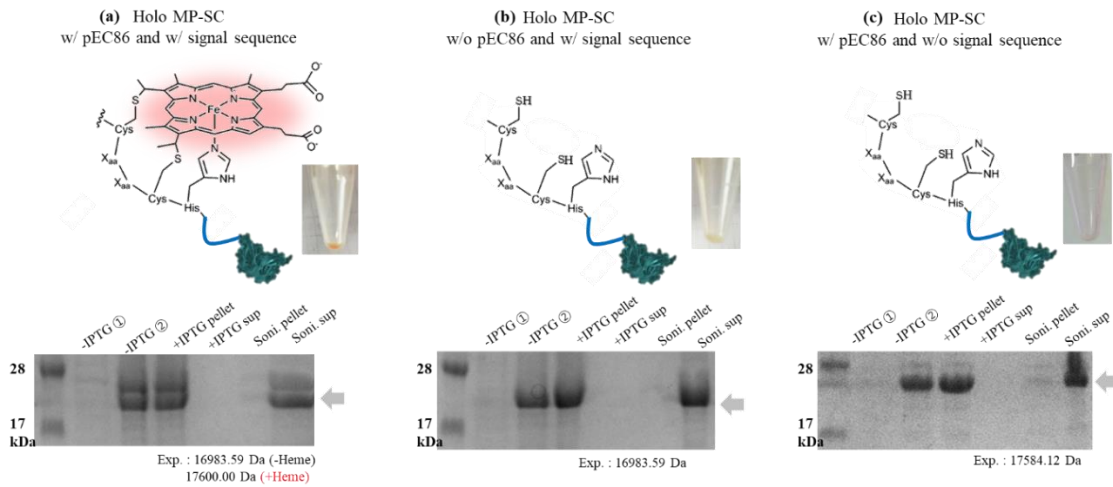


Figure A2. Expression test of microperoxidase fusion proteins

A.3 Characterization of microperoxidase fusion proteins

The mass value of purified proteins was determined by mass spectrometry. Two mass values were detected – heme incorporated or not incorporated MP-SC (Figure A3a). Next, heme incorporation ratios were confirmed using UV/vis spectroscopy (Figure A3b). The absorbance of heme shows a maximum at 404 nm. The absorbances were detected and calculated at 280 nm and 404 nm to confirm how much heme binds to MP-SC using the respective extinction coefficient. 16 % of the total purified MP-SC contains heme. Therefore, pure heme attached MP-SC should be purified using several purification methods.

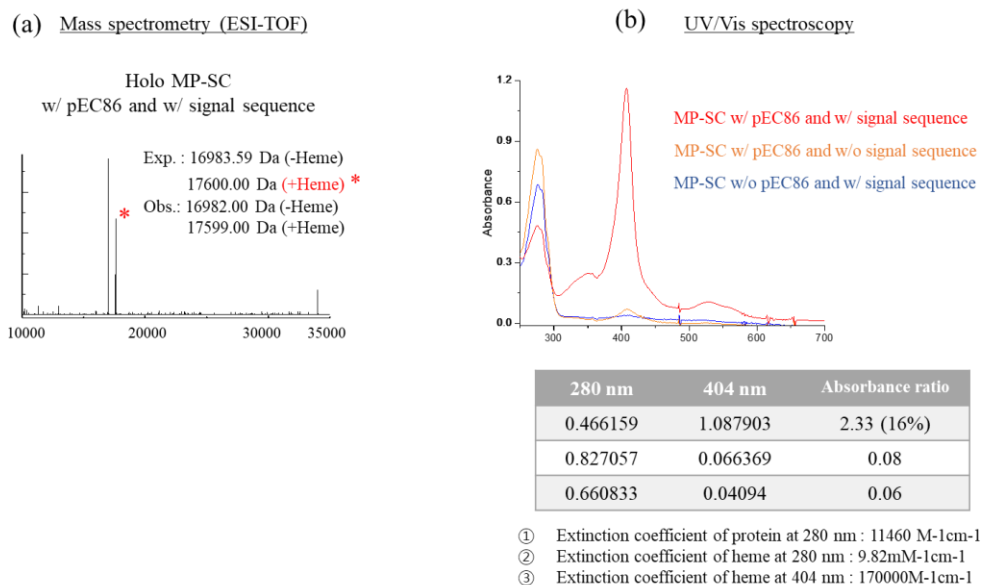


Figure A3. Characterization of microperoxidase-SpyCatcher

A.4 Catalytic activity of microperoxidase fusion proteins.

The catalytic activity of MP-SC was compared to that of HRP in a concentration dependent manner. The concentration of the enzyme was determined as heme concentration using UV/vis spectroscopy. TMB substrates were loaded in an enzyme-loaded plate. After 1 min, the absorbance was measured at 450nm using a plate reader. MP-SC showed 1000 times lower activity than HRP.

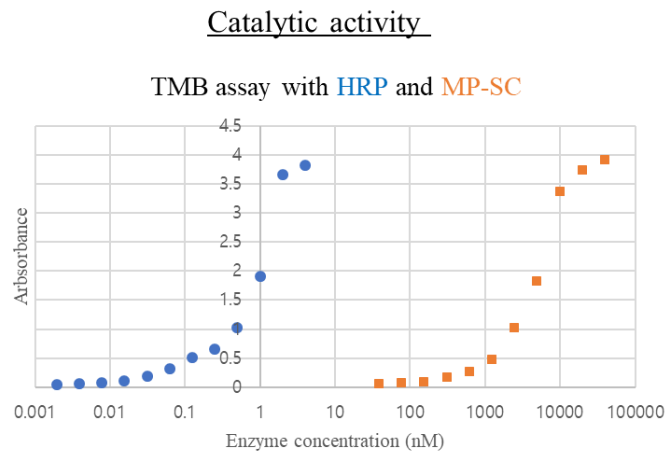


Figure A4. Comparison of catalytic activity of peroxidases

Appendix B

Target-specific Labeling Tools to Detect Intracellular Proteins

B. Target-specific Labeling Tools to Detect Intracellular Proteins

B.1 Introduction

The selective detection of intracellular target proteins is important but challenging, and their microscopic visualization has become a powerful tool to understand molecular and cellular processes. First, target proteins can be detected by fusing protein domains that can generate fluorescence or luminescence as fluorescent reporters. However, large structured tags such as fluorescent proteins, GFP can affect the location and function of the tagged proteins.¹⁰ An alternative method of visualizing proteins in cells is to use target-specific fluorescent probes by combining fluorescent molecules with targeting ligands, including antibodies, targeting peptides, or affibody molecules.¹¹ Epitope tags, short peptides that can be recognized by targeting ligands, such as antibodies, are widely used in fluorescent labeling for microscopy analysis, especially in numerous cases where high-quality antibodies are directed against the target protein are unavailable. High specificity and efficiency of fluorescent probes against epitope tags are essential for successful detection and visualization of target proteins. The FLAG®, myc- and HA-tags have often been used for immunostainings. Still, due to the large size of the antibodies used as binders, they are suboptimal for super-resolution microscopy and exceedingly difficult to express within cells. Besides, self-labeling enzymes can be genetically fused with target proteins for labeling such as HaloTag, SNAP-tag, and BL tag.¹² They can form covalent linkages to exogenously added fluorescent ligand and allow microscopic investigations of the labeled fusion proteins. In this case, we should change suitable ligand according to the system to be applied. Also, the size of these tags can cause resolution problems in super-resolution microscopy.

To solve these limitations, we introduced SpyTag/SpyCatcher (ST/SC) protein ligation system, which was used to label target protein site-specifically in cells. SpyTag peptide and SpyCatcher protein recognize each other and form the covalent isopeptide bond with high affinity.^{13,14} SpyTag can be fused to a target protein with minimal risk of disrupting target function. SpyCatcher can be modified to be chemically conjugated with fluorophore by adding active amino acid such as cysteine.¹³ SpyTagged target proteins were recognized by fluorophore-conjugated SpyCatcher and detected by fluorescent cell imaging, in the cytoplasm and the organelle lumen, respectively. In this study, site-specific labeling tools were developed to visualize the protein localization in the cell using SpyTag/SpyCatcher.

B.2 Results and Discussion

Various proteins in subcellular organelles are labeled by SpyTag/SpyCatcher.

To examine whether SC could be ligated to ST in the cell, we utilized SC as a scaffold protein and substituted serine residue at position 10 of SC with cysteine (SC_{S10C}) to a conjugate fluorescent dye. SC_{S10C} was overexpressed in bacteria and purified with simple one-step Ni-NTA agarose column chromatography. Purified SC_{S10C} was conjugated with fluorescein-5-maleimide (F5M-SC) or Alexa Fluor 647 maleimide (Alexa647-SC) via thiol-maleimide Michael-type addition. To quantify the molar ratio of the SC and fluorescent dyes (F5M or Alexa647) in dye conjugated-SC, we obtained the absorbance of dye conjugated-SC at 280 nm and 494 or 594 nm that indicated the presence of protein and fluorophore, respectively, and calculated molar concentration. UV/Vis absorption spectra showed this labeling ratio is 1:1 ratio, which ensures one cysteine is labeled by a maleimide activated dye (Fig. S1). ST is a small peptide and has minimal risk of disrupting the function of target, so it was genetically inserted to a portion of the extracellular surface with HaloTag, which has its fluorescence ligand and is used as a marker of protein expression. SpyTag-HaloTag fusion protein (ST-HT-TM) was transiently expressed at the cell membrane in HEK293T cells, pre-incubated with 10 μ M F5M-SC for 45 min, co-treated with 5 μ M permeant HaloTag ligand TMR for 15 min, washed and imaged. Confocal images show that only cells labeled with red TMR ligand are labeled with F5M-SC binding to the cell membrane-localized ST in live cells, with minimal background (Figure B1a). Permeant HaloTag ligand TMR labeled cytosolic ST, which failed to move from the cytosol to the cell surface, whereas F5M-SC labeled the cell membrane-localized ST specifically. Almost identical results were obtained with F5M-SC bound to the cell membrane-localized ST in permeabilized cells (Figure B1a). Ligation of ST/SC was confirmed by western blot using cell lysate. F5M-SC ligated with ST both in the live cell surface before lysis and in the supernatant after lysis (Figure B2a). These data showed that dye conjugated SC could specifically label SpyTagged cell membrane-localized proteins in permeabilized or live cells. To demonstrate that the ST/SC system had sufficient efficiency in detecting intracellular proteins, ST-HT was transiently expressed in cytosol, nucleus, mitochondria. We first tested whether dye conjugated SC can label intracellularly expressed ST in live cells. As expected, F5M-SC or Alexa647-SC did not label the inaccessible intracellular ST, whereas permeant HaloTag ligand TMR or Oregon green 488 ligand could label intracellularly expressed HaloTag in live cells (Figure B1b-B1d). However, when cells were permeabilized, F5M-SC or Alexa647-SC was able to label the intracellularly expressed ST (Figure B1b-B1d). Ligation of ST/SC was confirmed by western blot using cell lysate. F5M-SC and Alexa647-SC did not ligate intracellular ST in live cells, but they ligated ST in the supernatant after lysis (Figure B2b-B2d). These data showed that dye conjugated SC could label SpyTagged intracellularly localized proteins in permeabilized cells.

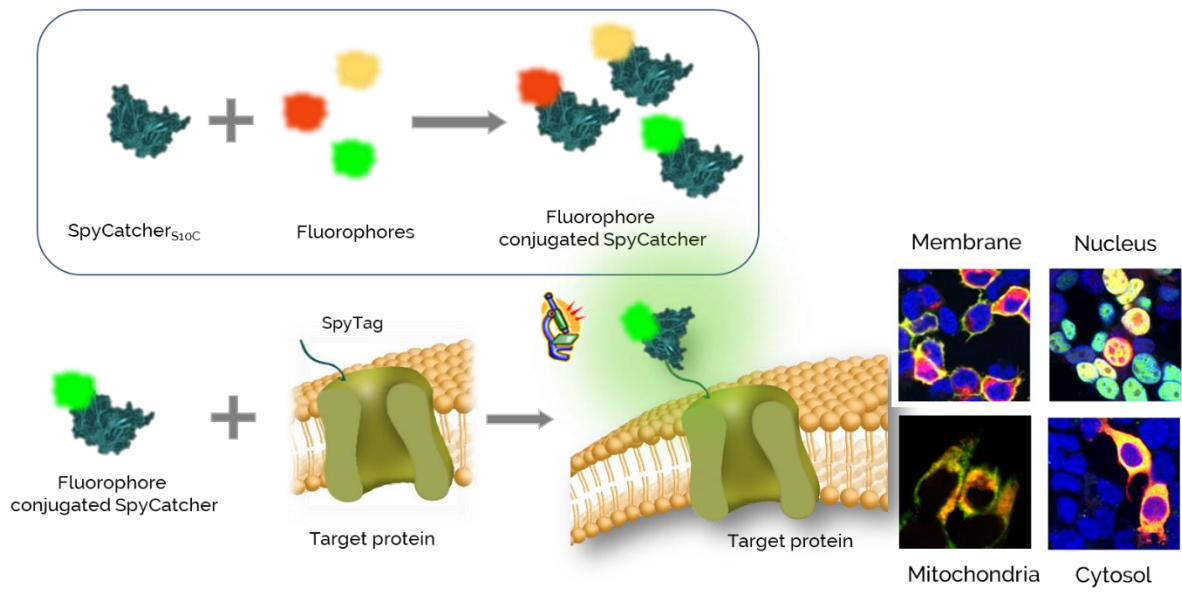


Figure B1. Schematic representation of target-specific labeling tools

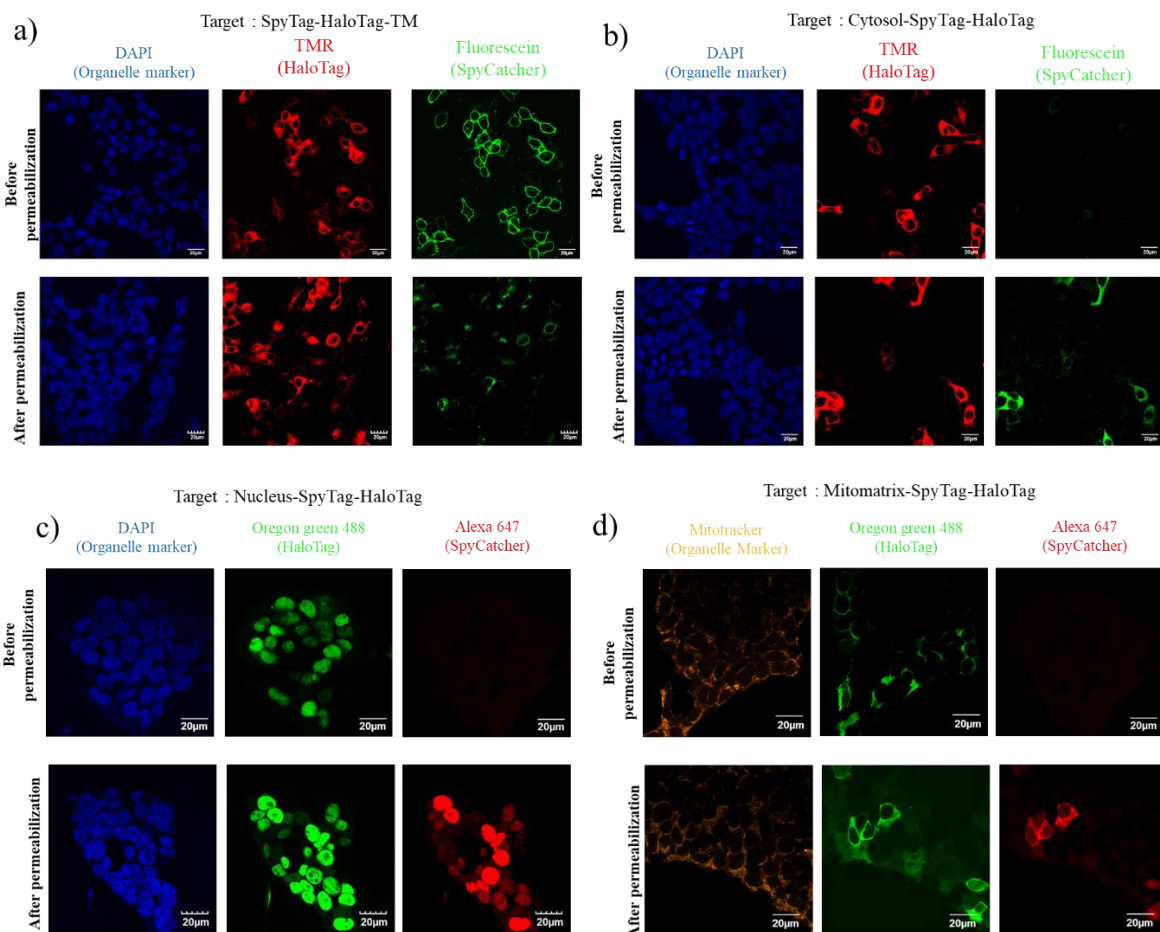


Figure B2. Fluorescent microscopic images with target-specific labeling tools

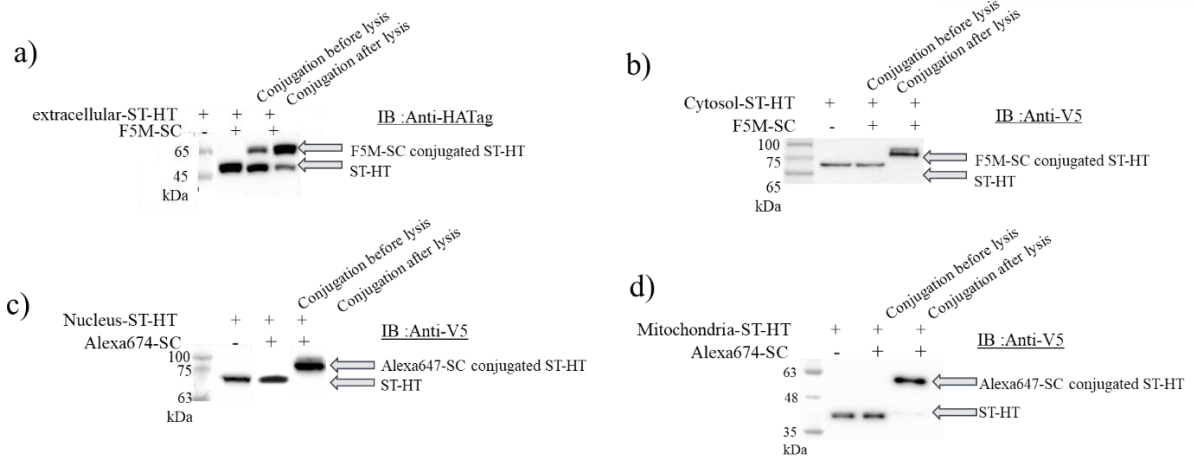


Figure B3. Confirmation of SpyTag/SpyCatcher ligation using western blots

C. References

1. Braun, M.; Thony-Meyer, L., Biosynthesis of artificial microperoxidases by exploiting the secretion and cytochrome c maturation apparatuses of Escherichia coli. *Proc Natl Acad Sci U S A* **2004**, *101* (35), 12830-5.
2. Cowley, A. B.; Lukat-Rodgers, G. S.; Rodgers, K. R.; Benson, D. R., A possible role for the covalent heme-protein linkage in cytochrome c revealed via comparison of N-acetylmicroperoxidase-8 and a synthetic, monohistidine-coordinated heme peptide. *Biochemistry* **2004**, *43* (6), 1656-66.
3. Tsou, C. L., Cytochrome c modified by digestion with proteolytic enzymes. 1. Digestion. *Biochem J* **1951**, *49* (3), 362-7.
4. Dallacosta, C.; Monzani, E.; Casella, L., Reactivity study on microperoxidase-8. *J Biol Inorg Chem* **2003**, *8* (7), 770-6.
5. Arslan, E.; Schulz, H.; Zufferey, R.; Kunzler, P.; Thony-Meyer, L., Overproduction of the Bradyrhizobium japonicum c-type cytochrome subunits of the cbb3 oxidase in Escherichia coli. *Biochem Biophys Res Commun* **1998**, *251* (3), 744-7.
6. Lombardi, A.; Nastri, F.; Pavone, V., Peptide-based heme-protein models. *Chem Rev* **2001**, *101* (10), 3165-89.
7. Asher, W. B.; Bren, K. L., A heme fusion tag for protein affinity purification and quantification. *Protein Sci* **2010**, *19* (10), 1830-9.
8. Choi, J. H.; Lee, S. Y., Secretory and extracellular production of recombinant proteins using Escherichia coli. *Appl Microbiol Biotechnol* **2004**, *64* (5), 625-35.
9. Kleingardner, E. C.; Asher, W. B.; Bren, K. L., Efficient and Flexible Preparation of Biosynthetic Microperoxidases. *Biochemistry* **2017**, *56* (1), 143-148.
10. Kremers, G. J.; Gilbert, S. G.; Cranfill, P. J.; Davidson, M. W.; Piston, D. W., Fluorescent proteins at a glance. *J Cell Sci* **2011**, *124* (Pt 2), 157-60.
11. Ogawa, M.; Kosaka, N.; Choyke, P. L.; Kobayashi, H., In vivo molecular imaging of cancer with a quenching near-infrared fluorescent probe using conjugates of monoclonal antibodies and indocyanine green. *Cancer Res* **2009**, *69* (4), 1268-72.
12. Hoelzel, C. A.; Zhang, X., Visualizing and Manipulating Biological Processes by Using HaloTag and SNAP-Tag Technologies. *Chembiochem* **2020**, *21* (14), 1935-1946.
13. Pessino, V.; Citron, Y. R.; Feng, S. Y.; Huang, B., Covalent Protein Labeling by SpyTag-SpyCatcher in Fixed Cells for Super-Resolution Microscopy. *Chembiochem* **2017**, *18* (15), 1492-1495.
14. Zakeri, B.; Fierer, J. O.; Celik, E.; Chittock, E. C.; Schwarz-Linek, U.; Moy, V. T.; Howarth, M., Peptide tag forming a rapid covalent bond to a protein, through engineering a bacterial adhesin. *P Natl Acad Sci USA* **2012**, *109* (12), E690-E697.